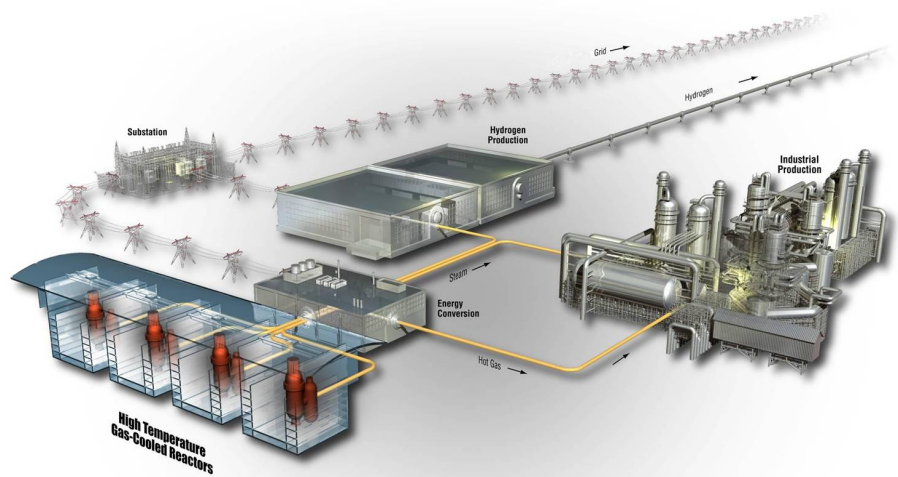


# COMBINE7.1—A Portable ENDF/B-VII.0 Based Neutron Spectrum and Cross-Section Generation Program

W. Y. Yoon  
R. A. Grimesey  
D. W. Nigg  
R. L. Curtis  
H. D. Gougar

September 2011

The INL is a  
U.S. Department of Energy  
National Laboratory  
operated by  
Battelle Energy Alliance



**DISCLAIMER**

This information was prepared as an account of work sponsored by an agency of the U.S. Government. Neither the U.S. Government nor any agency thereof, nor any of their employees, makes any warranty, expressed or implied, or assumes any legal liability or responsibility for the accuracy, completeness, or usefulness, of any information, apparatus, product, or process disclosed, or represents that its use would not infringe privately owned rights. References herein to any specific commercial product, process, or service by trade name, trade mark, manufacturer, or otherwise, does not necessarily constitute or imply its endorsement, recommendation, or favoring by the U.S. Government or any agency thereof. The views and opinions of authors expressed herein do not necessarily state or reflect those of the U.S. Government or any agency thereof.

# **COMBINE7.1 – A Portable ENDF/B-VII.0 Based Neutron Spectrum and Cross-Section Generation Program**

W. Y. Yoon  
R. A. Grimesey  
D. W. Nigg  
R. L. Curtis  
H. D. Gougar

September 2011

**Idaho National Laboratory  
Next Generation Nuclear Plant Project  
Idaho Falls, Idaho 83415**

<http://www.inl.gov>

Prepared for the  
U.S. Department of Energy  
Office of Nuclear Energy  
Under DOE Idaho Operations Office  
Contract DE-AC07-05ID14517



Next Generation Nuclear Plant Project

**COMBINE7.1—A Portable ENDF/B-VII.0 Based  
Neutron Spectrum and Cross-Section Generation  
Program**

INL/EXT-08-14729  
Revision 2

~~August 2011~~  
September 2011

Approved by:

Woo Y. Yoon  
Woo Y. Yoon  
Author

7/27/2011  
Date

Diane V. Croson  
Diane V. Croson  
VHTR TDO Project Manager

9/1/11  
Date

Hans D. Gougar  
Hans D. Gougar  
VHTR TDO Deputy Technical Director

9/01/2011  
Date

## ABSTRACT

COMBINE7.1 is a FORTRAN 90 computer code that generates multigroup neutron constants for use in the deterministic diffusion and transport theory neutronics analysis. The cross-section database used by COMBINE7.1 is derived from the Evaluated Nuclear Data Files (ENDF/B-VII.0). The neutron energy range covered is from 20 MeV to 1.0E-5 eV. The Los Alamos National Laboratory NJOY code is used as the processing code to generate a 167 fine-group cross-section library in MATXS format for Bondarenko self-shielding treatment. Resolved resonance parameters are extracted from ENDF/B-VII.0 File 2 for a separate library to be used in an alternate Nordheim self-shielding treatment in the resolved resonance energy range. The equations solved for energy dependent neutron spectrum in the 167 fine-group structure are the  $B_3$  or  $B_1$  zero-dimensional approximations to the transport equation. The fine group cross sections needed for the spectrum calculation are first prepared by Bondarenko self-shielding interpolation in terms of background cross section and temperature. The geometric lump effect, when present, is accounted for by augmenting the background cross section. Nordheim self-shielded fine group cross sections for a material having resolved resonance parameters overwrite correspondingly the existing self-shielded fine group cross sections when this option is used. COMBINE7.1 coalesces fine group cross sections into broad group macroscopic and microscopic constants. The coalescing is performed by utilizing fine-group fluxes and/or currents obtained by spectrum calculation as the weighting functions. The multigroup constants may be output in any of several standard formats including INL format, ANISN 14\*\* free format, CCCC ISOTXS format, and AMPX working library format. ANISN-PC, a one-dimensional (1-D) discrete-ordinate transport code, is incorporated into COMBINE7.1. As an option, the 167 fine-group constants generated by zero-dimensional COMBINE portion in the program can be used to calculate regionwise spectra in the 1-D ANISN portion, all internally to reflect the 1-D transport correction. The regionwise spectra are then used to generate multigroup regionwise neutron constants.

The upgrading of COMBINE from version 6 to version 7 was driven by the need to capture the multiple levels of heterogeneity found in the core of a pebble bed high temperature reactor. This type of reactor exhibits considerable 1-D symmetry at each stage (spherical at the TRISO and pebble scales; cylindrical at the scale of the core). Therefore, the 1-D neutron transport calculation can be performed at up to three stages, e.g., from a TRISO fuel to pebble (or COMPACT) to 1-D full core wedge. With the 167-group cross sections coalesced from one stage automatically applied to the next. The 167-group cross sections are collapsed to the desired few group structure using the flux computed at the final transport stage. Because the transport equation can be solved in Cartesian (planar), cylindrical, or spherical geometry, COMBINE 7.1 can also be used for pincell (compact) calculations in prismatic HTGRs. Furthermore, a core-level 1-D cylindrical or Cartesian transport model may be comprised of a

regions exhibiting planar, cylindrical, or spherical geometry, or no structure at all (0-D). For example, a 1-D core wedge of a pebble bed reactor may consist of three 0-D homogeneous regions representing a uniform inner reflector, four or five spherical 1-D regions comprised of pebbles, a 1-D cylindrical region representing a control rod assembly, and outer regions composed of 0-D homogeneous outer reflector components. The transverse leakages (axial and azimuthal) are treated with group-wise buckling terms. This geometrical flexibility, combined with the computational efficiency of the 1-D transport algorithm, makes COMBINE 7.1 well-suited for pebble bed reactor fuel management calculations. For this reason, COMBINE 7.1 is incorporated into the INL's PEBBED code as a subroutine, enabling inline cross section generation for the 3-D core diffusion/depletion algorithm used in that code.

In addition, COMBINE7.1 has now the capability of adjoint flux calculation through the 1-D ANISN transport. Photon transport capability is also added. For this, a photon production and photo-atomic cross section library, MATNG.LIB, was generated in MATXS format through NJOY code. The photon production cross section matrix is of  $167 \text{ neutron} \times 18 \text{ photon}$  groups. Photo-atomic cross sections, including heating, are in 18 energy groups.



## **ACKNOWLEDGMENTS**

A number of individuals contributed to the successful development of the COMBINE7.1 code, which was derived from COMBINE5 and 6 codes. Gilbert Singer provided an initial standard FORTRAN version of the CVI free-format input processing routines used in COMBINE/PC. Jerry Judd, J. Russell Johnson, Blair Briggs, and Bruce Schnitzler contributed to the programming of several routines. Joshua Cogliati helped on the FORTRAN character to integer conversion. Dr. D. Parsons, formerly with the Idaho National Laboratory (INL), is greatly appreciated for the use of ANISN/PC. Dr. Hans Gougar extensively tested the COMBINE7.1 beta versions and his inputs were invaluable. The Next Generation Nuclear Program at INL deserves a special mention for helping realize the current code version.



# CONTENTS

ABSTRACT.....	v
ACKNOWLEDGMENTS .....	viii
ACRONYMS.....	xiv
1. INTRODUCTION.....	1
1.1 COMBINE7.1 Code Abstract .....	4
2. THEORETICAL FOUNDATIONS .....	6
2.1 Derivation of 0-D $B_N$ Equations .....	6
2.1.1 $B_3$ Approximation .....	8
2.1.2 $B_1$ Approximation .....	12
2.1.3 Convergence on Gauss-Seidel Iterative Scheme.....	14
2.2 Bondarenko Method.....	14
2.2.1 Fine-Group Cross Section Generation in Bondarenko Format .....	17
2.2.2 Bondarenko Self-Shielding Interpolation .....	18
2.3 Resonance Region.....	18
2.3.1 Resolved Resonances—Nordheim Numerical Method.....	18
2.3.2 Doppler Broadening of Resolved Resonance Parameters.....	21
2.3.3 Determination of $E_1/E_2$ and the Number of Meshes for a Resonance .....	22
2.3.4 Absorber Narrow Resonance-Moderator Asymptotic Flux Approximation.....	23
2.3.5 Self-Shielding Elastic Scattering Transfer Matrix .....	23
2.3.6 Numerical Integration with Simpson’s Rule.....	23
2.3.7 Group Averaging.....	24
2.3.8 Dancoff-Ginsburg Correction Factor Calculation.....	24
2.4 Age Equations .....	27
2.5 $P_n$ to $S_n$ Transport Corrections.....	27
2.6 Adjoint Problems .....	28
2.7 Photon Production and Photo-atomic Cross Section.....	28
3. 1-D TRANSPORT CALCULATION .....	29
3.1 Transverse Buckling in the Final Stage 1-D Transport Calculation .....	29
4. USER’S GUIDE.....	30
4.1 Derivation of Diffusion Coefficient and Transport Cross Section.....	30
4.2 Summary Edits for Broad Group Constants.....	31
4.2.1 Average Macroscopic Cross Sections .....	33
4.2.2 Monoenergetic Transport Cross Section.....	36
4.2.3 Average Microscopic Cross Sections.....	37
4.2.4 Effective Diffusion Theory Constants (Blackness Theory) .....	38
4.2.5 Mixed Number Density Constants .....	38
4.2.6 Multiplication Factors .....	40
4.2.7 The Spatial Coalescing Formulas .....	40
5. COMBINE7.1 FILES DESCRIPTION .....	44

6.	INPUT DATA FILE (COMBINE.INP) ORGANIZATION .....	46
6.1	Multistage-Multiregion 1-D transport Level Input Data Records.....	46
6.2	Problem Level Input Data Records .....	51
6.2.1	Title Record .....	52
6.2.2	Problem Basic Control Information Record 1010101 .....	52
6.2.3	Energy Group Structure Record 10102YY .....	53
6.2.4	Resonance Calculation Option Record 102010Y. ....	53
6.2.5	Macroscopic Interface File Option Record 1030101 .....	53
6.2.6	Microscopic Interface File Option Record 10302XX.....	53
6.3	Floating Point Data Records .....	54
6.3.1	General Floating Point Data Record 1041001 .....	54
6.3.2	Material Specification Record 10420XX.....	54
6.3.3	Material Resonance Specification Record 1043XXY.....	54
6.3.4	Material Dancoff Specification Record 1044XXY.....	56
6.3.5	Material General Resonance Data Record 10450XX .....	56
6.3.6	Material Self-Shielding Factor Records (146XXYY).....	57
6.3.7	Broad Group Buckling Factor Records (14700YY) .....	57
6.3.8	Broad Group Buckling Sign Records (14710YY) .....	57
6.3.9	Blackness calculation option Record (1480001).....	58
6.3.10	MND calculation option Record (1490001) .....	58
7.	LIBRARY DATA ORGANIZATION .....	59
7.1	Fine Energy Neutron Group Structure .....	59
7.2	Photon Group Structure .....	60
7.3	Materials in the “MATXS” Cross Section Libraries (MATXS and MATNG), and the “RERES” Resolved Resonance Library.....	60
7.4	MATXS.LIB File Description .....	65
7.5	Description of Resolved Resonance Library (reres.lib) Format.....	69
7.6	Cross section and constants internal record .....	70
7.6.1	First Data Record for Material k.....	70
7.6.2	Second Data Record for Material k.....	71
7.7	Thermal $S(\alpha,\beta)$ and Free Scattering Cross Section Internal Record .....	72
8.	PROGRAMMER’S GUIDE.....	73
8.1	Flow Diagram .....	73
8.2	Summary of Contents of Subroutines .....	75
8.2.1	Program COMBINE7.1 and Supporting Subroutines.....	75
9.	REFERENCES .....	83
	B. REFERENCE.....	91
	ISOTXS—Nuclide (Isotope) Ordered, Multigroup Neutron Cross Sections .....	93
	D. REFERENCE .....	108

## FIGURES

Figure 1. COMBINE7.1 implementation scheme.....	3
---	---

Figure 2. Modified inverse Levine factor as a function of Dancoff factor. ....	16
Figure 3. An example of Doppler broadened resonance cross sections. ....	22
Figure 4. Parameters of the rectangular cell.....	26
Figure 5. Spectrum group structure.....	32

## TABLES

Table A-1. The library material title record summary. ....	86
Table A-2. The library material floating point data summary. ....	87
Table B-1. Cross-section arrangement. ....	91
Table D.1. Criticality Validation Suite .....	102
Table D.2. Calculated ( $B_1$ ) $k_{\text{eff}}$ eigenvalues against the measured $k_{\text{eff}} = 1.000$ .....	107



## ACRONYMS

ABH	Amouyal/Benoist/Horowitz
ENDF	Evaluated Nuclear Data Files
INL	Idaho National Laboratory
MCNP	Monte Carlo Neutral Particle
MLBW	Multilevel Breit-Wigner
MND	mixed number density
NR	narrow resonance
0-D	zero-dimensional
1-D	one-dimensional
R-M	Reich-Moore
SLBW	single level Breit-Wigner

# COMBINE7.1—A Portable ENDF/B-VII.0 Based Neutron Spectrum and Cross-Section Generation Program

## 1. INTRODUCTION

COMBINE7.1 is a FORTRAN 90 computer code for generation of spectrum-averaged, multigroup, neutron, cross-section data suitable for use in the deterministic diffusion and transport theory reactor design analysis. The cross-section database used by COMBINE7.1 is derived from Evaluated Nuclear Data Files (ENDF/B-VII.0<sup>1</sup>). The neutron energy ranging from 20 MeV to 1.0E-5 eV is treated by a total of 167 discrete energy groups. The equations solved for the energy-dependent neutron spectrum are the B3 or B1 zero-dimensional (0-D) approximations to the transport equation.

COMBINE7.1 has evolved from its predecessor Versions 5 and 6. The earlier version, COMBINE/PC—a Portable ENDF/B Version 5 Neutron Spectrum and Cross-Section Generation Program<sup>2</sup> (COMBINE5)—combined the preexisting neutron spectrum codes, PHROG<sup>3</sup> (fast) and INCITE<sup>4</sup> (thermal spectrum), previously developed at Idaho National Laboratory (INL), by suitably integrating them into a single package, thus, the name COMBINE. The cross-section database used by COMBINE5 is derived from the ENDF/B-V.<sup>5</sup> In the fast spectrum calculation, the B3 spherical harmonics equations are solved by Gauss elimination and the B1 spherical harmonics equations are solved simultaneously, beginning with the highest energy group. In INCITE, the B1 thermal equations have been cast in the form of a normalized Gauss-Seidel iterative scheme where extrapolation and iteration in both directions have been included as options. The fast and thermal energy ranges are coupled by using slowing down theory and energy-dependent scattering and spectra data to generate average transfer cross sections from the PHROG broad groups into INCITE broad groups. The results are then normalized to the total scatter below the fast range cutoff as produced by PHROG.

The 1990 release of ENDF/B-VI nuclear data<sup>6</sup> of ENDF-6 format created problems for the INL's Version 5 processing codes used to generate cross-section libraries for COMBINE5, requiring major revisions of these codes. An alternative to the modifications of the INL's processing codes was to utilize the NJOY code system<sup>7</sup> developed at the Los Alamos National Laboratory. NJOY optionally processes all resonance self-shielding through the Bondarenko approximation. In the Bondarenko model,<sup>8</sup> the narrow resonance (NR) approximation and the  $B_N$  approximation for large systems are invoked.<sup>9</sup> Two cross section libraries were generated by NJOY for the fast (72 group) and thermal (101 energy points) spectrum calculations, maintaining the same energy structures as in COMBINE5. The fast cross section library was based on sets of background cross sections and temperatures for Bondarenko self-shielding interpolation. The geometric effects of fuel lump and lattice are accounted for by the combination of Rational Approximation and Dancoff-Ginsburg correction, including a double heterogeneity due to fuel grains present within the macroscopic fuel lump by augmenting the background cross section. The weakness of the Bondarenko model occurs for thermal reactor analysis in the "epithermal" energy region from about 4 eV to around 200 to 300 eV.<sup>10</sup> In this region, the resonances are no longer "narrow" and the flux shape given by Bondarenko method is no longer sufficiently accurate. An alternate approach at the expense of more computer time is the Nordheim resonance integral treatment method.<sup>11</sup> A separate resolved resonance library was also created that included formats in single level Breit-Wigner (SLBW), Multilevel Breit-Wigner (MLBW), Reich-Moore (R-M), and no resonance extracted directly from ENDF/B-VI nuclear data files to be used in the Nordheim self-shielding treatment in the resolved resonance energy range. The Version 5 code was modified to handle the new cross section and resolved resonance libraries. The new code was designated as COMBINE6.<sup>12</sup> The ENDF/B-VI derived thermal cross-section library is based on the infinite dilution and temperature dependence is only present if thermal scattering data is available for an isotope. This format of the thermal cross-section library is same as that of COMBINE5's. The INCITE portion of COMBINE5 is therefore fully retained, including the

Amouyal/Benoist/Horowitz (ABH)<sup>13</sup> option for self-shielding in the thermal energy range. The energy range treated is from 0.001 eV to 16.905 MeV spanned by a total of 166 discrete energy points/groups. A routine was also retained to calculate a Dancoff-Ginsburg correction factor in conjunction with the resonance calculation for either a rectangular or hexagonal arrangement of cylindrical absorber pins. Several routines to process MLBW and R-M resonance formats were adopted from the NJOY code. Nordheim self-shielded cross sections, when requested for a material having resolved resonance parameters, overwrite the corresponding multigroup Bondarenko self-shielded cross sections. An iterative scheme was also introduced for better fission-rate weighted  $\chi$  values. In both COMBINE5 and COMBINE6, the energy boundary between the fast spectrum module and thermal spectrum module can be chosen by the user at one of the eight overlapping mutual energy group boundaries, the highest being 2.3824 eV and the lowest 0.414 eV. No resonance treatment is considered below the chosen energy boundary. No thermal upscattering is allowed into the energy above the highest boundary. Thermal upscattering does not take place between the highest (2.3824 eV) and chosen boundary of less energy, even though it is possible from below to above the boundary when the boundary is below the highest. The adequate self-shielding treatment of resonances in the thermal energy range is critical where thermal upscattering is also significant because of high operating temperature. Overlap and interference effect of resonances among admixed absorbing isotopes was not accounted for.

COMBINE7.1 has been modified to resolve the above issues. The  $B_1$  and  $B_3$  algorithms for the full range slowing down solution in a homogeneous medium, including thermal upscattering, were identified and implemented to unify fast and thermal spectrum calculations. The neutron energy ranging from 20 MeV to 1.0E-5 eV is treated by a total of 167 discrete energy groups, adding one more group (20–16.905 MeV) to the previous versions' group structure. The thermal upscattering takes place between 1.0E-5 and 5.0435 eV (high enough for most reactor applications) with no energy boundary restriction. Up to g-wave resonances are now treated to obtain the elastic scattering cross section, although the isotropic scattering is still used for energy transfer. In the Nordheim resonance treatment, up to three admixed resonance absorbers can be present to account for the resonance overlap and interference effect. Thermal upscattering was also added in the resonance treatment solution. The interpolation algorithm in the Bondarenko scheme to self-shield cross sections has been modified for improvement and revamped to afford additional temperature-only-dependent thermal scatterings, free and/or  $S(\alpha, \beta)$ . The interpolation is now performed first for the background cross sections at each temperature and the generated cross sections for the set of preselected temperatures are then interpolated for the problem-dependent temperature. Negative buckling ( $B^2$ ) algorithms have been implemented in addition to a real B (square root of buckling): one with the positive imaginary B and the other with the negative imaginary B. Previously, only the positive and real B of cosine spatial shape was allowed. The mixed use of three different modes of buckling in the broad groupwise input is implemented. All resonances are Doppler broadened by the method called "kernel broadening" as practiced in NJOY, thus eliminating the need to evaluate Doppler line functions ( $\psi$  and  $\chi$ ) previously calculated in the SLBW treatment. The GAM-1 resolved-resonance calculation routine,<sup>14</sup> a fast alternative to the much more accurate but time consuming Nordheim numerical method, was scrapped, since speed is no longer a factor. Many of the INCITE routines were removed or combined with PHROG because of the unified energy scheme.

The necessity of better treat spatial self-shielding and reflector effects when dealing with neutron-optically thin reactors like the annular core design of gas-cooled, graphite-moderated, high-temperature reactors such as that proposed for the Next Generation Nuclear Plant requires the transport correction in generating the cross sections for use in reactor physics. A one-dimensional (1-D) discrete-ordinate transport code (ANISN-PC<sup>15</sup>) is thus incorporated into COMBINE7.1 to reflect 1-D transport correction. With this incorporation, a fuel such as TRISO/PEBBLE can be better modeled to generate cross sections for the pebble bed reactor analyses. The 167 fine-group constants generated by the 0-D COMBINE portion for multiregions via stack cases/problems are fed into ANISN to calculate regionwise spectra, which are used in the COMBINE to generate the regionwise spatial self-shielded broad group constants.

The 1-D neutron transport can be performed up to three stages, e.g., from a TRISO fuel to PEBBLE to 1-D full core wedge. With the 1-D capability, the ABH thermal self-shielding is no longer needed, so this portion is eliminated in COMBINE7.1. The detail of ANISN code will be deferred to its manual.

In addition, COMBINE7.1 now has the capability of adjoint flux calculation through the 1-D ANISN transport for sensitivity study. Photon transport capability is also added. For this, a photon production and photo-atomic cross section library (MATNG.LIB) was generated in MATXS format through NJOY code. The photon production cross section matrix is of 167 neutron  $\times$  18 photon groups. Photo-atomic cross sections, including heating, are in 18 energy groups, ranging from 11 MeV to 100 keV. Figure 1 shows the COMBINE7.1 implementation scheme.

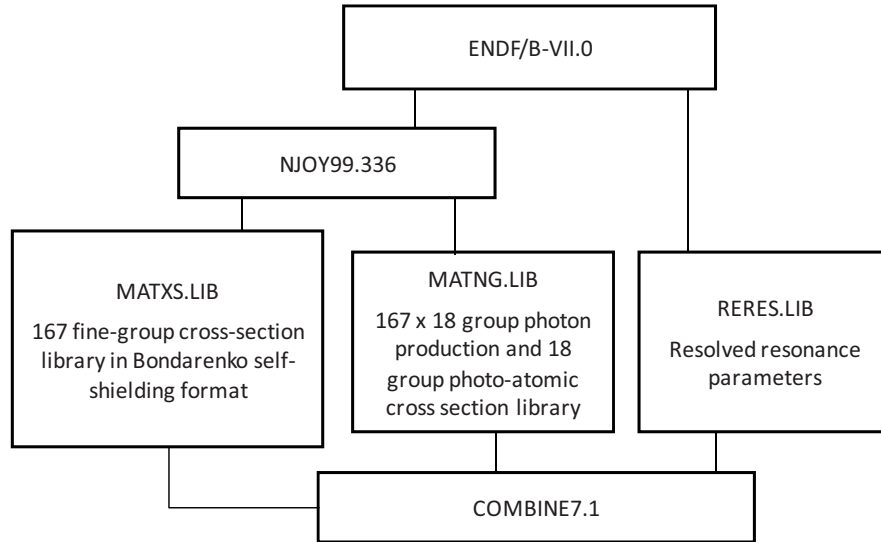


**Figure 1. COMBINE7.1 implementation scheme.**

ENDF/B-VII.0 nuclear data was released in December 2006 using the same ENDF-6 format.<sup>1</sup> The cross-section database is now derived entirely from ENDF/B-VII.0 nuclear data with the exception of zirconium element cross-section data, which is based on ENF/B-VI.8 nuclear data, and Th-231, which is based on the Japanese Evaluated Nuclear Data Library JENDL-4.0. The NJOY99.336 version<sup>16</sup> was used to generate a 167 fine-group cross-section library, MATXS.LIB, in MATXS format (Bondarenko format) on sets of background cross sections and temperatures including thermal scattering cross sections. This cross-section library includes all the neutron reaction cross sections for activation and depletion calculation, damage, heating, kerma, and gas production cross sections in addition to those vector and matrix cross sections required for transport calculations. Only those materials designated by ENDF/B File 7 formats as moderators and included in NJOY99.336 contain thermal  $S(\alpha,\beta)$  scattering matrices. The nonmoderating materials in the library possess free thermal scattering matrices. Some moderating materials also have free thermal scattering matrices. A separate resolved resonance library, RERES.LIB, was also created that includes formats in SLBW, MLBW, R-M, and no resonance, extracting all resolved resonance parameters directly from ENDF/B-VII.0 nuclear data files. The “MATNG” photon library contains photon production cross sections in MATXS format for all those materials in the MATXS.LIB and photo-atomic cross section for all the corresponding elements. The photoatomic cross sections are however neither temperature nor background cross section dependent. The set of photo-atomic cross sections include the heat production cross section in addition to total, coherent and incoherent scattering, photoabsorption, and pair production cross sections. In COMBINE these cross sections are processed to be used suitably for photon transport and heating calculation. The neutron energy group structure is identical to that of MATXS.LIB and the photon energy group structure is identical to that of ORIGEN code. Therefore, the photon production matrix is of 167  $\times$  18 group structure.

Along with MATXS.LIB, RERES.LIB, and MATNG.LIB, the upgraded COMBINE version is now called COMBINE7.1.

As the code has evolved, further improvements are expected in the future. Calculation experiences involving pebble bed and other reactor types would help this Endeavour. Increasing the number of energy groups in the resolved energy region is highly desirable, however, at the expense of more computer time.

## 1.1 COMBINE7.1 Code Abstract

1. **Program Identification:** COMBINE7.1.
2. **Description of Problem:** COMBINE7.1 is a FORTRAN 90 computer code that generates multigroup neutron constants for use in the deterministic diffusion and transport theory neutronics analysis. The cross-section database used by COMBINE7.1 is derived from ENDF/B-VII.0. The neutron energy range covered is from 20 MeV to 1.0E-5 eV. It can generate photon cross sections and perform photon transport calculation. The photon energy range covered is from 11 MeV to 100 keV. It has the capability of adjoint neutron flux calculation.
3. **Method of Solution:** The energy range is broken into 167 fine groups for the spectrum calculation. The equations solved for energy dependent neutron spectrum are the  $B_3$  or  $B_1$  0-D approximations to the transport equation. The resulting matrix of flux equations is then solved using standard numerical techniques to obtain the spectral weight function for the generation of group-averaged constants. An alternate resolved resonance shielding of the fine mesh cross-section data is performed using the Nordheim method. Calculated cross sections may be issued in any of several standard formats. The neutron or photon transport is performed with the 1-D discrete-coordinates method.
4. **Related Material:** Two MATXS library files and a resolved resonance parameter library file are provided with the code package in ASCII format. Processors to convert the MATXS file to the required binary format or to convert the binary file to the ASCII file are as follows:

cv7_1.f90:	COMBINE7.1 Fortran 90 source program. It requires matxs.lib and reres.lib to run a problem. It requires matng.lib when photon cross section generation is requested.
cv7_1.exe	Executable compiled by Intel Fortran Compiler 10.1.011.
matxs.asc:	167 fine-group neutron cross section library in ascii format
matxs.lib:	167 fine-group neutron cross section library in binary format
matng.asc:	167 × 18 photon production matrix and 18 group photo-atomic cross section library in ascii format
matng.lib:	167 × 18 photon production matrix and 18 group photo-atomic cross section library in binary format
reres.lib:	resolved resonance library in ascii format
matxscv.f:	Fortran program to convert matxs.asc (ascii file) to matxs.lib (binary file)
matxsca.f:	Fortran program to convert matxs.lib to matxs.asc
matngcv.f:	Fortran program to convert matng.asc (ascii file) to matng.lib (binary file)
matngca.f:	Fortran program to convert matng.lib to matng.asc
anisn.pdf:	ANISN/PC Manual (pdf file).
benchmarks	file directory containing 19 benchmark runs
sample_inputs	file directory containing sample inputs

5. **Restrictions:** COMBINE7.1 is written to function properly on both 32-bit and 64-bit word length machines. Accuracy to four or five decimal places in the computed spectrum and cross sections may be expected. Since double precision optimization for some variables are made in the program, no double precision optimization is needed when compiling.
6. **Computers:** COMBINE7.1 is written in standard FORTRAN with the objective of total machine independence. The program has been successfully compiled by the Intel Visual Fortran Compiler (Version 10) and by the Lahey/Fujitsu Fortran compiler (LF95) on the Windows 32-bit and 64-bit platforms, and also by Intel compiler on the 64-bit unix platform.
7. **Run Time:** Variable from a few seconds to 30 minutes on PC-class hardware, depending primarily on the number and type of self-shielding treatment and multistage calculations required for a particular case.
8. **Programming Language:** Standard FORTRAN 90.
9. **Operating System:** COMBINE7.1 has successfully functioned under Windows and Linux operating systems.
10. **Machine Requirements:** As stated in item 6, Computers.
11. **Authors:** W. Y. Yoon  
R. A. Grimesey  
D. W. Nigg  
R. L. Curtis  
H. D. Gougar  
Idaho National Laboratory  
Battelle Energy Alliance  
P.O. Box 1625  
Idaho Falls, ID 83415

## 2. THEORETICAL FOUNDATIONS

### 2.1 Derivation of 0-D $B_N$ Equations

The equations solved by COMBINE are the energy-dependent  $B_1$  or  $B_3$  spherical harmonic approximations to the transport equation originally developed by D. S. Selengut.<sup>17</sup> A derivation of the  $B_N$  spherical harmonics equations is straightforward, but rather tedious because of the complicated expansion integrals. The physical model is a homogeneous, critical, 1-D bare slab core. As such, the time-independent, energy dependent, Boltzmann neutron transport equation in plane geometry may be written

$$\mu \frac{\partial \Phi(x, \mu, E)}{\partial x} + \Sigma_t(x, E) \Phi(x, \mu, E) = \iint \Sigma_s(x; \Omega', E' \rightarrow \Omega, E) \Phi(x, \mu', E') d\Omega' dE' + Q(x, \mu, E) \quad (1)$$

where:  $\Phi(x, E, \mu)$  is the neutron flux in the direction  $\mu = \cos \theta$  relative to the 1-D x axis of the slab at energy E and position x and  $\Omega$  and  $\Omega'$  are the azimuthal angles associated with  $\mu$  and  $\mu'$ , respectively;  $\Sigma_t$  is the total cross section; and  $\Sigma_s(x; \Omega', E' \rightarrow \Omega, E)$  is the neutron transfer cross section, including the multiplicity of neutrons emitted in each reaction event. Q represents the independent (or extraneous) neutron sources that are not dependent on the neutron density of the system. All cross sections here are macroscopic. It is then assumed that the angular variation of the transfer cross section,  $\Sigma_s$ , depends only on the scattering angle,  $\mu_0 = \Omega \cdot \Omega'$ , so  $\Sigma_s$  may be expanded in a set of Legendre polynomials of  $\mu_0$  as

$$\Sigma_s(x; \Omega', E' \rightarrow \Omega, E) = \sum_{l=0}^{\infty} \frac{2l+1}{4\pi} \Sigma_{sl}(x; E' \rightarrow E) P_l(\mu_0), \quad (2)$$

where the expansion coefficients  $\Sigma_{sl}(x; E' \rightarrow E)$  are given by

$$\Sigma_{sl}(x; E' \rightarrow E) = 2\pi \int_{-1}^1 \Sigma_s(x; E' \rightarrow E, \mu) P_l(\mu) d\mu. \quad (3)$$

If the expansion of Equation (3) is inserted into Equation (1), use of the addition theorem for Legendre polynomials and integration over azimuthal angles gives

$$\mu \frac{\partial \Phi(x, \mu, E)}{\partial x} + \Sigma_t(x, E) \Phi(x, \mu, E) = \sum_{l=0}^{\infty} \frac{2l+1}{2} P_l(\mu) \int_E^{\infty} \Sigma_s(x, E' \rightarrow E) \int_{-1}^1 \Phi(x; \mu', E') P_l(\mu') d\mu' dE' + Q(x, \mu, E). \quad (4)$$

The basis of the  $B_N$  method, as a means of estimating within-group neutron fluxes, is to assume the spatial distribution to be independent of neutron energy in plane geometry,

$$\Phi(x, \mu, E) = e^{-iBx} \psi(B, \mu, E) \quad (5)$$

where only the real part of  $e^{-iBx}$  satisfies the spatial boundary conditions for the scalar flux. The complex form of the spatial dependence, parameterized by the square root of the buckling (B), is necessary for the equations to remain homogeneous. In Equation (5) the spatial dependence of the flux is eliminated by assuming that the solution is separable in  $(E, \mu)$  and  $x$  and characterizing the spatial dependence of each of the variables by a simple buckling mode. If Equation (5) is inserted into the neutron transport Equation (4) with  $Q(x, \mu, E)$  replaced by an isotropic fission source,  $\frac{1}{2} \chi(E) e^{-iBx}$ , and the transfer cross section is

now designated as  $\Sigma_{sl}$  signifying the absence of fission contribution, the result is

$$\begin{aligned} & \Sigma_t(E) \left(1 - \frac{iB\mu}{\Sigma_t}\right) \psi(B, \mu, E) \\ &= \sum_{l=0}^{\infty} \frac{2l+1}{2} P_l(\mu) \int_{\Sigma_{sl}(E' \rightarrow E)} \int_{-1}^1 \psi(B, \mu', E') P_l(\mu') d\mu' dE' + \frac{1}{2} \chi(E). \end{aligned} \quad (6)$$

The neutron source is assumed to have the same spatial dependence as the flux. This assumption is also necessary in order for the equations to remain homogeneous. The source term,  $\chi(E)/2$ , in Equation (6) is the result of Legendre polynomial expansion and truncation to the first term, assuming the fission source to be isotropic in lab coordinates. It is also noted that independent (or extraneous) neutron sources, which are not dependent on the neutron density of the system, are not included in this equation. Equation (6) could be multiplied by  $P_n(\mu)$  and integrated over  $\mu$  from -1 to 1 to obtain equations satisfied by the Legendre components of  $\psi(B, \mu, E)$ . More rapid convergence of the expansion is achieved, however, when Equation (6) is divided by  $\Sigma_t(1 - iB\mu/\Sigma_t)$ , multiplied by  $P_n(\mu)$ , and then integrated to obtain, for  $n = 0, 1, 2, \dots$ ,

$$\phi_n(B, E) = \sum_{l=0}^{\infty} (2l+1) \frac{A_{nl}(B, E)}{\Sigma_t(E)} \int_{\Sigma_{sl}(E' \rightarrow E)} \Phi_l(B, E') dE' + \frac{A_{n0}(B, E)}{\Sigma_t(E)} \chi(E), \quad (7)$$

using the following definitions:

$$(i)^n \phi_n(B, E) \equiv \int_{-1}^1 \psi(B, \mu, E) P_n(\mu) d\mu. \text{ when B is real,} \quad (8)$$

$$\phi_n(B, E) \equiv \int_{-1}^1 \psi(B, \mu, E) P_n(\mu) d\mu. \text{ when B is imaginary (B = } \pm iC, \text{ where C is real),} \quad (9)$$

$$A_{nl}(B, E) \equiv \frac{(i)^{l-n}}{2} \int_{-1}^1 \frac{P_n(\mu) P_l(\mu)}{1 - \frac{iB\mu}{\Sigma_t(E)}} d\mu \text{ when B is real,} \quad (10)$$

$$A_{nl}(B, E) \equiv \frac{1}{2} \int_{-1}^1 \frac{P_n(\mu) P_l(\mu)}{1 - \frac{iB\mu}{\Sigma_t(E)}} d\mu \text{ when B is imaginary.} \quad (11)$$

When  $n = 0$ , for example, the value  $P_0(\mu)$  is 1; hence, it follows from Equation (8) that  $\Phi_0(B, E)$  is simply the total flux at E.

From Equations (10) and (11), the following symmetry and recursion relations can be derived:

$$(i)^{n-l} A_{nl} = (i)^{l-n} A_{ln} \text{ when B is real,} \quad (12)$$

$$A_{nl} = A_{ln} \text{ when B is imaginary,} \quad (13)$$

$$\frac{1}{B/\Sigma_t} (2l+1) A_{nl} - (l+1) A_{n,l+1} + l \cdot A_{n,l-1} = \frac{\delta_{nl}}{B/\Sigma_t} \text{ when B is real,} \quad (14)$$

$$\frac{1}{C/\Sigma_t} (2l+1)A_{nl} + (l+1)A_{n,l+1} + l \cdot A_{n,l-1} = \frac{\delta_{nl}}{C/\Sigma_t} \text{ when } B = iC \text{ and } C \text{ is real,} \quad (15)$$

$$\frac{1}{C/\Sigma_t} (2l+1)A_{nl} - (l+1)A_{n,l+1} - l \cdot A_{n,l-1} = \frac{\delta_{nl}}{C/\Sigma_t} \text{ when } B = -iC \text{ and } C \text{ is real.} \quad (16)$$

where  $\delta_{nl}$  is the Kronecker delta.

Now, all of the  $\Phi_n$  in Equation (7) are a real quantity.  $l$  is the limit for the Legendre expansion of the differential scattering cross section; the expansion is truncated at  $l + 1$ . However,  $l$  does not determine the order of the  $B_N$  equations. The integral in Equation (7) may be solved to any order  $n$  independent of the value of  $l$ . As  $n$  is increased beyond  $l$ , no particular advantage is gained in a spectrum code like COMBINE because the ultimate purpose of the solution fluxes is to collapse the cross sections to a few group libraries for spatial transport codes. For  $n > l$  there are no cross sections in the library because the elastic scattering matrix was truncated at  $l + 1$ . Therefore, there is no reason to include higher order fluxes than  $n = 3$  in the  $B_3$  solution. The same argument pertains to the  $B_1$  approximation; in this case  $n$  is truncated at 1.

The coefficients,  $A_{nl}$ , will become a function of  $\alpha = B/\Sigma_t$  and  $A_{00} = \beta = \frac{\tan^{-1} \alpha}{\alpha}$  when  $B$  is real or  $\alpha = C/\Sigma_t$  and  $A_{00} = \beta = (\tanh^{-1} \alpha) / \alpha$  when  $B = \pm iC$  with a real  $C$ .

### 2.1.1 $B_3$ Approximation

Evaluation of Equation (10) for the  $B_3$  approximation, limiting  $l$  and  $n$  to 3, is straightforward but rather tedious for the higher order coefficients:

$$A_{00} = \beta = \frac{\tan^{-1} \alpha}{\alpha}$$

$$A_{01} = -\frac{1-\beta}{\alpha}$$

$$A_{02} = -\frac{3}{2} \frac{(1-\beta)}{\alpha^2} + \frac{\beta}{2}$$

$$A_{11} = -\frac{1-\beta}{\alpha^2}$$

$$A_{12} = -\frac{3}{2} \frac{(1-\beta)}{\alpha^3} - \frac{\beta}{2\alpha}$$

$$A_{22} = \frac{1}{4\alpha} \left[ \left( \frac{9}{\alpha^3} + \frac{6}{\alpha} + \alpha \right) \beta - \frac{3}{\alpha} - \frac{9}{\alpha^3} \right]$$

$$\begin{aligned}
A_{03} &= \frac{1}{2\alpha} \left[ \left( \frac{5}{\alpha^2} + 3 \right) \beta - \frac{4}{3} - \frac{5}{\alpha^2} \right] \\
A_{13} &= \frac{1}{2\alpha^2} \left[ \left( \frac{5}{\alpha^2} + 3 \right) \beta - \frac{4}{3} - \frac{5}{\alpha^2} \right] \\
A_{23} &= -\frac{1}{4\alpha} \left[ \frac{15}{\alpha^4} + \frac{9}{\alpha^2} + \frac{4}{3} - \left( \frac{15}{\alpha^4} + \frac{14}{\alpha^2} + 3 \right) \beta \right] \\
A_{33} &= -\frac{1}{4\alpha^2} \left[ \frac{25}{\alpha^4} + \frac{65}{3\alpha^2} + 4 - \left( \frac{25}{\alpha^4} + \frac{30}{\alpha^2} + 9 \right) \beta \right].
\end{aligned} \tag{17}$$

Evaluation of Equation (11) with  $B = iC$  results in

$$\begin{aligned}
A_{00} &= \beta = \frac{\tanh^{-1} \alpha}{\alpha} \\
A_{01} &= \frac{1 - \beta}{\alpha} \\
A_{02} &= -\frac{3(1 - \beta)}{2} - \frac{\beta}{\alpha^2} \\
A_{11} &= -\frac{1 - \beta}{\alpha^2} \\
A_{12} &= \frac{3(1 - \beta)}{2} + \frac{\beta}{2\alpha} \\
A_{22} &= \frac{1}{4\alpha} \left[ \left( \frac{9}{\alpha^3} - \frac{6}{\alpha} + \alpha \right) \beta + \frac{3}{\alpha} - \frac{9}{\alpha^3} \right] \\
A_{03} &= -\frac{1}{2\alpha} \left[ \left( \frac{5}{\alpha^2} - 3 \right) \beta + \frac{4}{3} - \frac{5}{\alpha^2} \right] \\
A_{13} &= \frac{1}{2\alpha^2} \left[ \left( \frac{5}{\alpha^2} - 3 \right) \beta + \frac{4}{3} - \frac{5}{\alpha^2} \right] \\
A_{23} &= \frac{1}{4\alpha} \left[ \frac{15}{\alpha^4} - \frac{9}{\alpha^2} + \frac{4}{3} - \left( \frac{15}{\alpha^4} - \frac{14}{\alpha^2} + 3 \right) \beta \right] \\
A_{33} &= -\frac{1}{4\alpha^2} \left[ \frac{25}{\alpha^4} - \frac{65}{3\alpha^2} + 4 - \left( \frac{25}{\alpha^4} - \frac{30}{\alpha^2} + 9 \right) \beta \right].
\end{aligned} \tag{18}$$

Evaluation of Equation (11) with  $B = -iC$  results in

$$\begin{aligned}
A_{00} &= \beta = \frac{\tanh^{-1} \alpha}{\alpha} \\
A_{01} &= \frac{\beta - 1}{\alpha} \\
A_{02} &= -\frac{3(1-\beta)}{2} \frac{\beta}{\alpha^2} - \frac{\beta}{2} \\
A_{11} &= \frac{\beta - 1}{\alpha^2} \\
A_{12} &= \frac{3(\beta - 1)}{2} \frac{\beta}{\alpha^3} - \frac{\beta}{2\alpha} \\
A_{22} &= \frac{1}{4\alpha} \left[ \left( \frac{9}{\alpha^3} - \frac{6}{\alpha} + \alpha \right) \beta + \frac{3}{\alpha} - \frac{9}{\alpha^3} \right] \\
A_{03} &= -\frac{1}{2\alpha} \left[ \left( \frac{5}{\alpha^2} - 3 \right) \beta - \frac{4}{3} + \frac{5}{\alpha^2} \right] \\
A_{13} &= \frac{1}{2\alpha^2} \left[ \left( \frac{5}{\alpha^2} - 3 \right) \beta + \frac{4}{3} - \frac{5}{\alpha^2} \right] \\
A_{23} &= \frac{1}{4\alpha} \left[ -\frac{15}{\alpha^4} + \frac{9}{\alpha^2} - \frac{4}{3} + \left( \frac{15}{\alpha^4} - \frac{14}{\alpha^2} + 3 \right) \beta \right] \\
A_{33} &= -\frac{1}{4\alpha^2} \left[ \frac{25}{\alpha^4} - \frac{65}{3\alpha^2} + 4 - \left( \frac{25}{\alpha^4} - \frac{30}{\alpha^2} + 9 \right) \beta \right]. \tag{19}
\end{aligned}$$

Thus, using the coefficients defined by Equations (17), (18), and (19), Equation (7) defines the  $B_3$  fluxes, which are all real. When the square root of the buckling ( $B$ ) is real, the spatial distribution is of cosine( $Bx$ ), where  $B^2$  is the geometric buckling of the fundamental mode of the critical homogeneous geometry. When  $B = iC$  with a real constant  $C$ , the spatial distribution is of positive exponential form with the negative buckling. In this case, there is a neutron leakage into the region, i.e., a negative leakage, which might be useful under certain circumstances. When  $B = -iC$  with a real constant  $C$ , the spatial distribution is of negative exponential form with the negative buckling and the solution would behave like the case with the positive buckling. In the COMBINE7.1 coding, the series expansions of  $\tan^{-1} \alpha$  and  $\tanh^{-1} \alpha$  are utilized to calculate these coefficients. The fundamental limitation of the cases with the negative buckling is in the fact that solutions involve a hyperbolic tangent,  $\tanh^{-1}(B/\Sigma_t)$ . As can be seen in

$\tanh^{-1}(B/\Sigma_t) = \frac{1}{2} \log \left[ (1 + B/\Sigma_t) / (1 - B/\Sigma_t) \right]$ ,  $B/\Sigma_t$  should be less than 1. Normally,  $B/\Sigma_t$  is much less than 1; however, it can be reset to a value less than 1 (0.8, e.g.) to avoid divergence when it is large.

The energy dependence of Equation (7) is approximated by a 167 fine group representation, spanning the energy range from 20 MeV to 1.0E-5 eV, for solution of the neutron spectrum. Integrating Equation (7) over the group energy interval, i.e.,  $E_g \leq E \leq E_{g-1}$  and truncating to L+1 terms generates

$$\begin{aligned} & \phi_n^g \\ &= \sum_{l=0}^L (2l+1) \frac{A_{nl}^g}{\Sigma_t^g} \sum_{s=l}^G \sum_{s'l \rightarrow g} \phi_l^{s'} \frac{\Delta g'}{\Delta g} + \frac{A_{n0}^g}{\Sigma_t^g} \frac{\chi^g}{\Delta g} \end{aligned} \quad (20)$$

where

$$\phi_n^g = \int_{E_g}^{E_{g-1}} \phi_n(E) \frac{dE}{E} / \Delta g$$

$$\Delta g = \int_{E_g}^{E_{g-1}} \frac{dE}{E}.$$

The maximum group number is designated as G in Equation (20). It is noted that the fluxes are now expressed as per-unit energy in lethargy coordinates. Equation (20) includes neutrons scattered down from all higher energy groups. It also includes neutrons scattered up from all lower energy groups if thermal upscattering occurs.

The  $B_3$  solution to Equation (20) is given by the following matrix equation for each energy group g:

$$\left[ I - C_g \right] \Phi_g = R_g \quad (21)$$

$$\Phi_g = \left[ \Phi_0^g, \Phi_1^g, \Phi_2^g, \Phi_3^g \right] \quad (22)$$

$$C_{nl}^g = (2l+1) \frac{A_{nl}^g}{\Sigma_t^g} \sum_{s'l}^{g \rightarrow g} : \quad (23)$$

where I is the four-rowed unit matrix,  $C_g$  is the matrix with 4 rows and 4 columns, and  $n, l$  are the row and column index, respectively, for  $C_g$  in Equation (21).

$$R_n^g = \frac{A_{n0}^g}{\Sigma_t^g} \frac{\chi^g}{\Delta g} + \sum_{l=0}^3 (2l+1) \frac{A_{nl}^g}{\Sigma_t^g} \sum_{s'=1, s' \neq g}^G \sum_{s'l}^{s' \rightarrow g} \Phi_l^{s'} \frac{\Delta g'}{\Delta g} \quad (24)$$

$$R_g = \left[ R_0^g, R_1^g, R_2^g, R_3^g \right]. \quad (25)$$

When there is no thermal upscattering, Equation (21) is solved by Gauss elimination, sweeping from the highest energy to the lowest energy. When the thermal upscattering is present, it is solved by the combination of Gauss elimination and Gauss-Seidel iterative scheme. In this case, the thermal upscattering terms will be included, initially using assumed flux guess.

The fission source,  $\chi$ , can be chosen from a fissile/fissionable isotope or calculated from the steady-state and fission rate weighted source spectrum. The steady-state fission spectrum for an isotope,  $i$ , is defined by

$$\chi_{i,g}^{SS} = \frac{\sum_{g'} \sigma_{f,g' \rightarrow g} \Phi_{g'} + \chi_g^D \sum_{g'} \nu_{g'}^D \sigma_{f,g'} \Phi_{g'}}{\sum_g \sum_{g'} \sigma_{f,g' \rightarrow g} \Phi_{g'} + \sum_g \chi_g^D \sum_{g'} \nu_{g'}^D \sigma_{f,g'} \Phi_{g'}}. \quad (26)$$

The fission rate weighted spectrum is then

$$\chi_g = \frac{\sum_i \chi_{i,g}^{SS} \sum_{g'} \nu_{tot,g'}^i N_i \sigma_{f,g}^i \Phi_{g'}}{\sum_i \sum_{g'} \nu_{tot,g'}^i N_i \sigma_{f,g'}^i \Phi_{g'}}. \quad (27)$$

The flux as defined in Equation (41) and included in the cross section library is initially used in Equation (27) and then the  $B_N$  spectrum calculated flux when once more spectrum calculation is performed.

### 2.1.2 $B_1$ Approximation

The  $B_1$  equations can be the degenerate forms of  $B_3$ . Instead,  $B_1$  equations with real  $B$ , for instance, are derived from Equation (7), emphasizing the physical approximations

$$\begin{aligned} \phi_0(B, E) &= \frac{\beta}{\Sigma_t(E)} \int_{T_{S0}} (E' \rightarrow E) \phi_0(B, E) dE' + 3 \frac{(\beta-1)}{\alpha \Sigma_t} \int_{T_{S1}} (E' \rightarrow E) \phi_1(B, E) dE' + \frac{\beta}{\Sigma_t} \chi(E) \end{aligned} \quad (28)$$

$$\begin{aligned} \phi_1(B, E) &= -\frac{(\beta-1)}{\alpha \Sigma_t(E)} \int_{\Sigma_{S0}} (E' \rightarrow E) \phi_0(B, E) dE' + 3 \frac{(1-\beta)}{\alpha^2 \Sigma_t(E)} \int_{\Sigma_{S1}} (E' \rightarrow E) \phi_1(B, E) dE' - \frac{(\beta-1)}{\alpha \Sigma_t(E)} \chi(E). \end{aligned} \quad (29)$$

Solve Equations (28) and (29) for  $\phi_0$  and  $\phi_1$  to obtain

$$B \Phi_1 + \Sigma_t \Phi_0 = \int_{E'} \Sigma_{S0}(E' \rightarrow E) \Phi_0(E') dE' + \chi(E), \quad (30)$$

$$\gamma(E) \Sigma_t(E) \Phi_1(E) - \frac{B}{3} \Phi_0(E) = \int_{E'} \Sigma_{S1}(E' \rightarrow E) \Phi_1(E') dE' \quad (31)$$

where

$$\gamma(E) = \frac{1}{3} \frac{\beta \alpha^2}{(1-\beta)}.$$

$\Phi_0(E)$  and  $\Phi_1(E)$  are interpreted as the energy-dependent flux and current, respectively. By examining Equations (30) and (31), it is seen that the  $B_1$  approximation differs from the  $P_1$  approximation by the factor  $\gamma(E)$  in Equation (31). If  $\gamma(E)$  is set to equal to 1.0, Equations (30) and (31) become the continuity

equations for the  $P_1$  approximation. The factor  $\gamma(E)$  tends to improve the  $B_1$  estimation of the energy-dependent transport current,  $\Phi_1(E)$  for small homogeneous system.<sup>17</sup>

Similarly, for  $B = -iC$

$$-C\Phi_1 + \Sigma_t\Phi_0 = \int_{E'} \Sigma_{s0}(E' \rightarrow E)\Phi_0(E')dE' + \chi(E), \quad (32)$$

$$-\gamma(E)\Sigma_t(E)\Phi_1(E) - \frac{C}{3}\Phi_0(E) = \int_{E'} \Sigma_{s1}(E' \rightarrow E)\Phi_1(E')dE'. \quad (33)$$

For  $B = iC$

$$C\Phi_1 + \Sigma_t\Phi_0 = \int_{E'} \Sigma_{s0}(E' \rightarrow E)\Phi_0(E')dE' + \chi(E), \quad (34)$$

$$-\gamma(E)\Sigma_t(E)\Phi_1(E) + \frac{C}{3}\Phi_0(E) = \int_{E'} \Sigma_{s1}(E' \rightarrow E)\Phi_1(E')dE'. \quad (35)$$

Equations (30) and (31) in multigroup form reduce to

$$B\Phi_1^g + \Sigma_t^g\Phi_0^g = \sum_{g'=1}^G \Sigma_{s0}^{g' \rightarrow g}\Phi_0^{g'} \frac{\Delta g'}{\Delta g} + \frac{\chi^g}{\Delta g} \quad (36)$$

and

$$\gamma^g \Sigma_t^g \Phi_1^g - \frac{B}{3}\Phi_0^g = \sum_{g'=1}^G \Sigma_{s1}^{g' \rightarrow g}\Phi_1^{g'} \frac{\Delta g'}{\Delta g}. \quad (37)$$

Equations similar to (36) and (37) are derived for imaginary  $B$  from Equations (32) through (35) with variations of sign. These equations are solved simultaneously as

$$\Phi_0^g = \frac{R_0^g (\gamma^g \Sigma_t^g - \Sigma_{s1}^{g \rightarrow g}) - BR_1^g}{(\Sigma_t^g - \Sigma_{s0}^{g \rightarrow g}) (\gamma^g \Sigma_t^g - \Sigma_{s1}^{g \rightarrow g}) + \frac{B^2}{3}} \quad (38)$$

$$\Phi_1^g = \frac{R_1^g + \frac{B}{3}\Phi_0^g}{\gamma^g \Sigma_t^g - \Sigma_{s1}^{g \rightarrow g}} \quad (39)$$

where

$$R_0^g = \sum_{g'=1, g' \neq g}^G \Sigma_{s0}^{g' \rightarrow g}\Phi_0^{g'} \frac{\Delta g'}{\Delta g} + \frac{\chi^g}{\Delta g} \quad \text{and} \quad R_1^g = \sum_{g'=1, g' \neq g}^G \Sigma_{s1}^{g' \rightarrow g}\Phi_1^{g'} \frac{\Delta g'}{\Delta g}.$$

When upscattering is present, Gauss-Seidel iterative scheme is used.

### 2.1.3 Convergence on Gauss-Seidel Iterative Scheme

The calculation will be converged when the following equations are satisfied at all energy points:

$$\left| \frac{\phi_i^{(m+1)} - \phi_i^{(m)}}{\phi_i^{(m+1)}} \right| < \varepsilon \text{ and } \left| \frac{J_i^{(m+1)} - J_i^{(m)}}{J_i^{(m+1)}} \right| < \varepsilon,$$

where  $\varepsilon$  is the user input convergence criteria. The results are then normalized to have one total scalar flux.

## 2.2 Bondarenko Method

The multigroup approximation requires that the groupwise cross sections and energy texture be necessarily coarse with respect to the resonance structure in many materials. The resonance results in self-shielding effect. The magnitude of this self-shielding effect is in general a complicated function of the geometry and composition of the system. However, it has been found that a simple model called the Bondarenko Method<sup>8</sup> or Background Cross Section Method<sup>18</sup> does a surprisingly good job of representing the effects for many applications.<sup>9</sup> This method was adopted in the NJOY's GROUPT and MATXS modules and the TRANSX code.<sup>10</sup> COMBINE7.1 followed those steps taken in the NJOY and TRANSX codes. The flux is assumed to vary inversely as the total macroscopic cross section. In the Bondarenko model, the NR approximation and the  $B_N$  approximation for large systems are invoked.<sup>9</sup> The model flux for the group averages for isotope  $i$  is written as

$$\Phi_i^l(E) = \frac{C(E)}{[\sigma_0^i + \sigma_i^l(E)]^{l+1}} \quad (40)$$

where  $C(E)$  is the smooth part of the shape of the flux,  $\sigma_i^l(E)$  is the microscopic total cross section for isotope  $i$ , and  $\sigma_0^i$  is called the background cross section (it represents the effects of all the other isotopes). The effect of the total cross section in the denominator is to put a dip in the flux for each peak in the cross section, and  $\sigma_0^i$  controls the relative size of the dip. A resonance material in a dilute mixture or in small pieces does not disturb a smooth flux very much by its presence—this is called the infinitely dilute case. When  $\sigma_0^i$  approaches a very large number, it becomes an infinitely dilute case. The  $l$  dependence shown here is appropriate for a large system with nearly isotropic scattering (the  $B_0$  approximation), and it was used when the MATXS file was generated from NJOY.

The multigroup form of this model flux is

$$\Phi_{lg}^i = \frac{C_g}{[\sigma_{0,g}^i + \sigma_{t,g}^i]^{l+1}}. \quad (41)$$

The resonance absorption changes with the temperature because of Doppler broadening of the resonances. In order to take into account the effect of Doppler broadening, the basic cross sections in the resonance region must be adjusted appropriately for the broadening before they are used in computing group constants.

The Bondarenko method is basically an “infinite medium” method that parameterizes cross sections for a nuclide as a function of temperature,  $T$ , and the “background dilution” cross section,  $\sigma_0$ , of all other nuclides mixed with the nuclide. Simplistically, given the temperature and background dilution cross-section values, self-shielded cross sections are determined by interpolating in tables. Since self

shielding causes the background dilution values that a nuclide sets to change, an iterative procedure involving all nuclides is used. The geometric lump effect, when present, is accounted for by augmenting the background cross section.

For a homogeneous mixture, the appropriate background cross section is

$$\sigma_{0,g}^i = \frac{1}{N_i} \cdot \sum_{j \neq i} N_j \cdot \sigma_{t,g}^j(\sigma_{0,g}^i) \quad (42)$$

where  $N$  is the number density for the isotope and  $\sigma_{t,g}$  is the self-shielded total cross section of an energy group  $g$ . Because  $\sigma_{t,g}$  depends on  $\sigma_{0,g}$ , finding  $\sigma_{0,g}$  is an iterative process. For a mixture of resonance materials, interference between resonances in different materials is handled in an average sense only.

For a lump of resonance material embedded in a large moderating region, escapes from the lump also increase the background cross section. To account for this, the  $\sigma_{0,g}$  value is augmented by an escape cross section

$$\sigma_{e,g}^i = \frac{1}{N_i \bar{l}} \quad (43)$$

where  $\bar{l}$  is the mean chord length of lump given by

$$\bar{l} = \frac{4V}{S} \quad (44)$$

and where  $V$  and  $S$  are the volume and surface area of the lump. Multizone situations, such as reactor lattices, are accounted for by the use of Dancoff factor  $C$ , which, in effect, modify the escape probability and, hence, the value of  $\sigma_e$ . The mean chord length  $\bar{l}$  can be adjusted away from the geometric value of Equation (44) to compensate for the presence of other lumps (Dancoff correction) or for shortcoming in the escape probability model used to obtain Equation (43). In the rational approximation, the Dancoff correction is equivalent to increasing the mean chord length,  $\bar{l}$ , by the factor  $1/(1-C)$  or equivalently decreasing the surface area of lump by  $1-C$  as in

$$\sigma_{e,g}^i = \frac{1}{N_i \cdot \bar{l} \cdot \frac{1}{(1-C)}} \quad (45)$$

when Bell corrections are applied

$$\sigma_{e,g}^i = \frac{1}{N_i \cdot \bar{l}} \cdot \frac{b_1 \cdot (1-C)}{1 + (b_2 - 1) \cdot C} \quad (46)$$

where  $b_1$  and  $b_2$  are called Bell corrections. When  $b_1 = b_2$ , the constant is usually called the Levine factor and Equation (46) becomes

$$\sigma_{e,g}^i = \frac{1}{N_i \cdot \bar{l}} \cdot \frac{1}{\frac{1}{b} + \frac{C}{1-C}} \quad (47)$$

where

- $b = 1.26$  for the slab geometry
- $= 1.35$  for the cylindrical geometry
- $= 1.30$  for the spherical geometry.

The so-called Levine factors,  $b$ , are approximate geometry dependent factors that are approximately correct for inaccuracies in the Rational Approximation.

When a double heterogeneity occurs because of fuel grains present within the macroscopic fuel lump, the Dancoff factor  $C$  specifies the mutual shielding between these grains, independent of  $C$  for the lumps themselves. To better account for the double heterogeneity because of fuel grains present within the macroscopic fuel lump, a correction has been made to the escape probability and given by Stamatelatos and LaBauve<sup>19</sup> as

$$\sigma_{e,g}^i = \frac{1}{N_i \left[ \bar{l} \cdot \left( \frac{1}{b} + \frac{C}{1-C} \right) + \bar{l}_g \left( \frac{1}{a} + \frac{C'}{1-C'} \right) \right]} \quad (48)$$

where

$\bar{l}_g$  = the average chord length of a single isolated spherical fuel grain

$C'$  = the Dancoff factor for fuel grains

$a = 1.77$ , the Levine factor for spherical grains.

However, because of the inadequacy of the above applications, the escape probability in COMBINE7.1 is recast as

$$\sigma_{e,g}^i = \left[ N_i \cdot \bar{l} \cdot \left( b + \frac{C}{1-C} \right) \right]^{-1} \quad (49)$$

where  $b$  is a modified inverse Levine factor as a function of a single Dancoff factor  $C$  as shown in Figure 2.

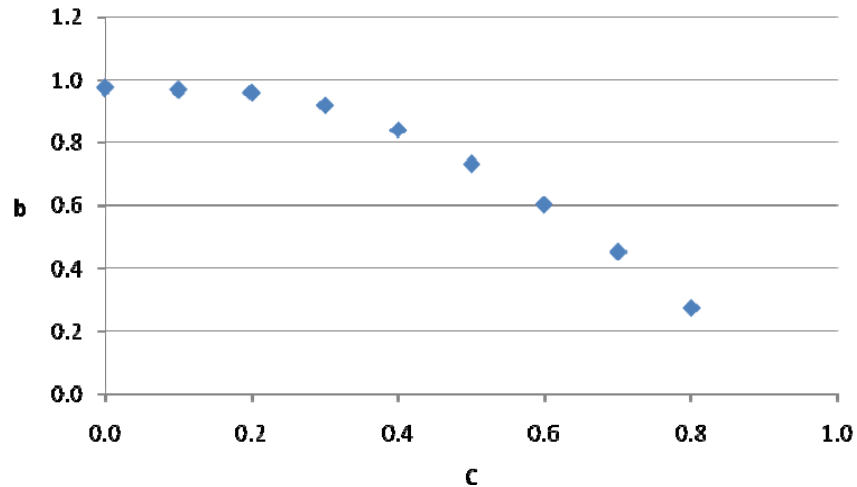


Figure 2. Modified inverse Levine factor as a function of Dancoff factor.

For the grain fuel, the mean chord length is based on the grain and the double heterogeneity effect is inclusive in this single Dancoff factor. The modified inverse Levine factor and some minor adjustment are derived empirically based on the more accurate Nordheim or Monte Carlo Neutral Particle (MCNP) calculations.

Finally, the following equation for the background cross section has been applied for cross-section interpolation

$$\sigma_{0,g}^i = \sigma_{e,g}^i + \frac{\sum_{i \neq j} N_j \cdot \sigma_{i,g}^j(\sigma_{0,g}^j)}{N_i} \quad (50)$$

### 2.2.1 Fine-Group Cross Section Generation in Bondarenko Format

In COMBINE7.1, a 167 fine group structure is used and the multigroup cross section constants are generated in this fine group structure to be used in the  $B_N$  solution.

The NJOY99.336 version<sup>16</sup> was used to generate a 167 fine-group cross-section library, MATXS.LIB, in MATXS format (Bondarenko format) on sets of background cross sections and temperatures including thermal scattering cross sections. For  $C(E)$  in Equation (40), an NJOY built-in spectrum, Thermal--1/E--Fast Reactor--Fission + Fusion, is used. The equations providing the fundamental definitions in NJOY for the multigroup cross sections and the group-to-group matrix are

$$\sigma_{t,l,g} = \frac{\int_g \sigma_t(E) \phi_l(E) dE}{\int_g \phi_l(E) dE}, \quad (51)$$

$$\sigma_{x,g} = \frac{\int_g \sigma_x(E) \phi_0(E) dE}{\int_g \phi_0(E) dE}, \quad (52)$$

$$\sigma_{X,l,g' \rightarrow g} = \frac{\int_g dE \int_{g'} dE' \sigma_{Xl}(E' \rightarrow E) \phi_l(E)}{\int_g \phi_l(E) dE}. \quad (53)$$

The energy-dependent cross-section database is now derived entirely from ENDF/B-VII.0 nuclear data with the exception of zirconium element cross-section data, which is based on ENF/B-VI.8 nuclear data, and Th-231, which is based on the JENDL-4.0. All materials have either S( $\alpha,\beta$ ) or free thermal scattering matrices.

During the course of COMBINE7.1 development, it was found that using the strictly Bondarenko-based U-238 cross sections caused problems against the benchmark experiments and against some equivalent MCNP calculations, occurring mostly for the intermediate spectrum cases. The problem is believed to be primarily because of the limited number of energy groups around the U-238 resonances. Some adjustments, based on the more accurate Nordheim self-shielding treatments and the MCNP results, were made to the U-238 cross sections in MATXS.LIB for the major resolved resonances and also some minor corrections were made in the program through background cross section interpolation.

With the modified inverse Levine factor, U-238 cross section adjustments, and some minor background cross section modifications, the results with the Bondarenko self-shielding approximations became consistent against the Nordheim self-shielding treatment or MCNP results. Increasing the number

of fine groups in the resolved resonance energy range at the expense of more computer time may make these adjustments unnecessary but is subject to a further study.

## 2.2.2 Bondarenko Self-Shielding Interpolation

Bondarenko self-shielding is performed in COMBINE7.1 by background cross section and temperature interpolation. The interpolation is first performed for the background cross sections at each temperature. The generated cross sections for the set of preselected temperatures are then interpolated for the problem-dependent temperature. In the background cross-section interpolation, a log-log  $N^{\text{th}}$  order for the vector cross sections, and log-linear  $N^{\text{th}}$  order Lagrangean schemes are employed with a variation to the first order for the extremely high or low problem-dependent background cross section. The temperature interpolation uses a log-log  $N^{\text{th}}$  order Lagrangean scheme. Iteration is necessary to arrive at the correct background cross sections. Six iterations are performed for all isotopes. The first iteration is based on the infinite dilution of the rest isotopes for total cross sections. The accuracy, convergence, and stability of these schemes have been sufficiently tested and are satisfactory.

## 2.3 Resonance Region

The material cross-section libraries supplied for each material have complete multigroup cross sections based on Bondarenko method. The weakness of the Bondarenko model occurs for thermal reactor analysis in the “epithermal” energy region from about 4 eV to around 200 or 300 eV.<sup>10</sup> In this region, the resonances are no longer narrow, and the flux shape given by Equation (40) is no longer sufficiently accurate. For those materials where resolved resonance parameters are present via RERES.LIB, a Nordheim numerical solution<sup>11</sup> is applied as an option. Before  $B_1$  or  $B_3$  Equations are solved, the resonance parameters in the material libraries must be converted into average, self-shielded, temperature dependent, groupwise cross sections.

### 2.3.1 Resolved Resonances—Nordheim Numerical Method

The balance equation for the collision density in a homogeneous mixture of moderators and resonance absorbers in an infinite medium is<sup>20</sup>

$$F(E) = \phi(E) \Sigma_t(E) = \sum_k \int_E^{E/\alpha_k} \frac{\phi(E') \Sigma_s^k(E') dE'}{(1 - \alpha_k)E'} \quad (54)$$

where

$\phi(E)$  = scalar neutron flux

$\Sigma_t$  = total macroscopic cross section

$\Sigma_s^k$  =  $N_k \sigma_{sk}$  = macroscopic scattering cross section for material k

$N_k$  = atomic density of material k

$\sigma_k$  = microscopic cross section of material k

$\alpha_k$  =  $\left( \frac{A_k - 1}{A_k + 1} \right)^2$ ,  $A_k$  = ratio of isotopic mass to mass of the neutron for material k

$F(E)$  = collision density at energy E.

The right-hand side of Equation (54) requires a different integration limit for each moderator  $k$ . The flux  $\phi(E)$  at each resolved resonance undergoes a severe depression at each strongly absorbing resonance. One or many resonances may fall within any given COMBINE multigroup. The average, self-shielded, capture integral in each multigroup  $g$  within the resonance range is then given by

$$I_{cg}^k = \int_{E_g}^{E_{g+1}} \phi(E) \sigma_c^k(E) dE \quad (55)$$

where  $\phi(E)$  is the solution of Equation (54) over the energy interval for the multigroup and  $\sigma_c$  is the capture cross section. Equation (54) is solved in lethargy space where

$$du = -\frac{dE}{E}$$

$$dE = -E du$$

$$E = E_1 e^{-u}$$

Therefore,  $dE = E_1 e^{-u} du$ .

Equation (55) is transformed to<sup>11</sup>

$$I_{cg}^k = E_1 \int_{u_{g-1}}^{u_g} \phi[E(u)] \sigma_c^k[E(u)] e^{-u} du$$

$$I_{cg}^k = E_1 \int_{u_{g-1}}^{u_g} F[u(E)] \frac{\sigma_c^k(u) e^{-u}}{\Sigma_t(u)} du \quad (56)$$

where  $F[u(E)]$  is the collision density per unit energy in lethargy coordinates. The mixed lethargy-energy form of Equation (56) results from the fact that the integration is performed on a lethargy mesh, but the resonance cross sections are calculated in energy space because the cross sections are not easily transformed to lethargy coordinates. Equations similar to Equation (56) may be written for the fission and elastic scattering integrals using  $\sigma_f^k(u)$  or  $\sigma_s^k(u)$  in place of  $\sigma_c^k(u)$ .

If absorption occurs in an isolated lump surrounded by an infinite sea of moderators, the introduction of the lump escape probability<sup>21</sup>  $P_0(\bar{l}, \Sigma_t)$ , is given in terms of the average chord length of the lump,  $\bar{l}$ . This enables Equation (54) to be modified to closely approximate the heterogeneous absorption rate in the lump-moderator assembly. The collision density in the lump now consists of two distinct types of events:

1. Those neutrons that have had their last collision in the lump, which is given by the right-hand side of Equation (54) multiplied by the probability of colliding in the lump,  $[1 - P_0(\bar{l}, \Sigma_t)]$ , times  $V_F$ , the volume of the fuel lump.
2. Those neutrons that stream into the lump at lethargy  $u(E)$  from outside the lump, multiplied by the moderator escape probability<sup>21</sup>  $P_M(\bar{l}, \Sigma_t)$ , times the volume of the external moderator,  $V_M$ , contained in a unit cell.

$$V_F F(u) = V_F \left[ 1 - P_0(\bar{l}, \Sigma_t) \right] \sum_k \frac{1}{1 - \alpha_k} \int_{u - \epsilon_k}^u F(u') \frac{\Sigma_s^k(u')}{\Sigma_t(u')} du' + V_M P_M \phi_M(u) \Sigma_M(u) \quad (57)$$

where

$$\varepsilon_k = 1/n \left( \frac{1}{\alpha_k} \right)$$

and  $\phi_M(u)$  is the average, asymptotic, equilibrium neutron flux in the moderator residing outside the lump. The normalization of Equation (57) is arbitrary, since the point wise collision density  $F(u)$  will only be used to obtain average cross sections over the multigroups in the resolved resonance range.

$\phi[u(E)]$  is set equal to  $1/E$  in the region outside the lump, i.e.,  $\phi_{asym}[u(E)] = e^u / E_1$ .

The moderator terms in Equation (57) may be removed by means of the reciprocity relation<sup>9</sup>

$$P_M V_M \Sigma_M = P_F V_F \Sigma_{tF} \quad (58)$$

Equation (57) then becomes

$$F(u) = (1 - P_0) \sum_{k=1}^7 \frac{1}{1 - \alpha_k} \int_{u-\varepsilon_k}^u F(u') \frac{\sigma_s^k(u')}{\sigma_t(u')} du' + P_0 \sigma_t(u) \frac{e^u}{E_1} \quad (59)$$

where  $\sigma_s^k$  and  $\sigma_t$  are given by Equations (62) and (63), expressed in terms of the scattering per absorber atom.

$$P_0 = P_0(\bar{l}, \Sigma_t) \quad (60)$$

where

$$\bar{l} = \bar{l}_0 = \frac{4V}{S}, \text{ single isolated lump}$$

$$\begin{aligned} \frac{V}{S} &= \text{ratio of volume of the absorber lump to the surface area} \\ &= 1/2 \times \text{half thickness—plate geometry} \\ &= 1/2 \times \text{radius—cylindrical geometry} \\ &= 1/3 \times \text{radius—spherical geometry} \end{aligned}$$

The escape probability  $P_0$  is tabulated<sup>11</sup> for single isolated lumps. When a Dancoff factor  $C$  is incorporated to represent the mutual shielding in a repetitive array,<sup>22</sup> the escape probability  $P_0$  is modified to be<sup>11,23</sup>

$$P = \frac{P_0(1-C)}{\left[ 1 - (1 - \bar{l} \Sigma_t P_0) C \right]} \quad (61)$$

where  $P_0$  in Equation (60) is the escape probability for a single isolated lump,  $P$  represents the mutually shielded value,  $C$  is the Dancoff Ginsberg correction factor for a regular array of lumps. For the grain fuel, the mean chord length is based on the grain and the double heterogeneity effect is inclusive in this single Dancoff factor.

In Equation (59), up to seven moderators are included for the down scatter source within the lump, the first always being the absorber atom itself. Three additional moderators and three additional admixed resonance absorbers with different masses can also be included.<sup>3</sup> This limit is felt to be sufficient for almost any fuel pin one would encounter in practice.

The cross sections in Equation (59) are evaluated relative to the number of absorber atoms as in

$$\sigma_s^k = \frac{\sum_s^k}{N_a} \quad (62)$$

where  $N_a$  = atom density of the absorber atom in the lump.

$$\sigma_t = \sigma_a + \sigma_s + \sigma_m^1 + \sigma_m^2 + \sigma_m^3 + \sigma_a^1 + \sigma_s^1 + \sigma_a^2 + \sigma_s^2 + \sigma_a^3 + \sigma_s^3 \quad (63)$$

where:  $\sigma_a$  and  $\sigma_s$  are the absorption and resonance scattering, respectively, of the absorber atom itself;  $\sigma_m^i$  represents the three moderator's scattering cross sections per absorber atom;  $\sigma_a^i$  represents the three admixed absorber's absorption cross sections per absorber atom; and  $\sigma_s^i$  represents the three admixed absorber's scattering cross sections per absorber atom. The absorption cross section of the three additional moderators is assumed to be very small compared with the principal absorber or the admixed absorbers.

Equation (59) has proven itself to be remarkably accurate in many applications. A number of unique approximations are used in deriving Equation (59), the most important of which is the "flat flux assumption."<sup>24</sup> The spatial dependence of the flux across the lump has been subsumed into the escape probability  $P_0$ , which permits the elimination of the spatial dependence of the flux in Equation (59).  $P_0$  is evaluated as a function of energy only. The approximation which makes this possible is that at each energy the escape probability is evaluated as if only the average flat flux in the lump were known relative to the asymptotic flat flux existing outside the lump. The escape probability  $P_0$  under the flat flux approximation is then given by<sup>24</sup>

$$P_0 \approx \frac{\bar{\phi}_{lump}}{\bar{\phi}_{asym}} \quad (64)$$

If an average flat flux can be assumed in the lump, the escape probability absorbs the spatial dependence in Equation (59).  $P_0(\bar{l}, \Sigma_t)$  is evaluated at each energy across the resonance since  $\Sigma_t(E)$  is a strong function of energy at resonance. Equation (64) is a truly remarkable result that makes possible a separate two-stage solution to a difficult problem; the first stage being the calculation of the escape probability  $P_0$ .<sup>11</sup> Equation (59) is solved numerically on a very fine energy mesh across each lethargy group where one or more resonances may reside.

### 2.3.2 Doppler Broadening of Resolved Resonance Parameters

Subroutines adopted from the NJOY code and incorporated in COMBINE7.1 numerically Doppler broaden the SLBW, MLBW, and R-M format resonance parameters by the kernel broadening method.<sup>25</sup> The subroutines were verified by kernel broadening the SLBW option and comparing with that using the  $\psi$ - $\chi$  function that was used in the previous COMBINE versions. At each mesh point the capture, fission, and elastic cross sections are calculated, accumulating contributions from all the resonances in the same resonance range. Figure 3 shows the Doppler broadened cross section as an example.

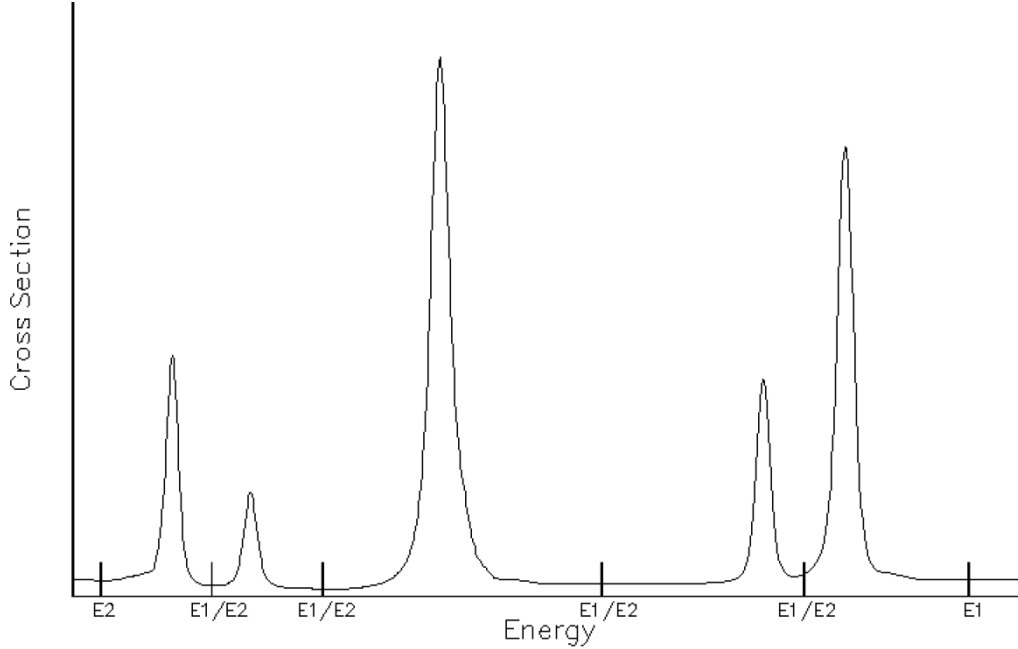


Figure 3. An example of Doppler broadened resonance cross sections.

### 2.3.3 Determination of $E_1/E_2$ and the Number of Meshes for a Resonance

The first energy,  $E_1$ , corresponds to the first fine group energy boundary encountered just below the upper limit of the highest resolved resonance energy range. It can be the user input at any fine group energy boundary lower than that. The next  $E_1$  (or  $E_2$ ) is at the midpoint between the next two neighboring resonances, and so on. The lowest  $E_2$  is also adjusted to correspond to the fine group energy boundary. For each resonance, a resonance integration interval is formed by  $E_1$  and  $E_2$ . Considering an equal lethargy interval solution, a mesh size and the number of mesh intervals within the resonance integration are calculated according to the following recipe, which was adopted from GAM-II code<sup>23</sup> and modified.

$$r = 5.0 + 0.5 \sqrt{K * 273.0 * |E_0| / AWRI / \Gamma} \quad (65)$$

$$\varepsilon = 0.75 / [AWR * \text{int}\{0.5 * r * \sqrt{1.0 / (K * 273.0 * AWRI) * |E_0|} + 1.0\} * \text{fmult}] \quad (66)$$

$$\text{mesh} = \frac{\log(E_1 / E_2)}{\varepsilon} \quad (67)$$

where: mesh is the number of mesh intervals,  $K$  is the Boltzmann constant =  $8.6173 \times 10^{-5}$  eV/K, the constant 273.0 defines the mesh reference temperature  $T_0$ ,  $AWRI$  is the ratio of mass of a particular isotope to that of a neutron,  $\Gamma$  is the total resonance width,  $E_1$  and  $E_2$  are the high and low energy boundaries of the integration for a resonance,  $E_0$  is the resonance energy, and  $\text{fmult}$  is the user input control parameter to make mesh coarse or finer (default= 1.0).

The number of mesh intervals is then made to be an even number so that the total number of mesh points becomes odd for Simpson's integration. The last mesh point of the previous resonance integration interval corresponds to the first mesh point of the present resonance integration interval, and so on. The lethargy mesh is generated independently for each resonance from midpoint to midpoint between resonances; therefore, the mesh spacing from resonance to resonance varies. The highest  $E_1$  and lowest  $E_2$  can be controlled by user input, other than the default values set in "reres.lib" and adjusted to the

group boundaries in the code. The maximum allowable number of mesh intervals in a resonance integration interval is coded to be 1400. When the admixed resonance absorbers are present, the Doppler broadened cross sections are generated over these mesh points.

### 2.3.4 Absorber Narrow Resonance-Moderator Asymptotic Flux Approximation

In the Narrow Resonance (NR) approximation, the resonances are so narrow that all moderators, including the absorber, can scatter past the resonance. The scattering cross section over most of this range is essentially just that for potential scattering  $\sigma_p$ . The integral term in Equation (57) becomes

$$\frac{1}{1-\alpha_k} \int_{u-\varepsilon_k}^u F(u') \frac{\sigma_s^k(u')}{\sigma_t(u')} du' = \frac{\sigma_p^k}{1-\alpha_k} \cdot \int_{u-\varepsilon_k}^u \phi(u') du' = \frac{\sigma_p^k}{1-\alpha} \cdot \int_{u-\varepsilon_k}^u \frac{e^{u'}}{E_1} du' = \sigma_p^k \frac{e^u}{E_1}, \quad (68)$$

when the asymptotic flux,  $\phi_{asym}[u(E)] = e^u / E_1 = w(u)$ , is applied.

The criteria to determine this approximation is when  $\ln(\frac{E_i}{\alpha E_i}) / \varepsilon > 1404$ .

In the thermal energy range,  $E \leq 5kT$ , the flux shape is rather Maxwellian than  $e^u/E_1$ ,<sup>26</sup>

$$\phi_{asym}[u(E)] = 5.936526 / (kT)^2 \cdot E_1 e^{-u} e^{\frac{E_1 e^{-u}}{kT}} = w(u). \quad (69)$$

### 2.3.5 Self-Shielding Elastic Scattering Transfer Matrix

The solution of Equation (20) or (38) and (39) requires the self-shielded resolved resonance contributions to the elastic scatter matrix for the Legendre moments through  $L = 3$  or  $L = 1$ , respectively. Departing from the previous versions, a simple normalization scheme is employed for this, utilizing the already available transfer matrix from Bondarenko self-shielded transfer matrix,

$$\sigma_{s,g' \rightarrow g}^l = (\sigma_{s,g' \rightarrow g}^l)_{Bondarenko} \cdot \frac{(\sigma_{s,g'}^0)_{Nordheim}}{(\sigma_{s,g'}^0)_{Bondarenko}}. \quad (70)$$

### 2.3.6 Numerical Integration with Simpson's Rule

Combining the integral form, absorber NR-moderator asymptotic flux approximation, and the thermal upscattering term, the numerical integration is expressed as

$$F(u) = \left\{ 1 - (1-P(u)) \frac{\varepsilon}{3\sigma_t(u)} \left[ (\delta(N_0) \frac{\sigma_{s0}(u)}{\alpha_0} + \sum_i^3 \delta(N_{a_i}) \frac{\sigma_{sa_i}(u)}{\alpha_{a_i}} + \sum_j^3 \delta(N_{m_j}) \frac{\sigma_{sm_j}(u)}{\alpha_{m_j}}) \right] \right\}^{-1} \cdot \left\{ (1-P(u)) \varepsilon \left[ \frac{\delta(N_0)}{3\alpha_0} \frac{I}{u-n\varepsilon} F(u') \frac{\sigma_{sa}(u')}{\sigma_t(u')} + \sum_i^3 \frac{\delta(N_{a_i})}{3\alpha_{a_i}} \frac{I}{u-n\varepsilon} F(u') \frac{\sigma_{sa_i}(u')}{\sigma_t(u')} + \sum_j^3 \frac{\delta(N_{m_j})}{3\alpha_{a_i}} \frac{I}{u-n\varepsilon} F(u') \frac{\sigma_{sm_j}(u')}{\sigma_t(u')} \right] + \delta(up) \sum_{g'} F_{g'} \frac{\sigma_{sg' \rightarrow g}^{upscat}}{\sigma_{tg'}} \frac{\Delta g'}{\Delta g} \right\} + \left[ (1-P(u)) (\delta(NR) \sigma_{p0} + \sum_i^3 \delta(A_{a_i}) \sigma_{pa_i} + \sum_j^3 \delta(A_{m_j}) \sigma_{pm_j} + P(u) \sigma_t(u) \right] w(u) \quad (71)$$

where  $\delta (N_x)$  means Nordheim integral treatment application for the resonance absorber, admixed resonance absorbers, admixed moderators,  $\delta (NR)$ ,  $\delta (A_a)$ ,  $\delta (A_m)$  means application of absorber NR-moderator asymptotic flux approximation instead of Nordheim integral treatment,  $\delta (up)$  means application of upscattering when thermal upscattering is present

$$\begin{aligned} \int_{u-n\varepsilon}^{u-\varepsilon} F(u') \frac{\sigma_s(u')}{\sigma_t(u')} du' &= 2 \sum_{i=1}^2 (3-i) \sum_{j=1}^{\frac{n-i+1}{2}} F[u-(2j+i-2)\varepsilon] \frac{\sigma_s[u-(2j+i-2)\varepsilon]}{\sigma_t[u-(2j+i-2)\varepsilon]} \\ + F(u-\varepsilon n) \frac{\sigma_s(u-\varepsilon n)}{\sigma_t(u-\varepsilon n)} \end{aligned} \quad (72)$$

is the Simpson's rule integration.

When thermal upscattering is present, iteration is needed. Since the convergence is rapid when the available flux in the code is utilized, only one more iteration is performed.

### 2.3.7 Group Averaging

Two options are available for converting the resonance integrals in Equation (53) into average multigroup cross sections, depending on whether one desires averages over the whole cell or just over the absorber lump. The average cross section is defined by

$$\sigma_{xg} = \frac{E_1 \int_{u_{i-1}}^{u_i} F(u) \frac{\sigma_x(u)}{\sigma_t(u)} e^{-u} du}{E_1 \int_{u_{i-1}}^{u_i} \phi(u) e^{-u} du} \quad (73)$$

where  $\sigma_x$  is the reaction cross section being averaged,  $F(u)$  is given by Equation (59), and  $\sigma_t$  is given by Equation (63). The reaction cross section is averaged over the absorber lump flux (default),

$$\phi(u) = F(u)/\sigma_t(u) = \text{lump flux, or over the cell flux } \phi(u) = \phi_{asym}(u) = \frac{1}{E} = \frac{e^u}{E_1} \approx \text{cell flux.}$$

After obtaining capture/fission and scattering cross sections from Nordheim treatment, these cross sections overwrite the previous Bondarenko based cross sections.

### 2.3.8 Dancoff-Ginsburg Correction Factor Calculation

Computation of the Dancoff Factor C for arbitrary shapes and spacing of lumps is very difficult. An external code like SUPERDAN can provide Dancoff factors.<sup>27</sup> INTRAPEB and PEBDAN codes<sup>36</sup> are developed at INL for estimating the Dancoff factors in Pebble beds. MCNP can also provide Dancoff factors, either by calculating the probability that a neutron leaving a fuel kernel (or lump) enters another kernel without a collision or calculating (1 – probability that a neutron leaving kernel will have a collision in the moderator).

Most accurate determinations have been performed for regular arrays of cylindrical fuel pins. One option in COMBINE is the exact calculation described below. In the event that a precise calculation is not possible because of geometric irregularity or nonavailability, Bell offers an approximate formula based on the most general assumptions, which can be used as a last resort. Bell's formula can be written as<sup>28</sup>

$$C \approx \frac{\lambda_1}{\frac{4V_1}{S_a} + \lambda_1} \quad (74)$$

where

$S_a$  = surface area of the absorbing lump

$V_1$  = the average external moderator volume per absorber lump

$\lambda_1$  = the external moderator mean-free-path in the same units as  $V_1$  and  $S_a$ .

Equation (74) is deceptive in its simplicity, considering the exact definition in Equation (75). It is exact in the limits of very large or very small lumps. The rational approximation for  $P_o$  has been used in deriving Equation (74) along with other assumptions, so it should be used only as a first order approximation when no other method is available. Equation (74) can be used with any regular or irregular geometry and is independent of geometric details other than average values of  $V_1$  and  $S_a$ . A precise calculation of  $C$  for cylindrical pins is included in COMBINE and is described below.

The cylindrical pin Dancoff correction is computed in COMBINE following the methods of Gelling and Sauer.<sup>29</sup> This correction may be calculated for an infinite lattice composed of cylindrical pins in either a rectangle or a hexagon. Pins are assumed to be black to resonance-energy neutrons.

The Dancoff correction is defined as:<sup>24</sup>

$$C = \frac{\int dS \int \vec{n} \cdot \vec{\Omega} \exp[-\Sigma l(\vec{s}, \vec{\Omega})] d\Omega}{\int dS \int \vec{n} \cdot \vec{\Omega} d\Omega} \quad (75)$$

where  $l(\vec{s}, \vec{\Omega})$  is a chord that extends from the lump surface element  $dS$  in the direction  $\vec{\Omega}$  through the moderator to the point of intersection with a neighboring lump.  $\Sigma$  is the cross section for removal of neutrons from the energy range of the resonance and  $\vec{n}$  is the normal to the lump surface element.

In the case of a lattice composed of cylindrical pins, the Dancoff correction may be expressed as

$$C = \frac{4}{\pi} \int_0^{2\pi} \frac{d\rho}{2} \int_{-1}^1 \frac{d\xi}{2} K_{i3}[\Sigma R_0 \cdot S] \quad (76)$$

The parameters are defined in Figure 4, and

$$K_{i3} = \int_0^{\infty} \exp[-x \cosh(u)] \cosh^{-3} u du \quad (77)$$

is the Bickley function of the third order.

The 2-D lattice is represented exactly for a pin surrounded by up to four annular moderating regions and an external moderator. A library of pin configurations is contained within the code. A pin location is specified by the row  $n$  and the column  $m$ , where  $m$  and  $n$  are in units of pitch.

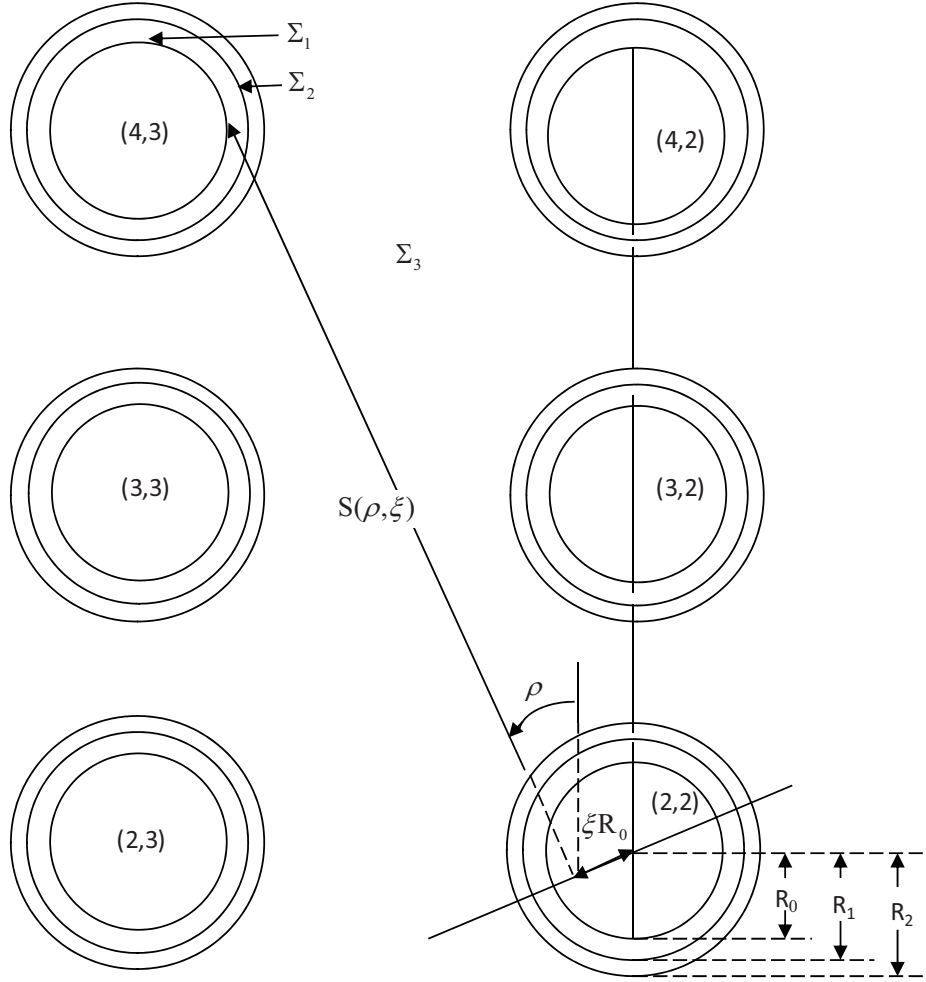


Figure 4. Parameters of the rectangular cell.

Heterogeneity of the moderating region is accounted for by defining the argument of the Bickley function<sup>29</sup> as

$$\sum R_0 \cdot S = R_0 \sum_{i=1}^N \Sigma_i S_i \quad (78)$$

where  $s_i$  is the length of the chord through region  $i$ , having total cross section  $\Sigma_i$ .

The integral in Equation (76) is evaluated using the trapezoidal approximation. Because of symmetry, the upper limit is taken as  $\pi/4$  for a rectangular lattice and  $\pi/6$  for a hexagonal lattice. The integral over  $\rho$  is evaluated by using 20 equal angular intervals, and for each value of  $\rho$  the integral over  $\xi$  is evaluated by using 100 increments of equal length. For each set of  $(\rho, \xi)$  values, the length of the chord  $S_i$  through each region is calculated and the Bickley function is evaluated by the approximation

$$K_{i3}(x) = \frac{e^{-x}}{(0.6366198x + 1.6211389)^{1/2}} \cdot \frac{x^2 + 6.399407x + 5.066719}{x^2 + 6.766116x + 5.066719} \quad (79)$$

This approximation yields values of  $k_{i3}(x)$  to an accuracy of  $\pm 0.05\%$ .

## 2.4 Age Equations

An option to perform an age calculation using a moments method available in the GAM-1 code has been retained in COMBINE. The derivation of this method is described in Reference 14 and has been omitted here. However, the final equations solved for the age are briefly described below. In multigroup form, the  $i$ th group moment equations for  $\phi_{00_i}$ ,  $\phi_{11_i}$ , and  $\phi_{20_i}$  are

$$\sum_{t_i} \phi_{00_i} = \sum_{j=1}^i (\sum_{s_{0_j \rightarrow i}} + \sum_{in_{j \rightarrow i}} + 2\sum_{n,2n_{j \rightarrow i}} + 3\sum_{n,3n_{j \rightarrow i}} + 4\sum_{n,4n_{j \rightarrow i}}) \phi_{00_j} \frac{\Delta_j}{\Delta_i} + S_i \quad (80)$$

$$\sum_{t_i} \phi_{11_i} = \sum_{j=1}^i \sum_{s_{1_j \rightarrow i}} \phi_{11_j} \frac{\Delta_j}{\Delta_i} + \phi_{00_i} \quad (81)$$

$$\sum_{t_i} \phi_{20_i} = \sum_{j=1}^i (\sum_{s_{0_j \rightarrow i}} + \sum_{in_{j \rightarrow i}} + 2\sum_{n,2n_{j \rightarrow i}} + 3\sum_{n,3n_{j \rightarrow i}} + 4\sum_{n,4n_{j \rightarrow i}}) \phi_{20_j} \frac{\Delta_j}{\Delta_i} + \frac{\phi_{11_i}}{3} \quad (82)$$

where all cross section definitions are the same as those described previously for the  $B_1$  solution. Solving each moment equation for the  $i$ th group we have the final solution equations:

$$\phi_{00_i} = \frac{\sum_{j=1}^{i-1} (\sum_{s_{0_j \rightarrow i}} + \sum_{in_{j \rightarrow i}} + 2\sum_{n,2n_{j \rightarrow i}} + 3\sum_{n,3n_{j \rightarrow i}} + 4\sum_{n,4n_{j \rightarrow i}}) \phi_{00_j} \frac{\Delta_j}{\Delta_i} + S_i}{\sum_{a_i} + \left[ \sum_{j=1, j \neq i}^{NOG} (\sum_{s_{0_i \rightarrow j}} + \sum_{in_{i \rightarrow j}} + \sum_{n,2n_{i \rightarrow j}} + \sum_{n,3n_{i \rightarrow j}} + \sum_{n,4n_{i \rightarrow j}}) \right] - (\sum_{n,2n_{i \rightarrow i}} + 2\sum_{n,3n_{i \rightarrow i}} + 3\sum_{n,4n_{i \rightarrow i}})} \quad (83)$$

$$\phi_{11_i} = \frac{\phi_{00_i} + \sum_{j=1}^{i-1} \sum_{s_{1_j \rightarrow i}} \phi_{11_j} \frac{\Delta_j}{\Delta_i}}{\sum_{t_i} - \sum_{s_{1_i \rightarrow i}}} \quad (84)$$

$$\phi_{20_i} = \frac{\frac{\phi_{11_i}}{3} + \sum_{j=1}^{i-1} (\sum_{s_{0_j \rightarrow i}} + \sum_{in_{j \rightarrow i}} + 2\sum_{n,2n_{j \rightarrow i}} + 3\sum_{n,3n_{j \rightarrow i}} + 4\sum_{n,4n_{j \rightarrow i}}) \phi_{20_j} \frac{\Delta_j}{\Delta_i}}{\sum_{a_i} + \left[ \sum_{j=1, j \neq i}^{NOG} (\sum_{s_{0_i \rightarrow j}} + \sum_{in_{i \rightarrow j}} + \sum_{n,2n_{i \rightarrow j}} + \sum_{n,3n_{i \rightarrow j}} + \sum_{n,4n_{i \rightarrow j}}) \right] - (\sum_{n,2n_{i \rightarrow i}} + 2\sum_{n,3n_{i \rightarrow i}} + 3\sum_{n,4n_{i \rightarrow i}})} \quad (85)$$

$$\tau_i = \frac{\phi_{20_i}}{\phi_{00_i}} = \text{age to group } i. \quad (86)$$

## 2.5 $P_n$ to $S_n$ Transport Corrections

The difference between the  $S_N$  and  $P_N$  require<sup>10</sup>

$$\sigma_{lg' \rightarrow g}^{SN} = \sigma_{lg' \rightarrow g}^{PN} \quad \text{for } g' \neq g \quad (87)$$

and

$$\sigma_{lg \rightarrow g}^{SN} = \sigma_{lg \rightarrow g}^{PN} - \sigma_{ltg}^{PN} + \sigma_g^{SN} \quad (88)$$

where  $\sigma_g^{SN}$  is not determined. The choice of  $\sigma_g^{SN}$  gives rise to a “transport approximation” and various recipes are in use:

- Consistent-P approximation is

$$\sigma_{lg \rightarrow g}^{SN} = \sigma_{lg \rightarrow g}^{PN} - (\sigma_{ltg}^{PN} - \sigma_{0tg}^{PN}) \quad (89)$$

- Inconsistent-P approximation is

$$\sigma_{lg \rightarrow g}^{SN} = \sigma_{lg \rightarrow g}^{PN} - (\sigma_{ltg}^{PN} - \sigma_{N+1tg}^{PN}) \quad (90)$$

- Diagonal transport approximation

$$\sigma_{lg \rightarrow g}^{SN} = \sigma_{lg \rightarrow g}^{PN} - (\sigma_{ltg}^{PN} - \sigma_{N+1tg}^{PN} + \sigma_{N+1g \rightarrow g}^{PN}) \quad (91)$$

- Bell-Hansen Sandmeier or extended transport approximation

$$\sigma_{lg \rightarrow g}^{SN} = \sigma_{lg \rightarrow g}^{PN} - (\sigma_{ltg}^{PN} - \sigma_{N+1tg}^{PN} + \sum_{g'} \sigma_{N+1g \rightarrow g'}^{PN}). \quad (92)$$

When the  $P_N$  to  $S_N$  correction is requested in the COMBINE7.1 input, the average of the above approximations is used for  $B_1$  calculation but only the consistent-P approximation is used for  $B_3$  calculation. This correction is applied only when CCCC ISOTXS cross section output is requested.

## 2.6 Adjoint Problems

The ANISN portion in the COMBINE7.1 can do adjoint neutron flux calculation, generating adjoint flux. This is done by transposing and reordering the groups. By input request, the adjoint cross sections can now be generated at the macroscopic level at the end of a COMBINE run. With the adjoint cross sections, a forward calculation can be done to obtain the adjoint flux.

## 2.7 Photon Production and Photo-atomic Cross Section

COMBINE7.1 now has the 1-D photon (gamma) transport capability, using the “matng.lib” library. This library contains the photon-production cross sections in the  $167 \times 18$  group structure and the photo-atomic cross sections in the 18-group structure. In addition to generating the neutron cross section file “combine.sig” for the neutron diffusion/transport, the code generates a spatially and energy collapsed macroscopic regionwise photon production and 18-group photoatomic cross section file “photon.sig” when requested. The self-shielding applied to the capture and fission cross sections are applied correspondingly to self-shield photon production cross sections before spatial collapsing. For photoatomic cross sections, there is no need for collapsing other than atom density based homogenization. Provided that the spatial neutron flux data of same group structure is provided from the reactor physics code, the code can generate the spatially distributed photon source, using the photon production cross sections from “photon.sig.” With thus generated distributed source and the photoatomic cross sections also from the “photon.sig” file, the code can perform 1-D photon transport calculation. With an edit of heat activity, it can provide the spatial gamma heating profile in addition to the photon flux profile.

### 3. 1-D TRANSPORT CALCULATION

The ANISN/PC code for 1-D transport theory calculations is incorporated in the COMBINE7.1. The ANISN portion solves the multigroup finite difference discrete ordinates equations with anisotropic scattering by using the fine group cross section constants, generated for the stacked 0-D or infinite media. Thus calculated fluxes are used to spatially collapse the fine group constants to better reflect the spatial self-shielding.

When the multigroup approximation has been applied, the steady-state Boltzmann transport equation for the directional flux density may be written as

$$\begin{aligned} & \Omega \cdot \nabla \psi_g(\mathbf{r}, \Omega) + \Sigma_{tg}(\mathbf{r}) \psi_g(\mathbf{r}, \Omega) \\ &= \sum_{g'=1}^{\text{IGM}} \int_{-1}^1 d\Omega' \left[ \chi_g \nu \Sigma_{fg'}(\mathbf{r}) + \Sigma_{sg' \rightarrow g}(\mathbf{r}, \Omega' \rightarrow \Omega) \right] \psi_{g'}(\mathbf{r}, \Omega') + Q_g(\mathbf{r}, \Omega) \end{aligned} \quad (93)$$

In the discrete ordinates method, the neutron transport equation is solved in a discrete set of directions only. Angular integrals are then approximated by sums over discrete directions and angular derivatives by differences.

The detail of ANISN/PC code can be found in the ANISN/PC manual<sup>15</sup> pdf file, included as a part of COMBINE7.1 code package.

Currently, COMBINE inputs for 1-D transport are interpreted for input to internal ANISN transport calculations when multistage COMBINE is performed. Also, 1-D transport calculation only can be performed with the minimum COMBINE input provided that full ANISN input file “anisn.inp” and cross section file “anisnc4.lib” are provided.

#### 3.1 Transverse Buckling in the Final Stage 1-D Transport Calculation

In the final stage 1-D transport calculation, a transverse buckling is used to generate the transverse leakage term. The transverse buckling can be constant or region and groupwise. The positive buckling means leakage and negative buckling means gain through  $B^2/(3\Sigma_{tr})$ . Negative bucklings should be used with caution as this approach has not been independently verified.

## 4. USER'S GUIDE

### 4.1 Derivation of Diffusion Coefficient and Transport Cross Section

Although it is not evident from a cursory examination of  $B_1$  equations, the mathematical structure of the system of equations resulting in Equations (30) and (31) is predetermined by the assumptions embodied in Equation (5). The assumptions, mathematically valid for a bare critical system satisfying simple diffusion boundary conditions, are characteristic of the broad generalities leading to the so-called First Fundamental Theorem of Reactor Theory.<sup>20</sup> The usual approach to the  $B_N$  energy-dependent equations involves taking the Fourier transform of the steady-state transport equation for a slab, with the implication that diffusion boundary conditions are somehow applicable to any order N.

The conceptual difficulty with this approach is that the resultant equations obscure any direct relationship between the spatial and energy dependence of the variables, unless the resultant equations are first subjected to Fourier inversion. Such a relationship is required to derive a rigorous definition of the energy-dependent diffusion coefficient by means of Fick's law. The procedure of deriving the  $B_1$  equations by use of Equation (5) and diffusion theory boundary conditions for the scalar flux enables one to accomplish this end in a straightforward way.

Equation (5) establishes the desired relationship between the variables subject to the boundary conditions at the extrapolated boundary of the slab. Only the real part of  $e^{-iBx}$  satisfies the boundary conditions for the spatially dependent scalar flux. The scalar flux is obtained from Equations (5), (8), and (9) in the conventional manner as

$$\Phi(x, \mu, E) = e^{-iBx} \psi(B, \mu, E)$$

$$\Phi_0(x, E) = \int_{-1}^1 \Phi(x, \mu, E) d\mu = e^{-iBx} \int_{-1}^1 \psi(B, \mu, E) d\mu = e^{-iBx} \phi_0(B, E). \quad (94)$$

From Fick's law, we obtain the relationship between the scalar flux and current

$$\vec{J}(x, E) = -D(E) \vec{\nabla} \Phi_0(x, E) = -\vec{k} D(E) \frac{d}{dx} \Phi_0(x, E) = D(E) B \phi_0(B, E) i \vec{k} e^{-iBx}. \quad (95)$$

where  $\vec{k}$  is the unit vector in the x direction.

Therefore,  $\vec{J}(x, E)$  is also separable in space and energy, a result consistent with Equation (5).

$$\therefore \vec{J}(x, E) = J(B, E) i \vec{k} e^{-iBx} \quad (96)$$

$$\text{where } J(B, E) = D(E) B \phi_0(B, E) \quad (97)$$

It has been pointed out that Equation (97) does not give a clear-cut relationship between  $J(E)$  and  $\phi_1(E)$  in Equations (30) and (31) since Fick's law is perfectly general. An alternate method of obtaining Equation (97) will be given, which helps clear up any ambiguity that may exist. Using the same assumptions and utilizing Equations (5), (8), and (9), we have

$$\vec{J}^*(x, E) = \vec{k} \int_{-1}^1 \mu \Phi(x, \mu, E) d\mu = \vec{k} \int_{-1}^1 \mu e^{-iBx} \psi(B, \mu, E) d\mu = i \vec{k} \phi_1(B, E) e^{-iBx} \text{ when } B \text{ is real,}$$

$= \bar{k} \phi_1(\mathbf{B}, E) e^{-i\mathbf{B}x}$  when  $\mathbf{B}$  is imaginary.

Introducing Fick's law without reference to the scalar flux boundary conditions we have

$$\vec{J}^*(x, E) = -D(E) \vec{\nabla} \Phi_0(x, E) = D(E) \mathbf{B} \phi_0(\mathbf{B}, E) i \bar{k} e^{-i\mathbf{B}x} .$$

Now equate  $\vec{J}^*(x, E)$  from the two preceding equations to obtain a result similar to Equation (97) as

$$\vec{J}^*(x, E) = \phi_1(\mathbf{B}, E) i \bar{k} e^{-i\mathbf{B}x} = D(E) \mathbf{B} \phi_0(\mathbf{B}, E) i \bar{k} e^{-i\mathbf{B}x} \text{ when } \mathbf{B} \text{ is real,}$$

$$= \phi_1(\mathbf{B}, E) \bar{k} e^{-i\mathbf{B}x} = D(E) \mathbf{B} \phi_0(\mathbf{B}, E) i \bar{k} e^{-i\mathbf{B}x} \text{ when } \mathbf{B} \text{ is imaginary;}$$

$$\therefore \vec{J}(\mathbf{B}, E) = \phi_1(\mathbf{B}, E) = D(E) \mathbf{B} \phi_0(\mathbf{B}, E) \text{ when } \mathbf{B} \text{ is real,}$$

$$= iD(E) \mathbf{B} \phi_0(\mathbf{B}, E) \text{ when } \mathbf{B} \text{ is imaginary.} \quad (98)$$

From Equation (98),  $D(E)$  is defined as

$$D(E) = \frac{\phi_1(\mathbf{B}, E)}{\mathbf{B} \phi_0(\mathbf{B}, E)} \text{ when } \mathbf{B} \text{ is real, } = \frac{\phi_1(\mathbf{B}, E)}{i\mathbf{B} \phi_0(\mathbf{B}, E)} \text{ when } \mathbf{B} \text{ is imaginary.} \quad (99)$$

Equation (99) gives an unambiguous definition of the diffusion coefficient within the framework of the  $B_1$  equations for a bare slab. The definition of the  $B_1$  transport cross section at energy  $E$  in the domain of Fick's law is

$$\Sigma_{tr}(E) = \frac{1}{3D(E)} = \frac{\mathbf{B} \phi_0(\mathbf{B}, E)}{3\phi_1(\mathbf{B}, E)} \text{ when } \mathbf{B} \text{ is real,}$$

$$\Sigma_{tr}(E) = \frac{1}{3D(E)} = \frac{i\mathbf{B} \phi_0(\mathbf{B}, E)}{3\phi_1(\mathbf{B}, E)} \text{ when } \mathbf{B} \text{ is imaginary.} \quad (100)$$

In order to use Equation (100), the current from the solution run needs to be nonzero. Thus, when a zero buckling is input to the code, neither the diffusion coefficient nor the transport cross section is calculated. This situation corresponds to an infinite medium problem for which there is no net neutron current flow. If a diffusion coefficient is desired for a near infinite medium situation, a small but finite buckling input to the code will produce the desired results. Different definitions of transport cross section, based on the  $B_1$  approximation to transport and the one-speed (monoenergetic) diffusion theory, are discussed in Section 4.2.1 and 4.2.2, respectively.

## 4.2 Summary Edits for Broad Group Constants

The equations for calculating the average cross sections are presented in this section in as complete a manners practical. This should facilitate the proper use of the average cross sections generated by the spectrum code.<sup>3,4</sup>

The COMBINE spectrum, cross-section library tape contains data tabulated for 167 fine lethargy groups. In a normal spectrum problem, the data are coalesced into a broad group structure, specified by the user, containing one or more fine groups per broad group. The coalescing is performed by utilizing

167 fine group fluxes and/or currents as the weighting functions. These energy dependent fluxes and currents may either be calculated for a particular reactor system or taken from an immediately preceding problem. The latter type of calculation is referred to as a cell calculation. The output from a spectrum problem normally includes average macroscopic cross-section data and may include average microscopic data for each material in the macroscopic calculation, if desired. As an alternative to the normal output, the user may request the calculation of macroscopic effective diffusion theory constants (blackness theory) in lieu of the normal cross section output.

Figure 4 illustrates the notation used in describing the average cross-section data and the relation of the fine-group data to the broad-group data generated in a spectrum problem. In Figure 4, broad group G contains the fine groups I through I+N and all averages for broad group G are performed over this range of fine groups. In the notation used above, NOG refers to the number of fine groups and NOAG refers to the number of broad groups.

Fine Groups	1	2	3	...	I-1	I	I+1	...	I+N-1	I+N	I+N+1	...	K-1	K	K+1	...	K+M-1	K+M	K+M+1	...	NOG-1	NOG
Broad Groups	1	...						G								G'						NOAG

Figure 5. Spectrum group structure.

The average cross sections are determined by the familiar relation

$$\bar{\Sigma} = \frac{\int_E \Sigma(E)w(E)dE}{\int_E w(E)dE} \quad (101)$$

where  $\bar{\Sigma}$  represents the energy dependent cross section  $\Sigma(E)$ , and  $w(E)$  is the energy dependent weighting function, normally either the fluxes or the currents. In the actual calculation, the continuous functions of the cross section and weighting parameter are represented by 167 fine group average values associated with a lethargy width,  $\Delta_i$ . Thus,

$$\bar{\Sigma} = \frac{\sum_i \Sigma_i w_i \Delta_i}{\sum_i w_i \Delta_i} \quad (102)$$

In all cases, the integrations are performed utilizing the trapezoidal rule.

### 4.2.1 Average Macroscopic Cross Sections

The macroscopic cross-section data generated by the COMBINE7.1 code is described below in considerable detail to facilitate its proper use. In all cases, the average quantity has been defined for the broad group G where:

$$\Sigma_i (cm^{-1}) = \sum_{k=1}^{NOI} N_k \sigma_i^k \Rightarrow \text{macroscopic cross section for } i^{\text{th}} \text{ fine group of a system containing NOI materials}$$

$N_k$  and  $\sigma_i^k$  are the atom density (# of atoms  $\times 10^{-24}$  per cubic centimeter) and microscopic cross section (barns/atom), respectively, for the  $k^{\text{th}}$  material

$\Delta_i \Rightarrow$  lethargy width of fine group  $i$

$\phi_i \Rightarrow$  average scalar flux in fine group  $i$

$J_i \Rightarrow$  average current ( $P_1$  flux) in fine group  $i$

$\psi_i \Rightarrow$  average  $P_2$  flux for group  $i$

$\chi_i \Rightarrow$  average  $P_3$  flux for group  $i$

$\bar{\Sigma}_{x_G} \Rightarrow$  average cross section for broad group G for a particular reaction denoted by  $x$

$\phi_G \Rightarrow$  integrated scalar flux for group G

$J_G \Rightarrow$  integrated current ( $P_1$  flux) for group G

$\psi_G \Rightarrow$  integrated  $P_2$  flux for group G

$\chi_G \Rightarrow$  integrated  $P_3$  flux for group G.

The integrated fluxes for broad group G are calculated as

$$\Phi_G = \sum_{i=1}^{i+N} \phi_i \Delta_i \quad (103)$$

$$J_G = \sum_{i=1}^{i+N} J_i \Delta_i \quad (104)$$

$$\psi_G = \sum_{i=1}^{i+N} \psi_i \Delta_i \quad (105)$$

$$\chi_G = \sum_{i=1}^{i+N} \chi_i \Delta_i \quad (106)$$

Average absorption cross section

$$\bar{\Sigma}_{a_G} = \frac{\sum_{i=I}^{I+N} \sum_{a_i} \phi_i \Delta_i}{\Phi_G}. \quad (107)$$

Average fission cross section

$$\bar{\Sigma}_{f_G} = \frac{\sum_{i=I}^{I+N} \sum_{f_i} \phi_i \Delta_i}{\Phi_G}. \quad (108)$$

Average number of neutrons per fission times the fission cross section

$$\bar{\nu \Sigma}_{f_G} = \frac{\sum_{i=I}^{I+N} \nu_i \sum_{f_i} \phi_i \Delta_i}{\Phi_G}. \quad (109)$$

Average number of neutrons produced per fission

$$\bar{\nu}_G = \frac{\bar{\nu \Sigma}_{f_G}}{\bar{\Sigma}_{f_G}}. \quad (110)$$

Average capture cross section

$$\bar{\Sigma}_{c_G} = \bar{\Sigma}_{a_G} - \bar{\Sigma}_{f_G}. \quad (111)$$

Average elastic, inelastic, (n,2n), (n,3n), or (n,4n) cross section for isotropic transfer from group G to G'

$$\bar{\Sigma}_{x_{G \rightarrow G'}} = \frac{\sum_{i=I}^{I+N} \sum_{k=K}^{K+M} \sum_{x_{i \rightarrow k}} \phi_i \Delta_i}{\Phi_G} \quad x_{i \rightarrow k} = \begin{cases} s_0 \text{ (elastic)} \\ \text{in (inelastic)} \\ n, 2n \text{ reactions} \\ n, 3n \text{ reactions} \\ n, 4n \text{ reactions} \end{cases}. \quad (112)$$

Average linearly anisotropic component of elastic or inelastic transfer cross section from group G to G'

$$\bar{\Sigma}_{x_{G \rightarrow G'}} = \frac{\sum_{i=I}^{I+N} \sum_{k=K}^{K+M} \sum_{x_{i \rightarrow k}} J_i \Delta_i}{J_G} \quad x_{i \rightarrow k} = \begin{cases} s_1 \text{ (elastic)} \\ \text{in (inelastic)} \end{cases}. \quad (113)$$

Average  $P_2$  component of the elastic transfer cross section from group G to G'

$$\bar{\Sigma}_{s_{2G \rightarrow G'}} = \frac{\sum_{i=I}^{I+N} \sum_{k=K}^{K+M} \sum_{s_{2i \rightarrow k}} \psi_i \Delta_i}{\Psi_G}. \quad (114)$$

Average  $P_3$  component of the elastic transfer cross section from group G to G'

$$\bar{\Sigma}_{s_{3G \rightarrow G'}} = \frac{\sum_{i=I}^{I+N} \sum_{k=K}^{K+M} \sum_{S_{3i \rightarrow k}} \chi_i \Delta_i}{\chi_G} . \quad (115)$$

Average total transfer cross section for transfer from group G to G'

$$\bar{\Sigma}_{t_{rG \rightarrow G'}} = \bar{\Sigma}_{s_{0G \rightarrow G'}} + \bar{\Sigma}_{inG \rightarrow G'} + 2\bar{\Sigma}_{n,2n_{G \rightarrow G'}} + 3\bar{\Sigma}_{n,3n_{G \rightarrow G'}} + 4\bar{\Sigma}_{n,4n_{G \rightarrow G'}} . \quad (116)$$

Average of isotropic elastic, inelastic, (n,2n), (n,3n), or (n,4n) total scattering cross section, which would include elastic thermal upscattering

$$\bar{\Sigma}_{t_{xG}} = \sum_{G'=1}^{NOAG} \bar{\Sigma}_{s_{G \rightarrow G'}} \quad \chi_{G \rightarrow G'} = \begin{cases} s_0 \text{ (elastic)} \\ in \text{ (inelastic)} \\ n, 2n \text{ reactions} . \\ n, 3n \text{ reactions} \\ n, 4n \text{ reactions} \end{cases} \quad (117)$$

Average  $P_1, P_2,$  and  $P_3$  component of the elastic total scattering cross section

$$\bar{\Sigma}_{t_{s1G}} = \sum_{G'=1}^{NOAG} \bar{\Sigma}_{s_{1G \rightarrow G'}} . \quad (118)$$

Average out-scatter cross section

$$\bar{\Sigma}_{outG} = \sum_{G'=1, G' \neq G}^{NOAG} \left[ \bar{\Sigma}_{s_{0G \rightarrow G'}} + \bar{\Sigma}_{inG \rightarrow G'} + \bar{\Sigma}_{n,2n_G} + \bar{\Sigma}_{n,3n_G} + \bar{\Sigma}_{n,4n_G} \right] \quad (119)$$

Average removal cross section

$$\bar{\Sigma}_{rG} = \bar{\Sigma}_{aG} + \bar{\Sigma}_{outG} . \quad (120)$$

Average total cross section

$$\bar{\Sigma}_{t_G} = \bar{\Sigma}_{aG} + \bar{\Sigma}_{s_{0G}} + \bar{\Sigma}_{inG} + \bar{\Sigma}_{n,2n_G} + \bar{\Sigma}_{n,3n_G} + \bar{\Sigma}_{n,4n_G} . \quad (121)$$

Integrated fission source

$$S_G = \sum_{i=I}^{I+N} S_i . \quad (122)$$

Average inverse velocity

$$\overline{(1/v)}_G = \frac{\sum_{i=I}^{I+N} (1/v)_i \Phi_i \Delta_i}{\Phi_G} . \quad (123)$$

Average diffusion coefficient (from Fick's law)

$$D_G = J_G / (B_G \Phi_G). \quad (124)$$

Average transport cross section

$$\Sigma_{trG} = 1/(3D_G) = (B_G \Phi_G)/(3J_G). \quad (125)$$

If a cell calculation is performed—a spectrum obtained from a previous problem is used as a weighting function to generate average cross sections for another material—the diffusion coefficients and transport cross sections are defined in terms of cross sections of the material being averaged. An appropriate definition can be obtained from Equation (37). By first solving Equation (37) for  $(B\Phi/3)$ , and then dividing both sides  $\Phi_1$ ). We then have

$$\Sigma_{trG} = \gamma_G \Sigma_{tG} - \left( \sum_{G'} \sum_{s_1}^{G' \rightarrow G} J_{G'} \right) / J_G \quad (126)$$

and

$$D_G = 1/(3\Sigma_{trg}) \quad (127)$$

These are the transport cross section and diffusion coefficient based on the  $B_1$  approximation to the neutron transport.

In addition to the usual average cross-section data described above, some other miscellaneous cross-section data are calculated and printed out for the user. These quantities include the absorption and out-scatter cross sections for each broad group corrected for the (n,2n), (n,3n), or (n,4n) reaction. In the usual few group diffusion code the out-scatter cross section is generally used both as a removal term and a source term. However, the standard out-scatter term calculated by COMBINE accounts for the loss of one neutron by an (n,2n), (n,3n), or (n,4n) reaction in a particular broad group. Therefore, when this same term is used as a source term for the next group in a few group diffusion theory calculation of reactivity, it represents only one-half, one-third, or one-fourth of the actual source into that group from the (n,2n), (n,3n), or (n,4n) transfer reaction. Thus, in the corrected cross-section data,

$$\bar{\Sigma}_{outG} = \sum_{G'=1, G' \neq G}^{NOAG} \left[ \bar{\Sigma}_{s_0G \rightarrow G'} + \bar{\Sigma}_{in_{G \rightarrow G'}} + 2\bar{\Sigma}_{n,2n_{G \rightarrow G'}} + \bar{\Sigma}_{n,3n_{G \rightarrow G'}} + \bar{\Sigma}_{n,4n_{G \rightarrow G'}} \right] \quad (128)$$

where now a corrected absorption term is defined as

$$\Sigma_{aG}^* = \Sigma_{aG} - \sum_{G'=G}^{NOAG} \Sigma_{n,2n_{G \rightarrow G'}} - 2 \sum_{G'=G}^{NOAG} \Sigma_{n,3n_{G \rightarrow G'}} - 3 \sum_{G'=G}^{NOAG} \Sigma_{n,4n_{G \rightarrow G'}} \quad (129)$$

to conserve neutrons.

#### 4.2.2 Monoenergetic Transport Cross Section

The monoenergetic (or one speed) transport cross section offers an alternative to the Fick's law definition given by Equation (125) or (126) and has the redeeming feature that is always positive regardless of the shape of the spectrum. It is the classical value based on its definition from the one-energy transport equation.<sup>9</sup> For broad group G, the macroscopic value is

$$\bar{\Sigma}_{trG} = \bar{\Sigma}_{tG} - \bar{\Sigma}_{ts_{1G}} \quad (130)$$

where the cross sections on the right-hand side are given by Equations (121) and (118). The microscopic transport cross section can be defined similarly, using microscopic cross sections, as

$$\overline{\sigma}_{tG}^k = \overline{\sigma}_{tG}^k - \overline{\sigma}_{ts1G}^k . \quad (131)$$

Both the Fick's Law (Equation 125 or 126 and 132) and monoenergetic definitions (Equations 129 and 130 of the transport cross section and corresponding diffusion coefficient are printed for each group defined at the completion of the spectrum calculation.

### 4.2.3 Average Microscopic Cross Sections

The average microscopic cross sections are defined in a manner similar to the macroscopic cross sections. The main difference is the use of the microscopic cross section,  $\sigma$ , in the place of the macroscopic cross section,  $\Sigma$ . The one exception is the definition of a microscopic transport cross section. A unique definition of a microscopic transport cross section presents a conceptual difficulty in the same way that a microscopic diffusion coefficient would. The macroscopic values are extensive quantities resulting from some form of Fick's law, and there is no corresponding, physically meaningful relationship for microscopic values. Rather, it has become traditional to define a microscopic transport cross section only in the metaphysical sense that "the whole is the sum of its assumed parts"; then, from this, the macroscopic diffusion coefficient follows as

$$D_G = \frac{1}{3 \sum_k N_k \overline{\sigma}_{tG}^k} = \frac{1}{3 \overline{\Sigma}_{tG}} . \quad (132)$$

This being the case, the only thing required to define the microscopic transport cross section  $\overline{\sigma}_{tG}^k$  in Equation (131) is a consistency relationship that will yield the proper macroscopic transport cross section for a particular mixture of materials as calculated by Equation (125). Any number of such consistency relationships could be defined and applied, as long as the macroscopic transport cross section in the denominator of Equation (132), computed from microscopic values, gives the same result as Equation (125).

One such equation that will yield the desired results is Equation (126), where  $\Sigma$  becomes the appropriate  $\sigma^k$  in each term of Equation (126). The broad microscopic transport cross section for the  $k^{\text{th}}$  isotope is then given by

$$\overline{\sigma}_{tG}^k = \gamma_G \overline{\sigma}_{tG}^k - \left( \sum_{G'} \sigma_{s1}^{G' \rightarrow G} J_{G'} \right) / J_G . \quad (133)$$

A measure of the "arbitrariness" of this definition of the microscopic transport cross section is that it is entirely possible that the microscopic transport cross section, as given by Equation (133), can be negative for one or several materials in the mixture, and yet, when multiplied by  $N_k$  and summed over all materials in the mixture, will yield the proper macroscopic transport cross section as given by Equation (125). This situation occurs when the mixture contains large amounts of a strong absorber and the resultant flux and current spectra are very hard. For moderating materials with a small absorption cross section, the second term in the numerator of Equation (133) can then be the leading term because of the high current weights given the transfer cross sections  $\sigma_{s1G' \rightarrow G}$  when G lies in the energy range of depressed flux and current at low energy. The resultant microscopic transport cross sections, even though

negative, are consistent in the sense of Equation (132), since “consistency” is all that is required of them in the definition.

The same pathologic situation can occur for cell materials being averaged over the flux and current from another spectral problem. If the spectral problem contained a very strong absorber producing a very hard spectra and the cell material does not contain much absorption, the macroscopic transport cross section from Equation (126) can be negative in low-energy groups. In this case, the negative result could be interpreted as indicating that the homogenization for the cell material was not judiciously chosen.

#### 4.2.4 Effective Diffusion Theory Constants (Blackness Theory)

Extensive use is made of diffusion theory in nuclear reactor design analysis; however, inherent in the diffusion theory approximation is its inadequacy in highly absorbing, low scattering regions such as control rods. Because many reactor systems include such regions, the blackness theory was developed to provide a convenient technique for handling these regions without recourse to a higher order transport solution. The approach is to treat the absorbing region as a fictitious diffusing medium of the same thickness but use blackness constants in the diffusion calculation, which yield more correct fluxes than could be obtained with the usual constants. The spectrum code incorporates an option to calculate blackness theory diffusion coefficients and absorption cross sections for use in highly absorbing regions of a system under study. The assumptions made in the development of the formulism used to calculate the effective constants are that the absorbing region is a thin slab and the immediately surrounding regions can be adequately handled by diffusion theory methods. These effective constants incorporate factors to account for the mesh structure used to describe the region in a finite difference solution of the diffusion equation. A complete development of this theory can be found in Reference 30 and a review of its use may be found in References 31 and 32.

#### 4.2.5 Mixed Number Density Constants

An input option allows for the production of mixed number density (MND) constants<sup>33</sup> for one single broad group in the thermal spectrum. No multiple thermal group MND constants are defined. The constants are defined as

$$\Sigma_{MND} = \overline{\Sigma V} = \frac{\int_0^{E_1} \Sigma(E) \phi_{SP}(E) dE}{\int_0^{E_1} \frac{1}{v(E)} \phi_{SP}(E) dE} = \frac{(\overline{\Sigma})_{SP}}{\left(\frac{1}{v}\right)_{SP}} \quad (134)$$

where

$\Sigma$  = the macroscopic absorption or fission cross section

$\phi_{SP}(E)$  = thermal flux spectrum solution

$E_1$  = upper energy of the single MND group

$v(E)$  = velocity at energy  $E$ .

$$D_{MND} = \overline{DV}_{\max} = \frac{\int_0^{E_1} D(E) M(E) dE}{\int_0^{E_1} \frac{M(E) dE}{v(E)}} = \frac{(\overline{D})_{\max}}{\left(\frac{1}{v}\right)_{\max}} \quad (135)$$

$$\sum_{tr}^{MND} = \frac{1}{3D_{MND}} \quad (136)$$

$$\sigma_{tr}^{MND} = \left( \frac{\bar{\sigma}_{tr}}{V_{\max}} \right) = \frac{\int_0^{E_1} \frac{M(E)dE}{V(E)}}{\int_0^{E_1} \frac{M(E)dE}{\sigma_{tr}(E)}} = \frac{\left( \frac{1}{V} \right)_{\max}}{\left( \frac{1}{\sigma_{tr}} \right)_{\max}} \quad (137)$$

where “max” indicates averaging over a Maxwellian spectrum and

$M(E)$  = Maxwellian distribution at temperature  $T$ ;

$$M(E)dE = \frac{E[\exp(-E/kT)]}{(kT)^2} dE \quad (138)$$

where  $k$  is Boltzmann's constant and the average energy =  $3/2kT$  and  $T$  corresponds to the ambient energy of the region.<sup>33</sup>

For each  $\sum$  in Equations (134) through (138), there is a corresponding microscopic  $\sigma$  calculated for the output files.  $\sigma_{tr}$  replaces  $D$ . There are also normalized MND constants defined as:

$$D^{NORM} = \frac{D_{MND}}{2.2 \times 10^5}$$

$$\sum_a^{NORM} = \frac{\sum_a^{MND}}{2.2 \times 10^5}$$

$$\sum_F^{NORM} = \frac{\sum_F^{MND}}{2.2 \times 10^5}. \quad (139)$$

Normalized microscopic values are defined as:

$$\sigma_{tr}^{NORM} = (2.2 \times 10^5) \sigma_{tr}^{MND}$$

$$\sigma_a^{NORM} = \frac{\sigma_a^{MND}}{2.2 \times 10^5}$$

$$\sigma_F^{NORM} = \frac{\sigma_F^{MND}}{2.2 \times 10^5}. \quad (140)$$

If the “unnormalized MND values” are used in a spatial diffusion calculation, the thermal flux will be values of neutron density. If normalized values are used, the thermal flux will be the 2,200 meters/sec thermal flux. Summary data printed (and punched) will include MND values of

$$\sum_{tr}, D, \sum_a, \sum_F, \nu \sum_F, \sigma_{tr}, 1/3\sigma_{tr}, \sigma_a, \sigma_F, \text{ and } \nu\sigma_F.$$

## 4.2.6 Multiplication Factors

Multiplication factors  $k_{\text{inf}}$  and  $k_{\text{eff}}$  are calculated for a COMBINE problem and printed after the broad group edits.  $k_{\text{inf}}$  is calculated as

$$k_{\text{inf}} = \frac{\sum_{G=1}^{GG} \nu \sum_{f_G} \phi_G}{\sum_{G=1}^{GG} \sum_{a_G} \phi_G} \quad (141)$$

where the numerator is the production rate of fission neutrons over the broad group spectra, the denominator is the absorption rate, and NOAG is the total number of broad groups. When  $B = C$  or  $B = -iC$  with a real constant  $C$ , then

$$k_{\text{eff}} = \frac{\sum_{G=1}^{NOAG} \nu \sum_{f_G} \phi_G}{\sum_{G=1}^{NOAG} (\sum_{a_G} + D_G C_G^2) \phi_G} \quad (142)$$

where  $D_G$  is the broad group diffusion coefficient and  $C_G^2$  are the buckling coefficients specified in the floating point input data.

When  $B = iC$ ,

$$k_{\text{eff}} = \frac{\sum_{G=1}^{NOAG} \nu \sum_{f_G} \phi_G}{\sum_{G=1}^{NOAG} (\sum_{a_G} - D_G C_G^2) \phi_G}, \quad (143)$$

since there is a negative leakage. In this case  $k_{\text{eff}}$  exceeds  $k_{\text{inf}}$ .

## 4.2.7 The Spatial Coalescing Formulas

The spatial coalescing is carried out by weighting the various cross sections and other neutron group constants as follows. The formulas employed in the INL's internal SCAMP code<sup>34</sup> were adopted in COMBINE7.1. The following formulas are applicable to both regionwise macroscopic and microscopic constants.

Absorption cross section

$$\Sigma_{R,G}^a = \left( \sum_{g \text{ in } G} \sum_{r \text{ in } R} \Sigma_{r,g}^a \int_{V_r} \Phi_g \, dv \right) / \left( \sum_{g \text{ in } G} \sum_{r \text{ in } R} \int_{V_r} \Phi_g \, dv \right). \quad (144)$$

The broad group fission cross section is found in the same manner as the absorption cross section.

$P_0$  Scattering cross section

$$\Sigma_{R,G \rightarrow G'}^0 = \left( \sum_{g' \text{ in } G'} \sum_{g \text{ in } G} \sum_{r \text{ in } R} \Sigma_{r,g \rightarrow g'}^0 \int_{V_r} \Phi_g \, dv \right) / \left( \sum_{g \text{ in } G} \sum_{r \text{ in } R} \int_{V_r} \Phi_g \, dv \right). \quad (145)$$

$P_1$  Scattering cross section

$$\Sigma_{R,G \rightarrow G'}^1 = \left( \sum_{g' \text{ in } G'} \sum_{g \text{ in } G} \sum_{r \text{ in } R} \Sigma_{r,g \rightarrow g'}^1 \int_{V_r} J_g \, dv \right) / \left( \sum_{g \text{ in } G} \sum_{r \text{ in } R} \int_{V_r} J_g \, dv \right). \quad (146)$$

The  $P_2$  and  $P_3$  scattering cross sections are found in the same manner as the  $P_1$  scattering cross section but using the  $P_2$  and  $P_3$  flux moment, respectively. However, the conventional scalar flux is used in the code instead of higher flux moments for the  $P_0$ ,  $P_1$ , and  $P_2$  scattering cross sections.

Total cross section:

$$\Sigma_{R,G}^T = \Sigma_{R,G}^a + \sum_{G'} \Sigma_{R,G \rightarrow G'}^0. \quad (147)$$

Diffusion coefficient based on Fick's law

$$D_{R,G} = J_G^R / (B_G^R \Phi_G^R), \quad (148)$$

where input ransverse buckling is used – maybe negative or not reliable.

Diffusion coefficient based on Fick's law pseudo extension

$$D_{R,G} = \left( \sum_{g \text{ in } G} \sum_{r \text{ in } R} \int_{V_r} |J_g| \, dv \right) / \left( \sum_{g \text{ in } G} \sum_{r \text{ in } R} \int_{V_r} |\text{grad} \Phi| \, dv \right), \quad (149)$$

where, in each space interval,  $\text{grad } \Phi = (\Phi_{m+1} - \Phi_m) / (x_{m+1} - x_m)$ .

Transport cross section based on the  $B_1$  approximation to transport

$$\Sigma_{R,G}^{tr} = \gamma_{R,G} \Sigma_{R,G}^T - (\Sigma_{R,G' \rightarrow G}^0 J_{R,G'}) / J_{R,G}. \quad (150)$$

Transport cross section based on the  $B_1$  approximation to transport and flux weighted instead of current

$$\Sigma_{R,G}^{tr} = \gamma_{R,G} \Sigma_{R,G}^T - (\Sigma_{R,G' \rightarrow G}^0 \Phi_{R,G'}) / \Phi_{R,G}. \quad (151)$$

Transport cross section based on the one-speed diffusion theory

$$\Sigma_{R,G}^{tr} = \Sigma_{R,G}^T - \Sigma_{R,G}^{S,J}, \quad (152)$$

where  $\Sigma_{R,G}^{S,J}$  is current weighted.

Transport cross section based on the one-speed diffusion theory

$$\Sigma_{R,G}^{tr} = \Sigma_{R,G}^T - \Sigma_{R,G}^{1\Phi}, \quad (153)$$

where  $\Sigma_{R,G}^{1\Phi}$  is flux weighted.

Fission spectrum

$$\chi_{R,G} = \left( \sum_{g \text{ in } G} \sum_{r \text{ in } R} \chi_{r,g} \int_{V_r} S_f \, dv \right) / \left( \sum_G \sum_{g \text{ in } G} \sum_{r \text{ in } R} \chi_{r,g} \int_{V_r} S_f \, dv \right). \quad (154)$$

where  $S_f^r = \frac{1}{\lambda} \sum_g v \Sigma_g^f \Phi_g$  and  $\lambda = \text{eigenvalue}$ .

Neutrons per fission times the fission cross section

$$v \Sigma_{R,G}^f = \frac{\left[ \left( \sum_{g \text{ in } G} \sum_{r \text{ in } R} v \Sigma_{r,g}^f \int_{V_r} \Phi_g \, dv \right) \left( \sum_G \sum_{g \text{ in } G} \sum_{r \text{ in } R} \chi_{r,g} \int_{V_r} S_f \, dv \right) \right]}{\left[ \left( \sum_{g \text{ in } G} \sum_{r \text{ in } R} \int_{V_r} \Phi_g \, dv \right) \left( \sum_{r \text{ in } R} \int_{V_r} S_f \, dv \right) \right]}. \quad (155)$$

Parallel buckling

$$B_{R,G}^2 \Big|_1 = \left[ \sum_{g \text{ in } G} C_\rho (x_u^\rho J_{u,g} - x_l^\rho J_{l,g}) \right] / \left( D_{R,G} \sum_{g \text{ in } G} \sum_{r \text{ in } R} \int_{V_r} \Phi_g \, dv \right), \quad (156)$$

where  $\rho=0, 1,$  and  $2$  for slab, cylindrical, and spherical geometry, respectively, and  $C_0=1, C_1=2\pi, C_2=4\pi$ .

Perpendicular buckling

$$B_{R,G}^2 \perp = \left( \sum_{g \text{ in } G} \sum_{r \text{ in } R} B_{R,g}^2 \int_{V_r} \Phi_g \, dv \right) / \left( \sum_{g \text{ in } G} \sum_{r \text{ in } R} \int_{V_r} \Phi_g \, dv \right) \quad (157)$$

where regionwise transverse buckling is used for

Flux volume integrals:

$$\Phi_{R,G} V_R = \sum_{g \text{ in } G} \sum_{r \text{ in } R} \int_{V_r} \Phi_g \, dv \quad (158)$$

Average fluxes:

$$\Phi_{R,G} = \sum_{g \text{ in } G} \sum_{r \text{ in } R} \int_{V_r} \Phi_g \, dv / \sum_{r \text{ in } R} \int_{V_r} \Phi_g \, dv \quad (159)$$

Average currents:

$$J_{R,G} = \sum_{g \text{ in } G} \sum_{r \text{ in } R} \int_{V_r} J_g \, dv / \sum_{r \text{ in } R} \int_{V_r} \Phi_g \, dv \quad (160)$$

Inner radial surface to average flux ratio:

$$R_{l,G} = \sum_{g \text{ in } G} \Phi_g^l / \Phi_{R,G} \quad (161)$$

Outer radial surface to average flux ratio:

$$R_{u,G} = \sum_{g \text{ in } G} \Phi_g^u / \Phi_{R,G} \quad (162)$$

The following glossary of terms is used in the above formulas:

a – superscript denoting absorption cross section

f – superscript denoting fission cross section

g – subscript denoting the  $g^{\text{th}}$  fine group of neutrons

G – subscript denoting the  $G^{\text{th}}$  broad group of neutrons

r – subscript denoting the  $r^{\text{th}}$  fine region

R – subscript denoting the  $R^{\text{th}}$  broad region

$\Phi$  – scalar flux

J – net current

v – volume

$\nu$  – neutron per fission

m – subscript denoting space point index

$l$  – subscript denoting space point number of lower boundary of broad region  $R$

u – subscript denoting space point number of upper boundary of broad region  $R$

x – space variable.

## 5. COMBINE7.1 FILES DESCRIPTION

Logical Unit	Name/status	Format	Usage
400	scratch	formatted	COMBINE input saved for later use
402	reres.lib	formatted	resolved resonance parameters library
403	anisn.inp	formatted	ANISN input
404	anisn.out	formatted	ANISN output
405	combine.inp	formatted	COMBINE input
406	combine.out	formatted	COMBINE output
407	scratch	unformatted	formerly nt8=8 in ANISN , flux and current storage (for IDAT1=2)
408	scratch	unformatted	Formerly nt9=9 in ANISN, flux and current storage (for IDAT1=1,2)
409	scratch	unformatted	Formerly nt1=1 in ANISN, XS and fixed source storage (for IDAT1=1,2)
410	scratch	unformatted	Formerly ntt=2 in ANISN, XS and fixed source storage (for IDAT1=1,2)
410+ica se	scratch	unformatted	temporary cross section files for cases to be 1-D transport (ANISN) corrected when ioned = 1, to be used in s.r. xscoal with ioned = 2.
427	scratch	direct access	photon cross sections, saved in s.r. bondar
428	scratch	direct access	average flux ratios (a region vs. broad region)
429	scratch	formatted	ANISN flux and higher moments saved for spatial cross section coalescing
430	combine.sig/ anisnc4.lib	formatted	formerly nt4=4 in ANISN, ISOTXS format input (for MTP /= 0)
431	neutron.flx	formatted	Opened when the photon transport calculation is requested (NPROB=-2)
432	scratch	direct access	total cross sections for Bondarenko self shielding for the 99 materials
433	scratch	direct access	total cross sections for Bondarenko self shielding for the 100 – 120 materials
434	scratch	formatted	Microscopic reaction cross section (167 fine group) file
435	anisnc4.flux	formatted	formerly 10 in ANISN, RTFLUX or ATFLUX format input
436	scratch	formatted	broad group and spatially coalesced macroscopic file when NSTAGE > 0 and NFREG > 0, copied to file 443 before calling s.r. pstpro
437	combine.flx	formatted	flux output
438	scratch	unformatted	shielded Bondarenko cross section file, adum, generated in s.r. bondar
439	scratch	unformatted	temporary self shielded static cross sections, adum, generated in s.r. spectrum
440	scratch	unformatted	(sigaz(i),sigfz(i),sigsz(i),amu1(i),i=1,np) for the principal resonance absorber after Doppler broadening
441	scratch	unformatted	temporary (sigaz(i),sigfz(i),sigsz(i),amu1(i),i=1,np) for the principal and admixed resonance absorbers before Doppler broadening
443	scratch	formatted	macroscopic file in s.r. xscoal/txscoal before calling s.r. pstpro
444	scratch	unformatted	temporary file for thermal scattering matrix
445	anisnc4.pun	formatted	formerly 7 in ANISN, used to save flux and currents
446	scratch	unformatted	(sigaz(i),sigfz(i),sigsz(i),amu1(i),i=1,np) for the first admixed resonance absorber after Doppler broadening
447	scratch	unformatted	(sigaz(i),sigfz(i),sigsz(i),amu1(i),i=1,np) for the second admixed resonance absorber after broadening
448	scratch	unformatted	(sigaz(i),sigfz(i),sigsz(i),amu1(i),i=1,np) for the third resonance absorber after Doppler broadening
449	scratch	unformatted	formerly 3 in ANISN, angular flux storage
450–569	scratch	unformatted	thermal cross section matrix for isotopes used in s.r. bondar
570	photon.sig	formatted	Opened when the photon transport calculation is

Logical Unit	Name/status	Format	Usage
			requested (NPROB = -2)
800+iprob	scratch	formatted	temporary saving for fine-group micro cross sections when nstage>0 and npun(lbj)=1
860+iprob	ztit(iprob)	formatted	broad-group micro cross sections when nstage>0 and npun(lbj)=1
900+ifreg	scratch	formatted	temporary finegroup macroscopic file when NSTAGE=3 and NFREG > 1 (1 ≤ ifreg ≤ NFREG), copied to file 443 for postprocessing and subsequent 1-D transport calculation or temporary broad group macroscopic file when NSTAGE=2 and NFREG>0, copied to file 443 before calling s.r. pstpro
431	scratch	Direct access	total cross sections for Bondarenko self shielding
432	scratch	unformatted	static (adum) cross section file for region 1 in ABH
433	scratch	unformatted	static (adum) cross section file for region 2 in ABH
434	scratch	unformatted	static (adum) cross section file for region 3 in ABH
436	scratch	unformatted	temporary flux and higher moments
438	scratch	unformatted	shielded bondarenko cross section file, adum, generated in s.r. bondar
440	scratch	unformatted	(sigaz(i), sigfz(i), sigsz(i), amul(i), i=1, np) for the principal resonance absorber after doppler broadening
441	scratch	unformatted	temporary (sigaz(i), sigfz(i), sigsz(i), amul(i), i=1, np) for the principal and admixed resonance absorbers before doppler broadening
442	scratch	unformatted	sa0, ss0, etc., and collision probability file for ABH
446	scratch	unformatted	(sigaz(i), sigfz(i), sigsz(i), amul(i), i=1, np) for the first admixed resonance absorber after doppler broadening
447	scratch	unformatted	(sigaz(i), sigfz(i), sigsz(i), amul(i), i=1, np) for the second admixed resonance absorber after broadening
448	scratch	unformatted	(sigaz(i), sigfz(i), sigsz(i), amul(i), i=1, np) for the third resonance absorber after Doppler broadening
449443	scratchscratch	unformattedformatted	formerly 3 in ANISN, angular flux storageformats and writes broad group output data in s.r. xscoal for post processing
444	scratch	unformatted	
450–499	scratch	unformatted	thermal cross section matrix cross sectionsmatrix for isotopes used in both s.r. bonche and bondar, is+449

## 6. INPUT DATA FILE (COMBINE.INP) ORGANIZATION

### 6.1 Multistage-Multiregion 1-D transport Level Input Data Records

Any variable names beginning with the letters I, J, K, L, M, or N are assumed to be of type INTEGER; otherwise, REAL. Each card is list-directed input.

**Record 1 Head Title** Up to 80 characters between the single or double quotes.

#### Record 2

Position	Name	Description of Data
Word 1	NPROB	$\geq 1$ Number of Problems ( $\leq 99$ ).
		-1 1-D neutron transport calculation only (requires files "anisnc4.lib" and "anisn.inp" present). Set 0 for Word 2 through Word 5. Cards 1 and 2 are only required.
		-2 1-D photon transport calculation only (requires files "photon.sig" and "neutron.flx" present). NSTAGE is used for the number of neutron groups. Set 0 for Word 3 through 6. Card 1, 2, 3, 5A, 5B, and 5C are only required.
Word 2	NSTAGE	Number of 1-D transport calculation stages.
		0 No 1-D transport calculation.
		$> 0$ Number of 1-D transport calculation stages (up to 3 stages). If NPROB = -2, NSTAGE = number of neutron groups in "neutron.flx"
Word 3	NFREG	0 If NSTAGE = 0 (0-D cell).
		$> 0$ Number of final regions if NSTAGE $> 0$ ( $\leq 50$ ).
		-1 One region requiring transbuckling buckling. Set NSTAGE = 1.
Word 4	NCOPF	Format flag for the final ASCII cross section output file.
		0 INL format.
		1 ANISN format.
		2 CCCC ISOTXS format (transport correction is performed for elastic cross sections in s.r. bondar).
		3 AMPX Working Library format for KENO5A.
-1 Generates additional "photon.sig" file, which contains photon production and photo-atomic cross sections, otherwise same as NCOPF = 0.		
Word 5	MIDEP	0 No additional special microscopic cross section such as (n,g), (n,p),... (n,heat), etc.
		1 Special microscopic cross sections such as (n,g), (n,p),... (n,heat), etc. are added in the microscopic output file "ZTIT" when NFREG $> 0$ . Also applies when NFREG = 0, NCOPF = 0, NSTAGE = 0, MICR = 1 (in 1010101 input record), and NPUN(I) = 1 (in 10302XX input record).
Word 6	IJNT	0 Regular cross section generation.
		1 For neutron only. Generates adjoint cross sections (macro only) if NPROB $> 0$ . If NPROB = -1 and IJNT = 1, a regular (forward) 1-D $S_n$ transport calculation will be performed, using the adjoint cross section file "anisnc4.lib," to obtain the djoint flux, provided that "anisn.inp" present.

These are the first and second cards in "combine.inp," which are always required. All words are required.

If NPROB  $> 0$  and NSTAGE=0, skip to Card 7A.

If NPROB  $> 0$  and NSTAGE=1 and NFREG=1, skip to 7A.

If NPROB  $> 0$  and NSTAGE=2, and NFREG=1, skip to Card 6A.

**Record 3 (if NFREG > 1 or NFREG = -1): Final Stage Neutron or Photon Transport Geometry**

Position	Name	Description of Data
Word 1	JGEOM	1-D geometry parameter
	1	Slab.
	2	Cylinder.
	3	Sphere.
Word 2	JSN	Order of angular quadrature (even integer only, 2/4/6/8/12/16 =S <sub>2</sub> / S <sub>4</sub> / S <sub>6</sub> .../ S <sub>16</sub> . 2 ≤ jsn ≤ 16 Level symmetric quadrature sets for slab, cylinder, and sphere geometry. -16 ≤ jsn ≤ -2 Gauss-Legendre quadrature sets for slab and spherical geometry only. 102 ≤ jsn ≤ 116 Double Gauss-Legendre quadrature sets for slab and spherical geometry only.
Word 3	ILB	Left boundary condition
	0	Vacuum(no reflection).
	1	Reflection (dΦ/dr=0).
	2	Periodic (angular flux leaving one boundary reenters at the other boundary).
	3	White boundary.
Word 4	IRB	Right boundary condition, same options as ILB.
Word 5	BK	Transverse buckling. For NPROB = -2 (photon transport), any (no effect).

If NPROB = -2 or BK >= 0, skip to Card 5A.

**Record 4A (if BK < 0): Number of Groups for Group and Regionwise Transverse Buckling**

Position	Name	Description of Data
Word 1	NGROUP	Number of groups for input transverse buckling. 1 < NGROUP <= 167

**Record 4B (if BK < 0): Energy Group Structure for the Transverse Buckling**

Position	Name	Description of Data
Word 1 to Word NGROUP	JGROUP(I)	Broad energy group structure starting with the <i>upper limit</i> of the first broad group. See Table 1 following input description. The upper limit of broad group number 1 must be the fine group number 1. I = 1,NGROUP.

**Record 4C (if BK < 0): Group and Regionwise Transverse Buckling**

Position	Name	Description of Data
Word 1 to Word NGROUP	BBK(I)	Buckling. I=1,NGROUP

Repeat Record 4C NFREG times.

**Record 5A (if NFREG > 1 or NFREG = -1 or NPROB = - 2): Final Stage Region Coordinates**

Position	Name	Description of Data
Word 1	XINT(1)	The left-most coordinate of the first zone.
Word 2	XINT(2)	The left-most coordinate of the second region.
Word NFREG	XINT(NREG)	The left-most coordinate of the last region.
Word NFREG+1	XINT(NREG+1)	The right-most coordinate of the last region.

**Record 5B (if NFREG > 1 or NFREG=-1): Final Stage Region Mesh Intervals**

Position	Name	Description of Data
Word 1	NINT(1)	Number of mesh intervals of the first region.
Word 2	NINT(2)	Number of mesh intervals of the second region.
Word NFREG	NINT(NREG)	Number of mesh intervals of the last region, total # of meshes $\leq 500$ .

**Record 5C (if NFREG > 1 or NFREG = -1): Final Stage Material Assignment to Region**

Position	Name	Description of Data
Word 1	MATR(1)	Material number assigned to the first region from the second word of Record 6A.
Word 2	MATR(2)	Material number assigned to the second region.
Word NFREG	MATR(NREG)	Material number assigned to the last region.

Note: No identical MATRs

**Record 6A (if NFREG > 1 or NFREG = -1): MATERIAL I description ( $1 \leq I \leq \text{NFREG}$ , sequential)**

Position	Name	Description of Data
Word 1	'm'	A single character without quotes.
Word 2	I	Material number 1, representing from JPROB(1) to KPROB(1).
Word 3	JPROB(I)	If (KPROB(I) > JPROB(I)), spatial coalescing into one region is performed after 1-D transport calculation according to Cards 6B, 6C, and 6D. (KPROB(I) - JPROB(I)) < 20.
Word 4	KPROB(I)	
Word 5	MATID(I)	Material ID, similar to 'mtlno' in the 1030101 card.
Word 6	ZTIT(I)	Title for this material (up to 18 characters between the two single or double quotes). Generates inl format "ztit" microscopic file regardless of "ncopf" designation.

If NFREG > 1 and JPROB(I) = KPROB(I), skip Cards 6B, 6C, and 6D.

**Record 6B (if KPROB(I) > JPROB(I) or NFREG = -1): "m" level 1-D transport Description**

Position	Name	Description of Data
Word 1	IRGEOM(I)	1-D geometry parameter ( see JGEOM in Card 3).
Word 2	IRSN(I)	Order of angular quadrature (even integer only, 2/4/6/8/12/16 =S <sub>2</sub> / S <sub>4</sub> / S <sub>6</sub> .../ S <sub>16</sub> (See JSN in Card 3).
Word 3	IRLB(I)	Left boundary condition (See ILB in Card 3).
Word 4	IRRB(I)	Right boundary condition, same options as IRLB(I).
Word 5	PF(I)	Packing fraction for the pebble bed application if applicable, otherwise 0.
Word 6	PEBRAD(I)	Pebble radius (cm) if applicable, otherwise 0.

Note: Word 4 and Word 5 are for diffusion coefficient correction to account for the neutron streaming in pebble beds as described in Reference 35.

**Record 6C (if KRPOB(1) > JPROB(1) or NFREG = -1): Coordinates for 1-D Transport**

$$NN = KPROB(I) - JPROB(I) + 1$$

Position	Name	Description of Data
Word 1	RINT(1)	The left-most coordinate of the fine first region.
Word 2	RINT(2)	The left-most coordinate of the second region.
Word NN	RINT(NN)	The left-most coordinate of the last region.
Word NN+1	RINT(NN+1)	The right-most coordinate of the last region.

**Record 6D (if KRPOB(1) > JPROB(1) or if NFREG = -1): Mesh Intervals for 1-D Transport**

Position	Name	Description of Data
Word 1	NRINT(1)	Number of mesh intervals of the first region.
Word 2	NRINT(2)	Number of mesh intervals of the second region.
Word NN	NRINT(NN)	Number of mesh intervals of the last region.

Repeat Records 6s ABS(NFREG) times.

**Record 7A: Problem I Description (1 ≤ I ≤ NPROB, sequential)**

Position	Name	Description of Data
Word 1	'p'	A single character without quotes.
Word 2	I	Problem number I.
Word 3	IONED	Type of problem to be performed. 0 Standard zero-dimensional COMBINE problem. 1 1-D first stage transport sequence, no spatial coalescing. 2 1-D first stage transport and then spatial coalescing into one region.
Word 4	NSTACK(I)	Number of cases in this problem (≤19). 1 If IONED = 0. > 1 Corresponds to the number of regions when IONED > 0.
Word 5	NSTACKID	Material ID of coalesced region, similar to 'mtlno' in the 1030101 card If NPROB=1, IONED = 0, and NSTACK(I) =1, NSTACKID = 0 is acceptable.

Note that when all stages (from first to third) are required, IONED in the first stage should be set to 2.

**Record 7B (if IONED > 0): "p" level 1-D Transport Description**

Position	Name	Description of Data
Word 1	IPGEOM(I)	1-D geometry parameter (See JGEOM in Card 3)
Word 2	IPSN(I)	Order of angular quadrature (See JSN in Card 3)
Word 3	IPLB(I)	Left boundary condition (See ILB in Card 3)
Word 4	IPRB(I)	Right boundary condition, same options as IRLB(1)

**Record 7C (if IONED > 0): Coordinates for 1-D transport**

Position	Name	Description of Data
Word 1	PINT(1,I)	The left-most coordinate of the fine first region
Word 2	PINT(2,I)	The left-most coordinate of the second region
Word NSTACK(I)	PINT(NSTACK(I),I)	The left-most coordinate of the last region
Word NSTACK(I)+1	PINT(NSTACK(I)+1,I)	The right-most coordinate of the last region.

**Record 7D (if IONED > 0): Mesh Intervals for 1-D Transport**

Position	Name	Description of Data
Word 1	NPINT(1,I)	Number of mesh intervals of the first region
Word 2	NPINT(2,I)	Number of mesh intervals of the second region
Word NSTACK(I)	NPINT(NSTACK(I),I)	Number of mesh intervals of the last region

Unless NPROB = -1 or -2, problem level input data records (Section 6.2) are required.

Repeat Records 7s and Section 6.2 input data records NPROB times.

Since the input is list-directed, each card consists of one line separated by commas or blanks, or multiple lines if values such as XINT require more than one line.

Microscopic cross sections are saved on “ztit” file, otherwise added to the macroscopic file as in the case of NSTAGE=0, or separately in the “combine.mic” file (only in INL format) when NSTAGE=1 and NFREG=1.

**Samples of “combine.inp” for NPROB = -1 or -2.**

**NPROB = -1 and IJNT=0.** Can be either regular or adjoint flux calculation depending on the ANISN input parameter ITH.

'Sn anisn neutron transport'

-1 0 0 0 0 0

**NPROB = -1 and IJNT=1.** Will perform a forward calculation, using the adjoint cross section file, to obtain the adjoint flux. Set ITH = 0 in the ANISN input.

'Sn anisn neutron transport'

-1 0 0 0 0 1

**NPROB = -2**

'Sn anisn photon transport'

-2 16 12 0 0 0

2 12 1 0 0.

0.0 30.8511 55.532 72.5 102.5 129.5 152.5 175.0 181.0 194.0 275.0 287.0 292.0

40 32 22 32 26 22 22 8 20 164 2 24

1 2 3 4 5 6 7 8 9 10 11 12

## 6.2 Problem Level Input Data Records

A problem consists of a title record, comment records (optional), data records, and a terminator record. A listing of the records is printed at the beginning of each problem. The order of the title, data, and comment records is unimportant, except that only the last title record or last data record having a particular data record number will be used.

When a format error is detected, a line containing a dollar sign (\$) located under the character causing the error and a comment giving the column of the error is printed. An error flag is set such that input processing continues, but the problem will be aborted at the end of input processing.

1. **Title Record.** *A title record must be entered for each problem.* A title record is identified by an equal sign (=) as the first nonblank character. The title record is normally placed first in the problem.
2. **Comment Records.** An asterisk (\*) or a dollar sign (\$) appearing as the first nonblank character identifies the record as a comment record. Blank records are treated as comment records. The only processing of comment records is the printing of contents. Comment records may be placed anywhere in the input file.
3. **Data Records.** The data records contain a varying number of fields, which may be integer, floating point, or alphanumeric. Blanks preceding and following fields are ignored.

The first field on a data record is a record number that must be an unsigned integer. If the first field has an error or is not an integer, an error flag is set. Consequently, data on the record are not used and the record will be identified by the record number in the list of unused data records. After each record number and the accompanying data are read, the record number is compared to previously entered record numbers. If a matching record number is found, the data entered on the previous record are replaced by the data on the current record. If the record being processed contains only a record number, the record number and the data entered on the previous record are deleted. If a record causes replacement or deletion of data, a statement is printed indicating that the record is a replacement.

A number field on a data record is started by either a digit (0 through 9), a sign (+ or -), or a decimal point (.). A comma or a blank (with one exception noted below) terminates a particular number field. The number field has a number part, and optionally, an exponent part. A number field without a decimal point or an exponent is an integer field; a number field with either a decimal point, an exponent, or both is a floating-point field. A floating-point field without a decimal point is assumed to have a decimal point immediately in front of the first digit. The exponent denotes the power of 10 to be applied to the number part of the field. The exponent part has an E and a sign (+ or -) followed by a number giving the power of 10. These rules for floating point numbers are identical to those for entering data in FORTRAN e or f format fields except that no blanks (one exception) are allowed between characters. Floating point data punched by FORTRAN programs can be read. To permit reading of floating point data, a blank following an E denoting an exponent is treated as a plus sign. Acceptable ways of entering floating-point numbers, all containing the quantity 12.45, are illustrated by six fields: 12.45, +12.45, 1245+2, 1.245+1, 1.245e1, and 1.245e+1.

4. **Terminator Records.** A record having a period as the first nonblank character is used as a terminator. Most previous input records are erased before the input to the next problem is processed. Therefore, each problem must contain a complete input data file sufficient for that type of problem. Also, the final problem is terminated by a period record.
5. **Data Record Summary.** A data record contains: the record number and a descriptive title of the data contained on the record; an explanation of any variable data input on this record; and the order of the data on the record, the variable name, and the input data requirements, where applicable. Any variable names beginning with the letters I, J, K, L, M, or N are of type INTEGER. Any variable names starting with another letter are of type REAL. After N words on a record, default values will be used for the rest. However, data items should not be skipped up to N words.

### 6.2.1 Title Record

A title record must be present for each problem and is identified by an equal sign (=) as the first character on the record.

### 6.2.2 Problem Basic Control Information Record 1010101

This record is required for each problem. The first four words are always required.  
(N words,  $4 \leq N \leq 9$ )

Position	Name	Description of Data
Word 1	NTYPE	Type of calculation to be performed. 1— Standard $B_1$ flux approximation if LEG = 1, or Standard $B_3$ flux approximation if LEG = 3. 2— Standard $P_1$ flux approximation if LEG = 1. $\gamma(E) = 1.0$ in Equation (31). 4— Cell calculation; fluxes, from the preceding problem will be used for averaging cross sections. Currents will be recalculated from Equations (37) using the $P_1$ approximation with $\gamma(E) = 1.0$ . 6— Blackness calculation; fluxes from the preceding problem will be used to obtain effective diffusion theory cross sections.
Word 2	LEG	1— $B_1$ or $P_1$ calculation. 3— $B_3$ calculation.
Word 3	NOI	Number of materials in the spectrum, cell or blackness calculation ( $1 < NOI \leq 120$ ).
Word 4	NOUG	Total number of broad groups in the spectrum, cell or blackness calculation ( $1 < NOUG < 167$ ).
Word 5	MICR	Microscopic cross section option (must be set to 1 if microscopic cross sections are to be output to the ASCII cross section file. 0— No average microscopic data desired. (Default) 1— Calculate average microscopic cross sections. Set to 1 if nstage=1.
Word 6	MSTU	Source option. 0 Unit source in fine group MGHS -1— Fission rate weighted spectrum will be used. N— Fission spectrum of the material XX in the 10420XX card (N = XX). When rabs in 1043XXY $\neq 0$ , MSTU is reset to -1. When NTYPE = 4, can be set to 0 (no effect).
Word 7	MGHS	Specifies fine group number for unit source. Required only if a unit source is desired, i.e., if MSTU=0. When NTYPE = 4, can be set to be 0 (no effect).
Word 8	MAXIT	Maximum number of iterations when up scattering is present. When 0, the code sets MAXIT = 500. The conversion iteration stops when satisfied either "CONV" or MAXIT criteria. When there is no up scattering, no iteration is needed.
Word 9	MAGE	Age calculation option. 0— No age calculation desired. (Default) 1— Age calculation desired.
Word 10	MNDFLG	0— No Mixed number density calculation. (Default) 1— Mixed number density calculation. Requires 1490001 record.

### 6.2.3 Energy Group Structure Record 10102YY

This record is required for the first case. The following cases or problems do not need this record. YY specifies up to 20 continuation records. (N words,  $1 \leq N \leq 167$ )

Position	Name	Description of Data
Word 1 to Word NOUG	NGP (I)	Broad energy group structure starting with the <i>upper limit</i> of the first broad group. ( $1 < I < 167$ ). See Table 1 following input description. The upper limit of broad group number 1 must be the fine group number 1 (corresponding to 20.0 MeV). $1 < \text{number of broad groups} < 167$

### 6.2.4 Resonance Calculation Option Record 102010Y.

This record is required only if Nordheim resonance calculations are to be performed for resonance materials. If this record is not present, NXSR = 0 for all materials. Y specifies up to 9 continuation records. (N words,  $1 \leq N \leq 50$ )

Position	Name	Description of Data
Word 1 to NOI	NXSR (I)	Resonance calculation option ( $1 < I < 50$ ).  0—Bondarenko self shielding treatment. 1—Nordheim self shielding treatment (use only for those isotopes with $iwr > 0$ , see Table 2).

### 6.2.5 Macroscopic Interface File Option Record 1030101

This record is only required for each problem for which macroscopic cross-section data are to be output to the interface file, combine.sig. (N words,  $2 \leq N \leq 5$ )

Position	Name	Description of Data
Word 1	IPUN	Macroscopic interface file data option. 1—Output the broad-group macroscopic cross sections to the ASCII cross-section file (combine.sig). 2—Output both the broad-group macroscopic cross sections (combine.sig) and the ASCII fine-group fluxes (combine.flx).
Word 2	MTLNO	Material number used to reference interface file macroscopic cross-section data. If $MTL(I) < 900$ , isotope chi values will be added in the '5d' record of the ISOTXS format, having ICHI set to 1, regardless whether they are all 0.0.
Word 3	IAD	Option parameter that will be placed in Columns 2 and 3 of the title record accompanying the macroscopic data to indicate to the diffusion or transport theory codes how these data are to be used in updating a cross-section library file associated with these codes. (Used only with INL format). 0—Completely replace material MTLNO on the library tape. (Default) 1—Replace only those values on the library tape for material MTLNO which are entered on the interface records.
Word 4	IDIFF	Option parameter that will be placed in columns 4 and 5 of the title record accompanying the diffusion or transport theory codes indicating whether to use the values of the diffusion coefficients or transport cross sections. (Used only with INL format). 0—Use the transport cross sections (Monoenergetic definition). (Default)

Position	Name	Description of Data
		1—Use the diffusion coefficients (Fick's law definition).

### 6.2.6 Microscopic Interface File Option Record 10302XX

These records are required only for those materials for which microscopic cross-section data are to be output to the interface file, combine.sig. The material number is indicated by XX ( $1 \leq XX \leq \text{NOI}$ ) (N words,  $2 \leq N \leq 4$ ). Also MICR on record 1010101 must be = 1.

Position	Name	Description of Data
Word 1	NPUN(I)	Microscopic interface file output option for material I. 0—Do not output microscopic data for this material. 1—Output self-shielded microscopic cross-section data are added in macroscopic output file (combine.sig). Set to 1 if nstage > 0.
Word 2	MTL(I)	Material number used to reference microscopic cross-section data for material I. This is used for INL and ISOTXS format output. For ANISN and AMPX format, the materials are output numbered in ascending order as processed. If MTL(I) < 900, isotope chi values will be added in the '5d' record of the ISOTXS format, having ICHI set to 1, regardless whether they are all 0.0. $0 < \text{MTL(I)} < 999$
Word 3	NAD(I)	Option parameter that will be placed in columns 2 and 3 of the title record accompanying the interface microscopic data for Material I to indicate to the diffusion or transport theory codes how these data are to be used in updating a cross-section library file associated with these codes. (Used only with INL format). 0—Completely replace material MTL(I) on library file. (Default) 1—Replace only those values on the library file for material MTL(I) that are entered on the records.
Word 4	NDIFF(I)	Option parameter that will be placed in columns 4 and 5 of the title record accompanying the interface microscopic data for material I to indicate to the diffusion or transport theory codes whether to use the values of either the transport cross section or the values of the quantity $1/(3\sigma_{tr})$ . (Used only with INL format). 0—Use the transport cross section (monoenergetic definition). (Default) 1—Use the quantity $1/(3\sigma_{tr})$ (Fick's law definition).

If nstage = 0 and npun(lbj) == 1, microscopic edit will be added in the macroscopic file (combine.sig).

If nstage = 1 and nfreg=1, inl format microscopic file, "combine.mic" is always generated.

If nstage > 1 and. nfreg >1, inl format microscopic files with names "ztit" in Record 6A are always generated.

## 6.3 Floating Point Data Records

### 6.3.1 General Floating Point Data Record 1041001

This record is required for each problem. (N words,  $1 \leq N \leq 3$ )

Position	Name	Description of Data
Word 1	BUCK	Constant buckling, cm-2 ( $B^2$ value must be nonzero and positive). -1.0—Read 14700YY and 14710YY records for broad group wise buckling and buck sign. Requires 14700YY and 14710YY records.
Word 2	BUCKSIGN	0.0—Exp (-iBx) spatial distribution, i.e., fundamental mode cosine shape. (Default) -1.0—Exp (-Bx) spatial distribution +1.0—Exp (+Bx) spatial distribution Applied when BUCK > 0.0.
Word 3	CONV	Convergence criteria for fluxes and currents or for renormalization factor. (If not specified or zero, the code sets CONV = 0.00001.)

### 6.3.2 Material Specification Record 10420XX

These records are required for each problem. The material number is indicated by XX ( $1 \leq XX \leq \text{NOI}$ ). (N words,  $3 \leq N \leq 6$ )

Position	Name	Description of Data
Word 1	BISO(I)	ENDF material identification number for Ith material.
Word 2	TISO(I)	Temperature (K) for Ith material.
Word 3	DENS(I)	Homogeneous atom density $\times 10^{-24}$ of the Ith material. May not be zero. Set to a very small number to force an infinite dilution calculation.
Word 4	THERMS(I)	0.0—static thermal scattering (no upscattering). (Default) 1.0—free gas thermal scattering (will include upscattering). (see Table 3) 2.0—S( $\alpha, \beta$ ) thermal scattering (will include upscattering). (see Table 3)
Word 5	EPFISS(I)	Total thermal energy yield/fission (w-sec/fiss). (Default = 0.0)
Word 6	SSFF(I)	Self-shielding factor flag for Ith material. 0.0—no input of additional self-shielding factors. (Default) 1.0—additional self-shielding factors input by broad group. The self-shielding factors are input on records 146XXYY. All cross sections already processed either by Bondarenko self-shielding treatment or by additional ABH or Nordeim treatment will be multiplied by these additional self-shielding factors. Care should be taken when this option is used.

### 6.3.3 Material Resonance Specification Record 1043XXY

These records are required only for those materials for which a resonance calculation is to be performed and for those materials for which resolved resonance parameters are present in “reres.lib.” XX indicates the material number where ( $1 < XX < \text{NOI}$ ) and Y specifies up to 9 continuation records. These records are used for the Nordheim resonance treatment when NXSR = 1.0 and also for the heterogeneous effect in the Bondarenko treatment when NXSR = 0.0. (N words,  $3 < N < 23$ )

Position	Name	Description of Data
Word 1	TEMP(I)	Temperature (K) of absorber lump.
Word 2	GEOM(I)	Geometry of absorber lump. 0.0—Homogeneous medium. DENS(I) is atom density. (see 10420XX record) 1.0—Slab Geometry heterogeneous. 2.0—Cylindrical Geometry heterogeneous. 3.0—Spherical Geometry heterogeneous.
Word 3	DZERO(I)	Heterogeneous absorber atom density in absorber lump $\times 10^{-24}$ . May not be zero. Set to a very small number to force an infinite dilution calculation.
Word 4	ABAR(I)	Lump dimension—radius of cylinder or sphere or thickness of slab in centimeters. Radius of fuel kernel in the TRISO type fuel.
Word 5	CIN(I)	Dancoff-Ginsburg fuel lump correction factor or option flag. (If no shadowing, CIN = 0.0, also CIN is not used if IGEOM(I) = 0.) 0.0 to 1.0—Value of the correction factor CIN which is to be read in. 2.0—Calculate correction factor (cylinders only). 3.0—Same as for “last material,” which required a correction factor. (Caution: The user should exercise care in using this option.) “Last Material” here means preceding MATXS ID in the order on library file.
Word 6	ELZERO(I)	Not used.
Word 7	CZERO(I)	Not used.
Word 8	S(I)	0.0—Use $\phi_{lump}$ . (Default). 1.0—Calculate volume fraction weighted cross sections between those over the lump flux ( $\phi_{lump}$ ) and those over the asymptotic flux ( $\phi_{asym}$ ) outside the lump.
Word 9	AMOD(I,1)	First admixed moderator ID. The XX in 10420XX record (not BISO). (Real)
Word 10	AMOD(I,2)	Second admixed moderator ID. The XX in 10420XX record. (Real)
Word 11	AMOD(I,3)	Third admixed moderator ID. The XX in 10420XX record. (Real)
Word 12	ADENM(I,1)	Atomic density of the first admixed moderator, AMOD(I,1).
Word 13	ADENM(I,2)	Atomic density of the second admixed moderator, AMOD(I,2).
Word 15	RABS(I,1)	First admixed resonance absorber ID. The XX in 10420XX record (not BISO). (Real). The material should have resolved resonance parameters present in reres.lib.
Word 16	RABS(I,2)	Second admixed resonance absorber ID. The XX in 10420XX record. (Real)
Word 17	RABS(I,3)	Third admixed resonance absorber ID. The XX in 10420XX record. (Real) For RABSs, resolved resonance parameters are present in “reres.lib.”
Word 18	ADENABS(I,1)	Atomic density of the first admixed resonance absorber, RABS(I,1).
Word 19	ADENABS(I,2)	Atomic density of the second admixed resonance absorber, RABS(I,2).
Word 20	ADENABS(I,3)	Atomic density of the third admixed resonance absorber, RABS(I,3).
Word 21	RTYPE1(I)	= 0.0—All waves available in RERES.LIB. (Default) > 0.0—s-wave only.
Word 22	RTYPE2(I)	= 0.0—Use $E_{high}$ as in the RERES.LIB. (Default) > 0.0—Reset $E_{high}$ to RTYPE2(I).
Word 23	RTYPE3(I)	= 0.0—Use $E_{low}$ as in the RERES.LIB. (Default, currently set to 0.0125 eV) > 0.0—Reset $E_{low}$ to RTYPE3(I).
Word 24	RTYPE4(I)	> 10.0—NINT(RTYPE4(I)) is the minimum number of mesh points per resonance (Default, set to 10). Currently, the code sets the maximum number of mesh points per resonance to 1400.

### 6.3.4 Material Dancoff Specification Record 1044XXY

These records are required for all materials for which a fuel lump Dancoff calculation is to be performed. XX indicates the material number where  $1 \leq XX \leq \text{NOI}$ , and Y specifies up to 9 continuation records. (N words,  $8 \leq N \leq 12$ )

Position	Name	Description of Data
Word 1	REG(I)	Number of nonabsorber regions in unit cell (REG(I) < 5).
Word 2	XK(I)	Lattice arrangement of cylindrical pins. 1.0—Rectangular. 2.0—Hexagonal.
Word 3	RADX(I,1)	Outer radius, in centimeters, of first nonabsorber region in unit cell, i.e., region immediately adjacent to absorber lump. ABAR(I) on record 10430IY is the radius of the absorber $R_0$ in Equations (76) and (78).
Word 4	RADX(I,2)	Outer radius of second nonabsorber region in unit cell.
Word 5	RADX(I,3)	Outer radius of third nonabsorber region in unit cell.
Word 6	RADX(I,4)	Outer radius of fourth nonabsorber region in unit cell.
Word 7	RADX(I,5)	Outer radius of fifth nonabsorber region in unit cell.
Word 8	SIG(1,1)	Macroscopic total cross section of first nonabsorber region in unit cell.
Word 9	SIG(I,2)	Macroscopic total cross section of second nonabsorber region in unit cell.
Word 10	SIG(I,3)	Macroscopic total cross section of third nonabsorber region in unit cell.
Word 11	SIG(I,4)	Macroscopic total cross section of fourth nonabsorber region in unit cell.
Word 12	SIG(I,5)	Macroscopic total cross section of fifth nonabsorber region in unit cell.

*NOTE: The macroscopic total cross section in each nonabsorber region is the average macroscopic scattering plus absorption cross section in the resolved resonance range  $\Sigma_i$  in Equation (78). The radius of the last nonabsorber region is the average radius of the unit cell based on the last moderator volume in the hexagonal or square lattice pitch.*

### 6.3.5 Material General Resonance Data Record 10450XX

These records are required only for those materials for which the user desires to modify the standard resonance calculational procedure. XX indicates that material number where  $1 \leq XX \leq \text{NOI}$ . (N words,  $1 \leq N \leq 3$ ).

Position	Name	Description of Data
Word 1	THERMUP(I)	0.0—No thermal upscattering in the Nordheim resonance treatment. (Default) 1.0—Thermal upscattering in the Nordheim resolved resonance treatment.
Word 2	FMULT(I)	A factor which will multiply the recommended mesh spacing to obtain a coarse or finer mesh to use in performing the resolved resonance calculation. Default value is 1.0. If less than 1.0, less meshes are used. If greater than 1.0, more meshes are used. The maximum number of mesh intervals per resonance, however, is limited to 904. The minimum is 10.
Word 3	XLMT(I)	0.0—All resonances are used in constructing cross sections. (Default) X—The number of neighboring resonances in either direction to be considered. (Not recommended)

### 6.3.6 Material Self-Shielding Factor Records (146XXYY)

These records are required only for those materials if self-shielding factors are to be input, i.e., if  $SSFF(I) = 1.0$  for material XX. NOUG values must be input. XX specifies the material number, where  $1 < XX < NOI$ , and YY specifies up to 20 continuation records.

Position	Name	Description of Data
Word 1 to NOUG	SSFGBG(J)	Self-shielding factors for material I (specified by XX) and broad group J, listed in consecutive order.  ( $1 < J < NOUG$ )  These data are necessary only for those materials that require self-shielding factors. Input self-shielding factors in the epithermal energy groups for materials with a resonance range will double self-shield resonance materials which are automatically self-shielded on records 1044XXY. Input self-shielding factors in this energy range should be 1.0 or an infinitely dilute resonance calculation should be performed to prevent double self-shielding of resonances (caveat emptor).

### 6.3.7 Broad Group Buckling Factor Records (14700YY)

This record is required only if broad group wise buckling is to be input, i.e., if  $buck \leq 0.0$  for the problem. NOUG nonzero and positive values must be input. YY specifies up to 20 continuation records. (NOUG words).

Position	Name	Description of Data
Word 1 to NOUG	BUCKBG(J)	Broad group wise buckling corresponding to 101020Y record. ( $1 \leq J \leq NOUG$ ) (must be nonzero and positive)

### 6.3.8 Broad Group Buckling Sign Records (14710YY)

This record is required only if broad group wise buckling is present in 14700YY record. NOUG values must be input. YY specifies up to 20 continuation records. (NOUG words).

Position	Name	Description of Data
Word 1 to NOUG	GBSIGN(J)	Broad group wise buckling sign corresponding to 14700YY record. ( $1 \leq J \leq NOUG$ ).  0.0— exp (-iBx) spatial distribution, i.e., fundamental mode cosine shape. -1.0— exp (-Bx) spatial distribution +1.0— exp (+Bx) spatial distribution

### 6.3.9 Blackness calculation option Record (1480001)

This record is required if the blackness calculation has been requested on Record 1010101 (NTYPE = 6). (N words,  $2 \leq N \leq 5$ ).

Position	Name	Description of Data
Word 1	TH	Thickness of highly absorbing region, in centimeters, for which a "Blackness theory" calculation of effective diffusion constants is desired.
Word 2	H	Width of mesh, in centimeters, used to describe the interior of a highly absorbing region in a diffusion theory calculation.
Word 3	CB	A quantity occurring in the blackness theory equations which can be approximated by $3 \left( \frac{\sum_{tr}}{\sum_t} \right)$ where $\sum_{tr}$ and $\sum_t$ represent the transport and total cross sections, respectively, for the regions immediately surrounding the blackness region. (Default = 3.0, assuming $\frac{\sum_{tr}}{\sum_t}$ to be unity)
Word 4	AK1	First blackness coefficient. (usually set to 1.0). (Default = 1.0)
Word 5	AK2	Second blackness coefficient. (usually set to 1.0). (Default = 1.0)

### 6.3.10 MND calculation option Record (1490001)

If the MND option has been requested on Card 1010101 (MNDFLG = 1), MND constants will be printed out for  $D$ ,  $\Sigma_a$ ,  $\Sigma_f$  macro and  $\sigma_{tr}$ ,  $\sigma_a$ ,  $\sigma_f$  microscopic cross sections. No MND constants will be output in the ASCII file. The other cross sections that are output will not be MND constants. (N words,  $2 \leq N \leq 2$ )

Position	Name	Description of Data
Word 1	IENDMN (Integer)	Highest fine energy group included in MND calculation.
Word 2	TPMND	Temperature of Maxwellian spectrum for MND calculation.

NOTE: *The MND option can only be used for a single thermal group. No multithermal group MND option is defined.*

## 7. LIBRARY DATA ORGANIZATION

### 7.1 Fine Energy Neutron Group Structure

Group Number	Upper Energy (eV)						
1	2.0000E+07	43	9.6112E+02	85	1.1300E+00	127	3.5000E-01
2	1.6905E+07	44	7.4852E+02	86	1.1250E+00	128	3.4000E-01
3	1.4918E+07	45	5.8295E+02	87	1.1100E+00	129	3.3000E-01
4	1.3499E+07	46	4.5400E+02	88	1.0900E+00	130	3.2000E-01
5	1.1912E+07	47	3.5358E+02	89	1.0800E+00	131	3.1000E-01
6	1.0000E+07	48	2.7536E+02	90	1.0700E+00	132	3.0000E-01
7	7.7880E+06	49	2.1445E+02	91	1.0600E+00	133	2.9000E-01
8	6.0653E+06	50	1.6702E+02	92	1.0500E+00	134	2.8000E-01
9	4.7237E+06	51	1.3007E+02	93	1.0250E+00	135	2.7000E-01
10	3.6788E+06	52	1.0130E+02	94	1.0000E+00	136	2.6000E-01
11	2.8650E+06	53	7.8893E+01	95	9.9000E-01	137	2.5000E-01
12	2.2313E+06	54	6.1442E+01	96	9.8000E-01	138	2.4000E-01
13	1.7377E+06	55	4.7851E+01	97	9.7000E-01	139	2.3000E-01
14	1.3534E+06	56	3.7267E+01	98	9.5000E-01	140	2.2000E-01
15	1.0540E+06	57	2.9023E+01	99	9.3000E-01	141	2.0000E-01
16	8.2085E+05	58	2.2603E+01	100	9.1000E-01	142	1.8000E-01
17	6.3928E+05	59	1.7603E+01	101	8.9000E-01	143	1.6000E-01
18	4.9787E+05	60	1.3710E+01	102	8.7600E-01	144	1.4000E-01
19	3.8774E+05	61	1.0677E+01	103	8.5000E-01	145	1.2000E-01
20	3.0197E+05	62	8.3153E+00	104	8.0000E-01	146	1.0000E-01
21	2.3518E+05	63	6.4760E+00	105	7.5000E-01	147	9.5000E-02
22	1.8316E+05	64	5.0435E+00	106	7.0000E-01	148	9.0000E-02
23	1.4264E+05	65	3.9279E+00	107	6.8300E-01	149	8.5000E-02
24	1.1109E+05	66	3.0590E+00	108	6.5000E-01	150	8.0000E-02
25	8.6517E+04	67	2.3824E+00	109	6.2500E-01	151	7.5000E-02
26	6.7379E+04	68	2.3300E+00	110	6.0000E-01	152	7.0000E-02
27	5.2475E+04	69	2.2900E+00	111	5.9000E-01	153	6.5000E-02
28	4.0868E+04	70	2.2000E+00	112	5.7500E-01	154	6.0000E-02
29	3.1828E+04	71	2.1000E+00	113	5.5000E-01	155	5.0000E-02
30	2.4788E+04	72	2.0000E+00	114	5.3200E-01	156	4.0000E-02
31	1.9305E+04	73	1.9000E+00	115	5.0000E-01	157	3.0000E-02
32	1.5034E+04	74	1.8600E+00	116	4.9000E-01	158	2.5000E-02
33	1.1709E+04	75	1.7800E+00	117	4.8000E-01	159	2.0000E-02
34	9.1188E+03	76	1.7000E+00	118	4.7500E-01	160	1.5000E-02
35	7.1017E+03	77	1.6000E+00	119	4.7000E-01	161	1.0000E-02
36	5.5308E+03	78	1.5000E+00	120	4.6000E-01	162	8.0000E-03
37	4.3074E+03	79	1.4400E+00	121	4.5000E-01	163	7.0000E-03
38	3.3546E+03	80	1.3500E+00	122	4.3000E-01	164	5.0000E-03
39	2.6126E+03	81	1.3000E+00	123	4.2000E-01	165	4.0000E-03
40	2.0347E+03	82	1.2500E+00	124	4.1400E-01	166	2.0000E-03
41	1.5846E+03	83	1.2000E+00	125	3.8000E-01	167	1.0000E-03
42	1.2341E+03	84	1.1500E+00	126	3.6000E-01		1.0000E-05

## 7.2 Photon Group Structure

Group Number	Upper Energy (eV)
1	1.1E+07
2	8.0E+06
3	6.0E+06
4	4.0E+06
5	3.0E+06
6	2.5E+06
7	2.0E+06
8	1.5E+06
9	1.0E+06
10	7.0E+05
11	4.5E+05
12	3.0E+05
13	1.5E+05
14	1.0E+05
15	7.0E+04
16	4.5E+04
17	3.0E+04
18	2.0E+04
	1.0E+04

## 7.3 Materials in the “MATXS” Cross Section Libraries (MATXS and MATNG), and the “RERES” Resolved Resonance Library

Element/ isotope	ENDF/B Material ID	Resolved Resonance in reres.lib *	Thermal Scattering **	Element/ Isotope	ENDF/B Material ID	Resolved Resonance in reres.lib	Thermal Scattering
H-1	124	0	f	Mg-24	1225	0	f
H-1	125	0	H in H <sub>2</sub> O	Mg-25	1228	0	f
H-1	126	0	H in ZrH	Mg-26	1231	0	f
H-1	127	0	H in Ch2	Al-27	1325	3	f
H-2	128	0	D in D <sub>2</sub> O, f	Al-27	1326	3	S(α,β)
H-3	131	0	f	Si-28	1425	3	f
He-3	225	0	f	Si-29	1428	3	f
He-4	228	0	f	Si-30	1431	3	f
Li-6	325	0	f	P-31	1525	0	f
Li-7	328	0	f	S-32	1625	2	f
Be-9	425	0	Be-metal	S-33	1628	2	f
Be-9	426	0	Be in BeO	S-34	1631	2	f
B-10	525	0	f	S-36	1637	0	f
B-11	528	0	f	Cl-35	1725	0	f
C	600	0	graphite, f	Cl-37	1731	0	f
N-14	725	0	f	Ar-36	1825	2	f
N-15	728	0	f	Ar-38	1831	2	f
O-16	825	0	f	Ar-40	1837	3	f
O-16	826	0	O in BeO	K-39	1925	2	f
O-16	827	0	O in UO <sub>2</sub>	K-40	1928	0	f
O-17	828	0	f	K-41	1931	2	f
F-19	925	0	f	Ca-40	2025	2	f
Na-22	1122	0	f	Ca-42	2031	2	f
Na-23	1125	2	f	Ca-43	2034	2	f

Element/ isotope	ENDF/B Material ID	Resolved Resonance in reres.lib *	Thermal Scattering **	Element/ Isotope	ENDF/B Material ID	Resolved Resonance in reres.lib	Thermal Scattering
Ca-44	2037	2	f	Kr-83	3640	2	f
Ca-46	2043	0	f	Kr-84	3643	2	f
Ca-48	2049	2	f	Kr-85	3646	2	f
Sc-45	2125	2	f	Kr-86	3649	2	f
Ti-46	2225	2	f	Rb-85	3725	2	f
Ti-47	2228	2	f	Rb-86	3728	2	f
Ti-48	2231	2	f	Rb-87	3731	2	f
Ti-49	2234	2	f	Sr-84	3825	2	f
Ti-50	2237	2	f	Sr-86	3831	2	f
V	2300	5	f	Sr-87	3834	2	f
Cr-50	2425	3	f	Sr-88	3837	2	f
Cr-52	2431	3	f	Sr-89	3840	0	f
Cr-53	2434	3	f	Sr-90	3843	0	f
Cr-54	2437	3	f	Y-89	3925	2	f
Mn-55	2525	2	f	Y-90	3928	2	f
Fe-54	2625	3	f	Y-91	3931	0	f
Fe-56	2631	3	f	Zr	4000	5	Zr in ZrH
Fe-56	2632	3	S( $\alpha,\beta$ )	Zr-90	4025	2	f
Fe-57	2634	3	f	Zr-91	4028	2	f
Fe-58	2637	3	f	Zr-92	4031	2	f
Co-58	2722	2	f	Zr-93	4034	2	f
Co-58m	2723	2	f	Zr-94	4037	2	f
Co-59	2725	3	f	Zr-95	4040	0	f
Ni-58	2825	3	f	Zr-96	4043	2	f
Ni-59	2828	2	f	Nb-93	4125	1	f
Ni-60	2831	3	f	Nb-94	4128	2	f
Ni-61	2834	3	f	Nb-95	4131	0	f
Ni-62	2837	3	f	Mo-92	4225	2	f
Ni-64	2843	3	f	Mo-94	4231	2	f
Cu-63	2925	3	f	Mo-95	4234	2	f
Cu-65	2931	3	f	Mo-96	4237	2	f
Zn	3000	5	f	Mo-97	4240	2	f
Ga-69	3125	2	f	Mo-98	4243	2	f
Ga-71	3131	2	f	Mo-99	4246	0	f
Ge-70	3225	2	f	Mo-100	4249	2	f
Ge-72	3231	2	f	Tc-99	4325	2	f
Ge-73	3234	2	f	Ru-96	4425	0	f
Ge-74	3237	2	f	Ru-98	4431	0	f
Ge-76	3243	2	f	Ru-99	4434	2	f
As-74	3322	2	f	Ru-100	4437	2	f
As-75	3325	2	f	Ru-101	4440	2	f
Se-74	3425	2	f	Ru-102	4443	2	f
Se-76	3431	2	f	Ru-103	4446	2	f
Se-77	3434	2	f	Ru-104	4449	2	f
Se-78	3437	2	f	Ru-105	4452	0	f
Se-79	3440	0	f	Ru-106	4455	0	f
Se-80	3443	2	f	Rh-103	4525	2	f
Se-82	3449	2	f	Rh-105	4531	1	f
Br-79	3525	2	f	Pd-102	4625	2	f
Br-81	3531	2	f	Pd-104	4631	2	f
Kr-78	3625	2	f	Pd-105	4634	2	f
Kr-80	3631	2	f	Pd-106	4637	2	f
Kr-82	3637	0	f	Pd-107	4640	2	f

Element/ isotope	ENDF/B Material ID	Resolved Resonance in reres.lib *	Thermal Scattering **	Element/ Isotope	ENDF/B Material ID	Resolved Resonance in reres.lib	Thermal Scattering
Pd-108	4643	2	f	Xe-124	5425	2	f
Pd-110	4649	2	f	Xe-126	5431	2	f
Ag-107	4725	2	f	Xe-128	5437	2	f
Ag-109	4731	2	f	Xe-129	5440	2	f
Ag-110m	4735	2	f	Xe-130	5443	2	f
Ag-111	4737	2	f	Xe-131	5446	2	f
Cd-106	4825	2	f	Xe-132	5449	2	f
Cd-108	4831	2	f	Xe-133	5452	0	f
Cd-110	4837	2	f	Xe-134	5455	2	f
Cd-111	4840	2	f	Xe-135	5458	1	f
Cd-112	4843	2	f	Xe-136	5461	2	f
Cd-113	4846	2	f	Cs-133	5525	2	f
Cd-114	4849	2	f	Cs-134	5528	2	f
Cd-115m	4853	2	f	Cs-135	5531	2	f
Cd-116	4855	2	f	Cs-136	5534	0	f
In-113	4925	2	f	Cs-137	5537	0	f
In-115	4931	2	f	Ba-130	5625	2	f
Sn-112	5025	2	f	Ba-132	5631	2	f
Sn-113	5028	2	f	Ba-133	5634	2	f
Sn-114	5031	2	f	Ba-134	5637	2	f
Sn-115	5034	2	f	Ba-135	5640	2	f
Sn-116	5037	2	f	Ba-136	5643	2	f
Sn-117	5040	2	f	Ba-137	5646	2	f
Sn-118	5043	2	f	Ba-138	5649	2	f
Sn-119	5046	2	f	Ba-140	5655	2	f
Sn-120	5049	2	f	La-138	5725	2	f
Sn-122	5055	2	f	La-139	5728	2	f
Sn-123	5058	0	f	La-140	5731	2	f
Sn-124	5061	2	f	Ce-136	5825	2	f
Sn-125	5064	2	f	Ce-138	5831	2	f
Sn-126	5067	0	f	Ce-139	5834	2	f
Sb-121	5125	2	f	Ce-140	5837	2	f
Sb-123	5131	2	f	Ce-141	5840	2	f
Sb-124	5134	0	f	Ce-142	5843	2	f
Sb-125	5137	0	f	Ce-143	5846	2	f
Sb-126	5140	2	f	Ce-144	5849	0	f
Te-120	5225	0	f	Pr-141	5925	2	f
Te-122	5231	2	f	Pr-142	5928	2	f
Te-123	5234	2	f	Pr-143	5931	2	f
Te-124	5237	2	f	Nd-142	6025	2	f
Te-125	5240	2	f	Nd-143	6028	2	f
Te-126	5243	2	f	Nd-144	6031	2	f
Te-127m	5247	0	f	Nd-145	6034	2	f
Te-128	5249	2	f	Nd-146	6037	2	f
Te-129m	5253	0	f	Nd-147	6040	2	f
Te-130	5255	2	f	Nd-148	6043	2	f
Te-132	5261	2	f	Nd-150	6049	2	f
I-127	5325	2	f	Pm-147	6149	2	f
I-129	5331	2	f	Pm-148	6152	0	f
I-130	5334	2	f	Pm-148m	6153	0	f
I-131	5337	0	f	Pm-149	6155	0	f
I-135	5349	0	f	Pm-151	6161	2	f
Xe-123	5422	0	f	Sm-144	6225	2	f

Element/ isotope	ENDF/B Material ID	Resolved Resonance in reres.lib *	Thermal Scattering **	Element/ Isotope	ENDF/B Material ID	Resolved Resonance in reres.lib	Thermal Scattering
Sm-147	6234	2	f	W-186	7443	2	f
Sm-148	6237	2	f	Re-185	7525	2	f
Sm-149	6240	2	f	Re-187	7531	2	f
Sm-150	6243	2	f	Ir-191	7725	2	f
Sm-151	6246	2	f	Ir-193	7731	2	f
Sm-152	6249	2	f	Au-197	7925	2	f
Sm-153	6252	2	f	Hg-196	8025	2	f
Sm-154	6255	2	f	Hg-198	8031	2	f
Eu-151	6325	2	f	Hg-199	8034	2	f
Eu-152	6328	2	f	Hg-200	8037	2	f
Eu-153	6331	2	f	Hg-201	8040	2	f
Eu-154	6334	2	f	Hg-202	8043	2	f
Eu-155	6337	2	f	Hg-204	8049	0	f
Eu-156	6340	2	f	Pb-204	8225	2	f
Eu-157	6343	2	f	Pb-206	8231	3	f
Gd-152	6425	3	f	Pb-207	8234	3	f
Gd-153	6428	3	f	Pb-208	8237	3	f
Gd-154	6431	3	f	Bi-209	8325	2	f
Gd-155	6434	3	f	Ra-223	8825	0	f
Gd-156	6437	3	f	Ra-224	8828	0	f
Gd-157	6440	3	f	Ra-225	8831	0	f
Gd-158	6443	3	f	Ra-226	8834	2	f
Gd-160	6449	3	f	Ac-225	8925	0	f
Tb-159	6525	2	f	Ac-226	8928	0	f
Tb-160	6528	3	f	Ac-227	8931	0	f
Dy-156	6625	2	f	Th-227	9025	0	f
Dy-158	6631	2	f	Th-228	9028	2	f
Dy-160	6637	2	f	Th-229	9031	2	f
Dy-161	6640	2	f	Th-230	9034	1	f
Dy-162	6643	2	f	Th-231	9037	0	f
Dy-163	6646	2	f	Th-232	9040	3	f
Dy-164	6649	2	f	Th-233	9043	0	f
Ho-165	6725	2	f	Th-234	9046	0	f
Ho-166m	6729	2	f	Pa-231	9131	3	f
Er-162	6825	2	f	Pa-232	9134	2	f
Er-164	6831	2	f	Pa-233	9137	3	f
Er-166	6837	2	f	U-232	9219	3	f
Er-167	6840	2	f	U-233	9222	3	f
Er-168	6843	2	f	U-233	9223	3	U in UO <sub>2</sub>
Er-170	6849	2	f	U-234	9225	2	f
Lu-175	7125	2	f	U-235	9228	3	f
Lu-176	7128	2	f	U-235	9229	3	U in UO <sub>2</sub>
Hf-174	7225	2	f	U-236	9231	2	f
Hf-176	7231	2	f	U-237	9234	1	f
Hf-177	7234	2	f	U-238	9237	3	f
Hf-178	7237	2	f	U-238	9238	3	U in UO <sub>2</sub>
Hf-179	7240	2	f	U-239	9240	1	f
Hf-180	7243	2	f	U-240	9243	1	f
Ta-181	7328	2	f	U-241	9246	1	f
Ta-182	7331	2	f	Np-235	9340	0	f
W-182	7431	2	f	Np-236	9343	2	f
W-183	7434	2	f	Np-237	9346	2	f
W-184	7437	2	f	Np-238	9349	0	f

Element/ isotope	ENDF/B Material ID	Resolved Resonance in reres.lib*	Thermal Scattering**	Element/ Isotope	ENDF/B Material ID	Resolved Resonance in reres.lib	Thermal Scattering
Np-239	9352	0	f	Cm-244	9637	2	f
Pu-236	9428	2	f	Cm-245	9640	2	f
Pu-237	9431	0	f	Cm-246	9643	2	f
Pu-238	9434	1	f	Cm-247	9646	1	f
Pu-239	9437	3	f	Cm-248	9649	1	f
Pu-240	9440	2	f	Cm-249	9652	2	f
Pu-241	9443	3	f	Cm-250	9655	2	f
Pu-242	9446	1	f	Bk-249	9752	2	f
Pu-243	9449	1	f	Bk-250	9755	2	f
Pu-244	9452	1	f	Cf-249	9852	2	f
Pu-246	9458	0	f	Cf-250	9855	1	f
Am-241	9543	1	f	Cf-251	9858	1	f
Am-242	9546	2	f	Cf-252	9861	1	f
Am-242m	9547	2	f	Cf-253	9864	1	f
Am-243	9549	1	f	Cf-254	9867	0	f
Am-244	9552	0	f	Es-253	9913	1	f
Am-244m	9553	0	f	Es-254	9914	0	f
Cm-241	9628	0	f	Es-255	9915	0	f
Cm-242	9631	1	f	Fm-255	9936	0	f
Cm-243	9634	1	f				

\* Presence of resolved resonance parameters in the reres.lib.

iwr = 0: No resonance parameters, includes only awr and ap

1: Single-Level Breit-Wigner (SLBW) format

2: Multilevel Breit-Wigner (MLBW) format

3: Reich-Moore (R-M) format

4: multi-isotope SLBW format

5: multi-isotope MLBW format

\*\* S( $\alpha,\beta$ ) thermal scattering, otherwise specified as "f," which is free-gas thermal scattering.

Cross sections are mostly processed at T=293, 900, 1300, and 2200 K and at  $\sigma_0 = 1.0e10e4, 1.0e2, 1.0$  barns. For some important isotopes, cross sections are processed with up to 10  $\sigma_0$  values and as low as 0.01 barns and up to 10 temperatures. For those having the S( $\alpha,\beta$ ) thermal scattering cross sections, the temperatures are dictated by the ENF/B-VII.0. The maximum temperature for free or S( $\alpha,\beta$ ) thermal scattering is 800 K for H-1 in H2O, 1200 K for H-1 in ZrH, 350 K for H-1 in CH2, 650 K for H-1 in D2O, 1200 K for Be, 1200 K for Be in BeO, 2000 K for graphite, 1200 K for O-16 in BeO, 1200 K for Zr in ZrH, 1200K for UO2, 800K for Al, 800K for Fe-56. Temperature in the combine input below the lowest or above the highest may cause a problem in the temperature interpolation.

## 7.4 MATXS.LIB File Description

```

-----
file structure
record type                               present if
=====
file identification                       always
file control                              always
set hollerith identification              always
file data                                 always
***** (repeat for all particles)
*      group structures                    always
*****
***** (repeat for all materials)
*      material control                    always
*
* ***** (repeat for all submaterials)
* *      vector control                    n1db.gt.0
* *
* * ***** (repeat for all vector blocks)
* * *      vector block                    n1db.gt.0
* * *****
* *
* * ***** (repeat for all matrix blocks)
* * *      matrix control                    n2d.gt.0
* * *
* * * ***** (repeat for all sub-blocks)
* * * *      matrix sub-block                n2d.gt.0
* * * *****
* * *
* * *      constant sub-block                jconst.gt.0
* * *
*****
-----

```

```

-----
file identification
hname, (huse(i), i=1,2), ivers
1+3*mult
format(4h 0v ,a8,1h*,2a8,1h*,i6)
hname      hollerith file name - matxs - (a8)
huse       hollerith user identification (a8)
ivers      file version number
mult       double precision parameter
           1- a8 word is single word
           2- a8 word is double precision word
-----

```

```

-----
file control
npart, ntype, nholl, nmat, maxw, length
format(6h 1d ,6i6)
npart      number of particles for which group
           structures are given
ntype      number of data types present in set
nholl      number of words in set hollerith
           identification record
nmat       number of materials on file
-----

```



---

```

material control
hmat,amass,(temp(i),sigz(i),itype(i),nld(i),n2d(i),
llocs(i),i=1,nsubm)
format(4h 5d ,a8,1p,2e12.5/(2e12.5,5i6))
hmat      hollerith material identifier
amass     atomic weight ratio
temp      ambient temperature or other parameters for
           submaterial i
sigz      dilution factor or other parameters for
           submaterial i
itype     data type for submaterial i
nld       number of vectors for submaterial i
n2d       number of matrix blocks for submaterial i
llocs     location of submaterial i

```

---

```

vector control
(hvps(i),i=1,nld),(nfg(i),i=1,nld),(nlg(i),i=1,nld)
format(4h 6d ,4x,8a8/(9a8))      hvps
format(12i6)                      iblk,nfg,nlg
hvps(i)  hollerith identifier of vector
           nelas      neutron elastic scattering
           n2n        (n,2n)
           nnf        second chance fission
           gabs       gamma absorption
           p2n        protons in, 2 neutrons out
           .          .
           .          .
           .          .
nfg(i)    number of first group in band for vector i
nlg(i)    number of last group in band for vector i

```

---

```

vector block
(vps(i),i=1,kmax)
kmax=sum over group band for each vector in block j
format(4h 7d ,8x,1p,5e12.5/(6e12.5))
vps(i)    data for group bands for vectors in block j.
           block size is determined by taking all the group
           bands that have a total length less than or equal
           to maxw.

```

---

```

scattering matrix control
hmtx,lord,jconst,
l(jband(l),l=1,noutg(k)),(ijj(l),l=1,noutg(k))
mult+2+2*noutg(k)
format(4h 8d ,4x,a8/(12i6))      hmtx,lord,jconst,
                                   jband,ijj
hmtx      hollerith identification of block
lord      number of orders present
jconst    number of groups with constant spectrum
jband(l)  bandwidth for group l
ijj(l)    lowest group in band for group l

```

---

```

    scattering sub-block
(scatt(k),k=1,kmax)
kmax=lord times the sum over all jband in the group range of
    this sub-block
format(4h 9d ,8x,1p,5e12.5/(6e12.5))
scatt(k)      matrix data given as bands of elements for initial
              groups that lead to each final group. the order
              of the elements is as follows: band for p0 of
              group i, band for p1 of group i, ... , band for p0
              of group i+1, band for p1 of group i+1, etc. the
              groups in each band are given in descending order.
              the size of each sub-block is determined by the
              total length of a group of bands that is less than
              or equal to maxw.
              if jconst.gt.0, the contributions from the jconst
              low-energy groups are given separately.

```

---



---

```

    constant sub-block
(spec(l),l=1,noutg(k)),(prod(l),l=11,ning(k))
l1=ning(k)-jconst+1
noutg(k)+jconst
format(4h10d ,8x,1p,5e12.5/(6e12.5))
spec          normalized spectrum of final particles for initial
              particles in groups l1 to ning(k)
prod          production cross section (e.g., nu*sigf) for
              initial groups l1 through ning(k)
              this option is normally used for the energy-independent
              neutron and photon spectra from fission and radiative
              capture usually seen at low energies.

```

---

## 7.5 Description of Resolved Resonance Library (reres.lib) Format

Card: title

For a material

Card: aid,iwr,awr,ap,elow,ehigh,nernis,mat (A10,I1,4E11.6,I11,I4)

If  $1 \leq iwr \leq 3$

For  $j=1, nernis$

Card: elt,eht,spi,ap,nls,naps,mat (4E11.6,2I11,I4)

For  $l=1, nls$

Card: nrj,qx,lrx,mat (I11,E11.6,I11,33X,I4)

For  $i=1, nrj$

Card: er,aj,gn,gg,gf,gt,mat (6E11.6,I4)

If  $iwr \geq 4$

Card: elt,eht,mat (2E11.6,44X,I4)

For  $j=1, nernis$

Card: awri,abn,naps,spi,ap,nls,mat (2E11.6,I11,2E11.6,I11,I4)

For  $l=1, \max(nls)$

Card: nrj,qx,lrx,mat (I11,E11.6,I11,33X,I4)

For  $i=1, nrj$

Card: igf,er,aj,gn,gg,gt,mat (I11,5E11.6,I4)

Repeat for materials

---

aid	material identification.
iwr	1 for single-level Breit-Wigner (SLBW), 2 for multilevel Breit-Wigner (MLBW), 3 for Reich-Moore, 4 for multiisotope SLBW, 5 for multiisotope MLBW.
awr	ratio of the material mass to that of a neutron.
ap	scattering radius in units of $10^{-12}$ cm.
elow	lower limit for the whole resolved resonance energy range (same as in ENDF/B-VII.0).
ehigh	upper limit for the whole resolved resonance energy range (same as in ENDFB-VII.0).
nernis*	number of energy ranges for $iwr=1, 2, 3$ or number of isotopes for $iwr=4, 5$ .
mat	ENDF/B-VII material identification number.
elt	lower limit for an energy range (adjusted for COMBINE7, differing from elow: see reres.lib).
eht	upper limit for an energy range.
nls	number of $l$ -values (neutron orbital angular momentum).
naps	flag controlling the use of the two radii.
nrj	number of resolved resonances for a given $l$ -value.
qx	Q-value to be added to the incident particle's center of-mass energy to determine the channel energy.
lrx	flag indicating whether this energy range contains a competitive width.
er	resonance energy.
aj	floating point value of $J$ (the spin, or total angular momentum of the resonance).
gn	neutron width, $\Gamma_n$ , evaluated at the resonance energy, er.
gg	radiation width, $\Gamma_g$ .
gf	fission width, $\Gamma_f$ ( $\Gamma_{fa}$ for R-M).
gt	resonance total width ( $\Gamma_{tb}$ for R-M).
awri	ratio of the mass of a particular isotope to that of a neutron
abn	the abundance of an isotope in the material
igf	isotope index

---

\* All have only one energy range except Pu-239 which has three energy ranges.

## 7.6 Cross section and constants internal record

The data in the internal master cross section library consist of alphanumeric, integer, and floating point records. The alphanumeric records are used for identification purposes, the integer data for the most part indicate the number and types of records to be read, and the floating point records make up the actual cross-section data.

The initial data records on the tape are used for identification and to indicate the number of materials, fission spectra, and energy groups in the library. Subsequent records describe the cross-section data, with similar types of data records being repeated for each material until all materials have been described. The materials are always arranged in the library so that the identification numbers are in ascending order. The cross-section data records in the library have been condensed as much as feasible to reduce the processing time. Therefore, the length and number of data records present for a particular material depend on the amount of data required to describe the pertinent cross sections. The minimum number of records in the library for any material is two and the maximum is four.

A detailed description of the arrangement of the data within the library, including the mnemonic names and meanings of the data in the order of their occurrences in the library is found below. The cross-section data records for each material are arranged as shown below and are repeated for each material.

### 7.6.1 First Data Record for Material k

Mnemonic Name	Description or Function of Data
BISO(IS)	Material number
LTOT	Integer indicating the total number of words of data contained in the cross-section vector ADUM
IWA	Absorption reaction flag. If IWA = 1, absorption cross sections are present.
IWF	Fission reaction flag. If IWF = 1, fission cross sections and the values of the average number of neutrons per fission are present. If IWA = 0, IWA is ignored.
IWS	=> No elastic scattering transfer matrices present 1 => Elastic scattering transfer matrices present
LOL(L)	Number of cross-section values in List L. L = 1 => inelastic transfer matrix is present if $ LOL1  = 1$ . L = 2 => N,2N transfer matrix is present if $ LOL2  = 1$ . L = 3 => P <sub>0</sub> and P <sub>1</sub> elastic transfer matrix is present if $ LOL3  = 1$ . L = 4 => P <sub>2</sub> and P <sub>3</sub> elastic transfer matrix is present if $ LOL4  = 1$ . L = 5 => P <sub>0</sub> , N, 3N transfer matrix is present if $ LOL5  = 1$ . L = 6 => P <sub>0</sub> , N, 4N transfer matrix is present if $ LOL6  = 1$ .

NOTE: *LOL(1) and LOL(2) negative implies P<sub>1</sub> inelastic or P<sub>1</sub>, N,2N matrices are also present in addition to P<sub>0</sub> matrices. In either case, P<sub>1</sub> matrix follows directly behind the P<sub>0</sub> matrix. The length of either matrix is  $|LOL(1)|$  or*

*$|LOL(2)|$ . LA and LD vectors apply to both P<sub>0</sub> and P<sub>1</sub> matrices in both cases. Only P<sub>0</sub>, N,3N and N,4N cross sections are allowed.*

Mnemonic Name	Description or Function of Data
LA(L)	Number of fine groups <i>scattered from</i> in list L, starting with the first fine group, i.e., number of the highest fine group for which scattering reaction of type I is present (threshold group).
LD(L)	Maximum number of fine groups scattered to in list L, i.e., the maximum number of groups downscattered (this value is constant for all groups in which a scattering reaction is tabulated for a particular material).
AW(IS)	The atomic weight ratio of this material.

## 7.6.2 Second Data Record for Material k

Mnemonic Name	Description or Function of Data
ADUM(I) (I = 1,LTOT)	<p>Vector containing the complete set of microscopic cross sections and values of neutrons produced per fission for material k. All scattering matrices are in this vector.</p> <p>The cross section values, if present, are contained in the vector in the following order:</p> <p>If IWA = 1, the first MAXG (the number of groups used) values are the absorption cross sections starting with group 1.</p> <p>If IWA = 1, and IWF = 1, the next MAXG values are the fission cross sections followed by MAXG values of neutrons produced per fission.</p> <p>If IWF = 1, the next MAXG values are the fluxes from MATXS.LIB followed by MAXG chi values (fission spectrum) for this material.</p> <p>If <math> LOL1  = 1</math>, the next LOL(1) values are the P0 inelastic cross sections for transfer from group I to group J. The list starts with I = 1 and contains the values for J ranging from 1 to LD(1) + 1. Then the values for I = 2 with J ranging from 2 to LD(1) + 2 are next, etc. until I = LA(1).</p> <p>There are LD(1) + 1 values listed for each I, as long as LD(1) + I ≤ MAXG. When LD(1) + I &gt; MAXG then only MAXG + 1 - I values are listed for I.</p> <p>If LOL1 = -1, the next LOL(1) values are the P1 inelastic cross sections for transfer from group I to group J. The structure of this list is identical to 4.</p> <p>If <math> LOL2  = 1</math>, next LOL(2) values are the P0 (n,2n) cross sections for transfer from group I to group J. The list is ordered as above for the inelastic data.</p> <p>If LOL2 = -1, the next LOL(2) values are the P1 (n,2n) cross sections for transfer from group I to group J. The structure of this list is identical to 6.</p> <p>If LOL3 = 1, the next LOL(3) values are the isotropic elastic scattering cross sections for transfer from group I to group J followed by the same number of values for the linearly anisotropic component of the elastic scattering cross sections from group I to group J.</p> <p>If LOL4 = 1, the next LOL(4) values are the P2 components of the elastic scattering cross sections for transfer from group I to J followed by the P3 components from group I to group J.</p> <p>If LOL5 = 1, the next LOL(5) values are the P0 (n,3n) cross sections for transfer from group I to group J. The list is ordered as above for the inelastic data. There is no P1 (n,3n) matrix.</p> <p>If LOL6 = 1, the next LOL(6) values are the P0 (n,4n) cross sections for transfer from group I to group J. The list is ordered as above for the inelastic data. There is no P1 (n,4n) matrix.</p>

## 7.7 Thermal $S(\alpha, \beta)$ and Free Scattering Cross Section Internal Record

itfile = 449 + is

l = group scattered from

jj = group scattered to

ljj = (l-1)\*maxg+jj

write (itfile) l, jj, therm0(ljj), therm1(ljj), therm2(ljj), therm3(ljj)

where

$1 \leq is \leq noi$  (noi = number of materials in the problem),

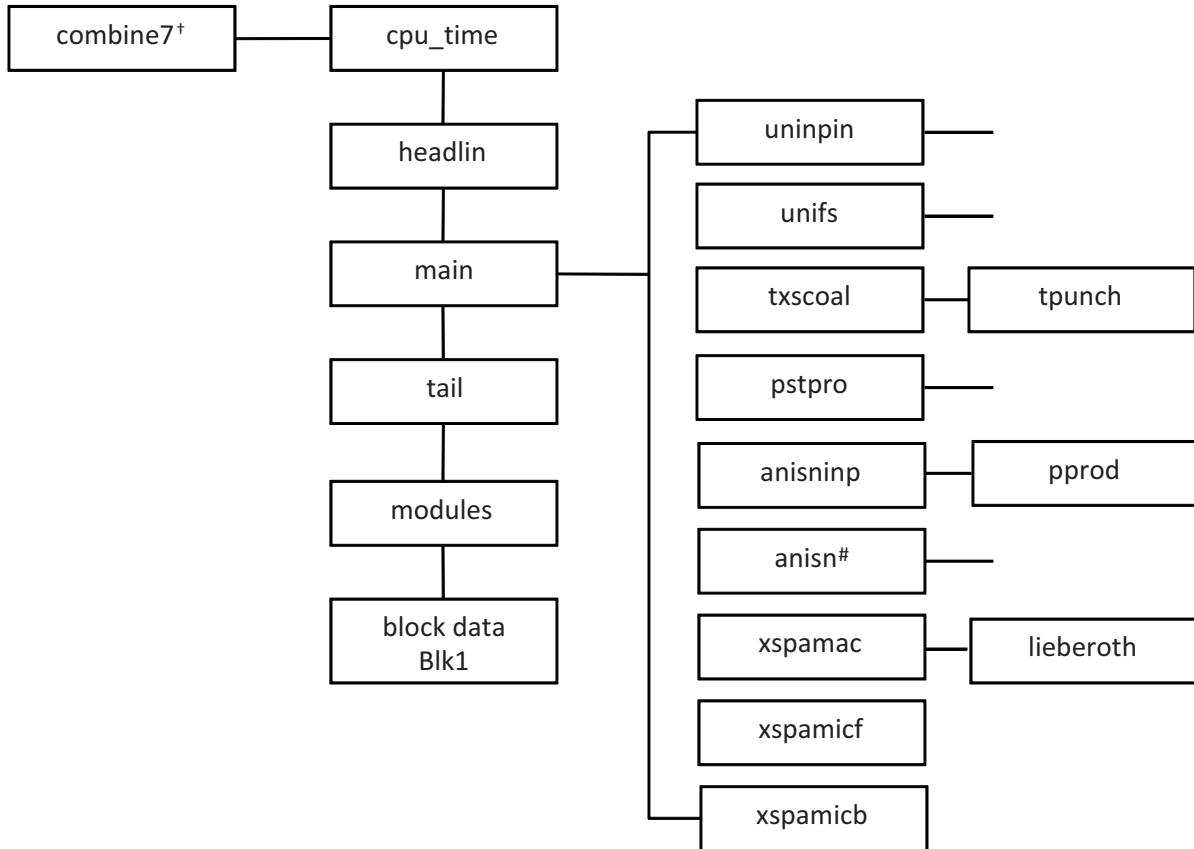
$65 \leq l \leq 167$  (fine groups in the thermal energy range),

$65 \leq jj \leq 167$  (fine groups in the thermal energy range)

## 8. PROGRAMMER'S GUIDE

COMBINE7.1 is written in FORTRAN 90 and is currently compiled using the Intel Visual Fortran compiler or the Lahey/Fujitsu (LF95) Fortran compiler on the Windows 32 platform. The Intel Visual Fortran compiler provides the faster run time. The source code is heavily commented to explain subroutine functions, data structures, etc. This section provides a short description of each subroutine and shows the overlay structure.

### 8.1 Flow Diagram



```

— uninpin - inp - inppck
- inpw
- inpcvi - inpalf
- inpalf
- unindat - uninin
- inp2 - iinkw
- inpmod - inpupk
- endck
- iinkw
- jinkw
- jnp2 - jinkw
- jnpmod - jnpupk
- err

— unifs - spectrum- mascot - output
- bondar - lethrg
- ginsburg- dancof
- skipr
- totes - skipr
- bonsig0
- phtonxs
- lethrg
- nordheim- reslib
- grid
- cross1 - facts
- facphi
- cross2 - facts
- facphi
- cross3 - facts
- facphi
- frobns - thrinv
- abcmat
- tbroad - movpanl
- broadn - bsigma - hunky - funky
- hnabb*
- funky
- admabs - reslib
- cross1 - facts
- facphi
- cross2 - facts
- facphi
- cross3 - facts
- facphi
- frobns - thrinv
- abcmat
- tbroad - movpanl
- broadn - bsigma - hunky - funky
- hnabb*
- funky
- resol - newbv - interp
- escape - newcyl
- newslb
- trapz
- samps*
- semps*
- somps*

```

				- sumps*
				- svmps*
				- swmps*
				- sxmps*
				- prnres
		- flux	- bone	
			- bthree	- eval
				- solv
			- age	
			- blknes	
	- xscoal	- coalesc		
		- mnd	- maxwel	
		- punch		
		- prtscat		
		- unpakk		
— pstpro	- stran	- contrl	- updn	
			- writhd	
			- writhk	
			- mapss	
			- amatin	
			- amating	
			- mapsa	- writfl
			- mapsag	
			- mapsi	
			- mapdr	
			- mapsk	

---

Note 1: † indicates “program,”  
 \*“function,”  
 otherwise, “subroutine.”  
 # see ANISN manual.

Note 2: SR.QUIT is used at several places to close temporary files and terminate execution.  
 An intrinsic subroutine, “exit” is used to terminate execution, close all files, and return control to the operating system.

## 8.2 Summary of Contents of Subroutines

### 8.2.1 Program COMBINE7.1 and Supporting Subroutines

Overall control of COMBINE7.1 is maintained in PROGRAM COMBINE7.1. It controls the flow of the overall program. COMBINE7.1 calls SR.MAIN to read and digest all of the input data, perform spectrum calculation, and process the cross-section output data into the user-specified final format. It also calls the date and time subroutines to produce the banner information printed at the beginning and end of the printed output.

#### SR. ABCMAT

Routine to do a matrix multiplication. Called from sr.frobns.

#### SR. ADMABS

Generates cross sections from the admixed absorber resonances.

#### SR. AGE

AGE calculates moments and Fermi age from the second moment when an age calculation is requested. These are Equations (80) through (86) in the text.

**SR.AMATIN**

Processes the neutral internal cross-section file prior to reformatting.

**SR.AMATING**

Processes the neutral internal cross-section file prior to reformatting.

**SR. ANISN**

Executes a one-dimensional discrete ordinates (ANISN) transport calculation using geometry and 167-group cross sections obtained from the slowing down solution. SR.ANISN is composed of a number of subroutines and functions the function and description of which is included in the ANISN-PC User's Manual.

**SR. ANISNINP**

Prepares an ANISN input deck using geometry and 167-group cross sections obtained from the slowing down solution.

**BLOCK DATA BLK1**

Collision Probabilities from case and Placzek pin locations for Dancoff calculation.

**SR.BLKNES**

BLKNES calculates thermal blackness coefficients for diffusion theory codes. BLKNES is called from SR.FLUX.

**SR.BONDAR**

Bondarenko self-shields and transfers all requested library material cross sections to the file unit 419. The file unit 419 is then library file with no additional material to be processed in SR. SPECTRUM.

**SR.BONE**

BONE solves the  $B_1$  or  $P_1$  groupwise fast spectrum equations by substitution. The solution proceeds from group 1 through group 167 with the thermal upscattering iterations. These are Equations (38) and (39) in the text. The 167 group isotropic neutron flux and current are returned. BONE is called from SR.FLUX.

**SR.BONSIG0**

Calculates the groupwise Bondarenko background cross sections for the Bondarenko self shielding. Includes the heterogeneous component.

**SR. BROADN**

Doppler broaden the resolved resonance cross sections.

**SR.BSIGMA**

A part of Doppler broadening algorithm. Called from SR.BROADN.

**SR.BTHREE**

BTHREE solves the  $B_3$  groupwise fast spectrum equations by the Gauss-Seidel iteration. These are Equations (21) through (25) in the text. The groupwise solution proceeds from group 1 through group 167 with the thermal upscattering iteration. Four Legendre moments for the  $B_3$  fluxes are returned for each microgroup. BTHREE is called from SR.FLUX.

**SR.COALSEC**

COALSEC calculates the broad group fluxes, currents, and cross sections from the fast spectrum flux/current weighted values. It is called to calculate both macroscopic and microscopic values based on Equations (103) through (133) in the text. COALSEC is called from SR.XSCOAL.

**SR.CONTRL**

Controller for final formatting of the ASCII cross-section output file.

**SR.CROSS1**

CROSS1 calculates the single level Breit-Wigner resolved resonance cross sections on energy mesh generated in SR.GRID. Doppler-broadening occurs in SR.TBORAD.

**SR.CROSS2**

CROSS2 calculates the multi level Breit-Wigner resolved resonance cross sections on energy mesh generated in SR.GRID. Doppler-broadening occurs in SR.TBORAD.

**SR.CROSS3**

CROSS3 calculates the Reich-Moore resolved resonance cross sections on energy mesh generated in SR.GRID. Doppler-broadening occurs in SR.TBORAD.

**SR.DANCOF**

DANCOF calculates the Dancoff-Ginsburg factor C for a set of square lattice or hexagonal lattice pins in regular arrays depending upon the type of lattice requested in the input. The factor C(I) for the I resonance material is returned for each calculation. The calculation is for Equations (86) through (88) in the text. DANCOFF is called from SR.GINSBURG.

**SR.ENDCK**

ENDCK prints an error message when errors are detected on an input card.

**SR.ERR**

ERR prints an error message indicating which items on a given input card are in error.

**SR.ESCAPE**

ESCAPE calculates the heterogeneous lump escape probability,  $P_0$ , used in Equation (59) for the solution of the resolved resonance collision density. ESCAPE calls SR.NEWCYL or SR.NEWSLB for table lookup values of cylindrical or slab geometries respectively. ESCAPE returns  $P_0$  the escape probability and is called from SR.RESOL.

**SR.EVAL**

EVAL evaluates the  $B_3$  coefficients  $A_{ij}$  in Equations (17), (18) and (19). EVAL is called from SR.BTHREE.

**SR.FACPHI**

Calculate phase shift for the resonance calculation. Called from SR.CROSS1, CROSS2, and CROSS3.

**SR.FACTS**

Calculates penetration and shift factors for the resonance calculation. Called from SR.CROSS1, CROSS2, and CROSS3.

**SR.FLUX**

Calls SR.BONE, BTHREE, AGE, and BLKNES for the  $B_1$  spectrum,  $B_3$  spectrum, age, and blackness calculation, respectively.

**SR.FROBNS**

Inverts a complex matrix. Called from SR.CROSS3.

**SR.FUNKY**

Designed to define functions that appear in Doppler broadening calculations.

**SR.GINSBURG**

A drive subroutine for Dancoff-Ginsburg factor calculation.

**SR.GRID**

GRID calculates a discrete lethargy mesh in energy space which is used in SR.CROSS1, CROSS2, and CROSS3 to calculate the resonance cross sections used in solving Equation (59) for the collision density and Equation (56) for the resonance integrals in the resolved resonance range. The lethargy mesh is generated independently for each resonance from midpoint to midpoint between resonances. The mesh interval is directly proportional to the resonance width and inversely proportional to the resonance energy. A maximum of 900 uniform mesh intervals are permitted for each resolved resonance. However, the mesh spacing from resonance to adjacent resonance varies with gamma, the width of each resonance. The mesh spacing may be controlled by the input parameters FMULT and XLMT defined in the input instructions. The default values, however, produce optimum results. The mesh is therefore non-uniform across the series of resonance levels upstream from any given mesh point in order to calculate scatter-in sources when solving Equation (59). GRID is called from SR.NORDHEIM.

**SR.HEADLIN**

Prints banner page. Calls date and time.

**FUNCTION.HNABB**

Calculates  $hn(a,b)$  for  $b \geq a$  by a direct Taylor series expansion of the defining integral. Used in Doppler broadening calculation.

**SR.HUNKY**

This routine is designed to define functions that appear in Doppler broadening calculations.

**SR.INP**

Driver for the free format input package. Sets up an array of input data and a table of pointers to the data to allow free field input processing. Supervises subroutines INPALF, INPCVI, INPPCK, INPW. See the extensive comments in these subroutines for details.

**SR.INP2**

Routine to transfer data from input card buffer to designated storage area in core. Supervises subroutines IINKW, INPMOD/INPUPK. See the extensive comments in these subroutines for details.

**SR.INTERP**

INTERP is called from SR.NEWBV which is called by SR.RESOL for the resolved resonance numerical solution. NEWBV is called by RESOL to set new back values for the scatter-in source on the right-hand side of Equation (59). INTERP is called by NEWBV to interpolate from old back values to the new back value mesh.

**SR.JNP2**

Copy of SR.INP2. Supervises subroutines JINKW, JNPMOD/JNPUPK. Used for overlay efficiency.

**SR.LETHRG**

LETHRG calculates broad group energy boundaries and lethargy widths from the input cut point. LETHRG is called from SR.BONDAR.

**SR.LIEBEROTH**

LIEBEROTH computes an energy-dependent multiplier to the diffusion coefficient that corrects the error in the inter-pebble leakage that is an artifact of the homogenization process. The correction is applied only when the spherical geometry is chosen and when the pebble packing fraction is a value between 0.01 and 0.99.

**SR.MAIN**

Calls SR.UNINPIN for input data processing.  
Calls SR.UNIFS for spectrum calculation.  
Calls SR.PSTPRO for cross section post processing.

**SR.MAPDR**

Generate directory record for AMPX material.

**SR.MAPSA**

Maps neutron cross sections into ANISN 14\*\* format.

**SR.MAPSAG**

Maps photo-atomic cross sections into ANISN 14\*\* format.

**SR.MAPSI**

Maps cross sections into CCCC ISOTXS format.

**SR.MAPSK**

Maps INL format data into KENO5A working library format and write.

**SR.MAPSS**

Maps cross sections into INL format.

**SR.MAXWEL**

MAXWEL generates a Maxwellian thermal flux spectrum at the input temperature requested to be used in the MND calculation of MND thermal constants. These are Equations (134) to (140) in the text. MAXWEL is called from SR.MND.

**SR.MND**

MND calculates Mixed Number Density constants when requested in the input. These are given in Equations

(226) to (232) in the text. MND constants may only be calculated for a single thermal energy group. The MND constants are then printed for scrutiny by the user. MND is called from SR.'s MICRO and INMN3.

**SR.MOVSPANL**

Move panel for Doppler broadening. Called from SR.TBROAD.

**SR.NEWBV**

NEWBV is called by SR.RESOL to calculate a set of new back values for the scatter-in source on the right-hand side of Equation (59). New back values are required because a new uniform mesh is required for Simpson's rule integration of the right-hand side of Equation (59) for the scatter-in source. SR.INTERP is called by NEWBV to interpolate to the new uniform mesh from old back values on the old non-uniform mesh generated for the cross-section calculation in SR.CROSS.

**SR.NEWCYL**

NEWCYL is called by SR.ESCAPE to do the tabular interpolation for the capture probability  $P_c$  for cylindrical pins. The escape probability  $P_0=1-P_c$ .

**SR.NEWSLB**

NEWSLB is called by SR.ESCAPE to do the tabular interpolation for the capture probability  $P_c$  for slab geometry. The escape probability  $P_0=1-P_c$ .

**SR.NORDHEIM**

Drive routine for Nordheim integral treatment for resonance integrals.

**SR.OUTPUT**

Writes out most of the data input.

**SR.PHOTONXS**

Generates photon production and photo-atomic cross sections and return them on unit 427.

**SR.PPROD**

Generates photon production, using neutron flux and photon production cross sections, and writes in as distributed source (17\*\*) for anisotropic input.

**SR.PRNRES**

PRNRES prints the results of the resolved resonance calculations by fine group. PRNRES is called from SR.NORDHEIM.

**SR.PRTSCAT**

PRTSCAT prints out the broad group scattering matrices for both macroscopic and microscopic cross-section data. PRTSCAT is called from SR.XSCOAL.

**SR.PSTPRO**

Controlled for ASCII flux and cross-section output file post processing.

**SR.PUNCH**

PUNCH formats and writes the device-specified broad group output data. PUNCH is called from SR.XSCOAL.

**SR.QUIT**

Exit subroutine. Closes files and terminates program.

**SR.MASCOT**

Initializes macroscopic scattering cross sections and calls SR.OUTPUT. Called from SR.SPECTRUM.

**SR.RESLIB**

Read resolve resonance parameters from the "reslib" file. Reverse the order from high to low energy.

**SR.RESOL**

RESOL performs the calculation of the resolved resonance integrals by means of the Nordheim numerical solution. It calls SR.CROSSs and TBROAD to generate the Doppler-broadened cross sections from the resolved resonance parameters. It solves Equation (59) at each fine lethargy mesh point for the collision density. It constructs resonance integrals from Equation (56). RESOL is called from SR.NORDHEIM.

**FUNCTION SAMPS**

SAMPS integrates the scatter-in source term on the right-hand side of Equation (59) for the principal resonance absorber by means of Simpson's rule. The integration is over the back-value mesh generated in SR.NEWBV. SAMPS is called from SR.RESOL.

**FUNCTION SEMPS**

SEMPs integrates the scatter-in source term on the right-hand side of Equation (59) for the first input moderator by means of Simpson's rule. The integration is over the back-value mesh generated in SR.NEWBV. SEMPS is called from SR.RESOL.

**SR.SKIPR**

Skip forward or backward on a coded or blocked binary tape. Works on the binary "matxs.lib."

**SR.SOLV**

SOLV solves the  $B_3$  Equation (21) by means of block Gauss elimination one group at a time from high to low in energy. SOLV is called from SR.BTHREE.

**FUNCTION SOMPS**

SEMPs integrates the scatter-in source term on the right-hand side of Equation (59) for the second input moderator by means of Simpson's rule. The integration is over the back-value mesh generated in SR.NEWBV. SEMPS is called from SR.RESOL.

**SR.SPECTRUM**

Drives spectrum calculation by first generating the required fine group cross sections and then calculating spectrum.

**SR.STRAN**

Driver for reformatting the ASCII cross-section output file from internal format to the user-requested final format. Sets up storage, etc.

**FUNCTION SUMPS**

SEMPs integrates the scatter-in source term on the right-hand side of Equation (59) for the third input moderator by means of Simpson's rule. The integration is over the back-value mesh generated in SR.NEWBV. SEMPS is called from SR.RESOL.

**FUNCTION SVMPS**

SEMPs integrates the scatter-in source term on the right-hand side of Equation (59) for the first input admixed resonance absorber by means of Simpson's rule. The integration is over the back-value mesh generated in SR.NEWBV. SEMPS is called from SR.RESOL.

**FUNCTION SWMPS**

SEMPs integrates the scatter-in source term on the right-hand side of Equation (59) for the second input admixed resonance absorber by means of Simpson's rule. The integration is over the back-value mesh generated in SR.NEWBV. SEMPS is called from SR.RESOL.

**FUNCTION SXMPS**

SEMPs integrates the scatter-in source term on the right-hand side of Equation (59) for the third input admixed resonance absorber by means of Simpson's rule. The integration is over the back-value mesh generated in SR.NEWBV. SEMPS is called from SR.RESOL.

**SR.TAIL**

Prints final banner. Print date, time, and elapsed run time.

**SR.TBROAD**

Manages the paging of cross section data for Doppler broadening.

**SR.THRINV**

Inverts symmetric matrix. Called from SR.FROBNS.

**SR.TOTCS**

Read total cross section from vector blocks in "matxs.lib" for all submaterials and save on direct access file, 'is' unit.

**SR.TPUNCH**

TPUNCH formats and writes the device-specified broad group output data. TPUNCH is called from SR.TXSCOAL.

**SR.TRAPZ**

TRAPZ performs a trapezoidal integration of seven dependent variables from SR.RESOL over uniform mesh for one energy group in the resolved resonance range. The seven integrals are returned. TRAPZ is called from SR.RESOL.

**SR.TXSCOAL**

Drives the coalescing option for 1-D (ANISN) problems.

**SR.UNIFS**

Calls SR.SPECTRUM, which drives the spectrum calculation. Also calls SR.XSCOAL, which drives the cross section coalescing.

**SR.UNINDAT**

UNINDAT reads the input integer data cards in the 1000000 series and maps the input data onto modules. The data are then checked for range errors and any errors are printed. UNINDAT is called from SR.UNINPIN.

**SR.UNININ**

UNININ initializes the input integer data arrays before the entry of change case data. This preserves unchanged values from the previous problem. UNININ is called from SR.UNINDAT.

**SR.UNINPIN**

UNINPIN controls the reading of all input data on 1000000 series cards using INP subroutines. SR.UNINDAT is called to map input data which is read onto modules. UNINPIN is called from PROGRAM COMBINE7.

**SR.UNPAKK**

Takes the cross section data present in the ADUM array read from unit 404(???) and packs them into the local variables. UNPAKK is called from SR.GETCHE and SR.XSCOAL.

**SR.UPDN**

Find the largest upscatter distance, largest downscatter distance, count total number of materials in the file, and manufacture an ISOTXS 6-character name for each material.

**SR.WRITFL**

Utility for writing ANISN, free form, ASCII input using repeats and fills as appropriate.

**SR.WRITHD**

Writes header information if ISOTXS cross-section output is specified.

**SR.WRITHK**

Writes header for KENO5 format.

**SR.XSCOAL**

Drives the coalescing option for 0-D (slowing down) problems.

**SR.XSPAMAC**

XSPAMAC drives the spatial (broad region) collapsing of 167-group macroscopic cross sections from the 1-D transport solution obtained from ANISN.

**SR.XSPAMICB**

XSPAMICF collapses the 167-group, region-wise microscopic cross sections into the broad energy group structure specified in the input.

**SR.XSPAMICF**

XSPAMICF drives the spatial (broad region) collapsing of 167-group microscopic cross sections from the 1-D transport solution obtained from ANISN.

## 9. REFERENCES

1. National Nuclear Data Center, *Evaluated Nuclear Data File (ENDF/B-VII.0)*, Brookhaven National Laboratory, December 15, 2006.
2. R. A. Grimesey, David W. Nigg, Richard L. Curtis, *COMBINE/PC-A Portable ENDF/B Version 5 Neutron Spectrum and Cross-Section Generation Program*, EGG-2589, Rev. 1, February 1991.
3. R. L. Curtis, et al., *PHROG -A FORTRAN-IV Program to Generate Fast Neutron Spectra and Average Multigroup Constants*, Idaho Nuclear Corp., IN-1435, April 1971.
4. R. L. Curtis and R. A. Grimesey, *INCITE: A FORTRAN-IV Program to Generate Thermal Neutron Spectra and Multigroup Constants Using Arbitrary Scattering Kernels*, Idaho Nuclear Corp., IN-1062, 1967.
5. National Nuclear Data Center, *Evaluated Nuclear Data File (ENDF/B-V)*, Brookhaven National Laboratory, 1979. R. Kinsey, *Data Formats and Procedures for the Evaluated Nuclear Data File ENDF*, BNL-NCS-50496, 1979.
6. National Nuclear Data Center, *Evaluated Nuclear Data File (ENDF/B-VI)*, Brookhaven National Laboratory, 1990. V. McLane, Editor, *ENDF-102 DATA FORMATS AND PROCEDURES FOR THE EVALUATED NUCLEAR DATA FILE ENDF-6*, BNL-NCS-44954-01/04-REV, July 1990.
7. R. E. MacFarlane and D. W. Muir, *The NJOY Nuclear Data Processing System Version 91*, Los Alamos National Laboratory, LA-12740-M, October, 1994.
8. I. I. Bondarenko, Ed., *Group Constants for Nuclear Reactor Calculations*, Consultants Bureau, New York, 1964.
9. G. I. Bell and S. Glasstone, *Nuclear Reactor Theory*, Van Nostrand Reinhold, New York, 1970.
10. R. E. MacFarlane, *TRANSX 2: A code for Interfacing MATXS Cross-Section Libraries to Nuclear Transport Codes*, LA-12312-MS, RSICC PSR-317, Los Alamos National Laboratory, July 1992.
11. L. W. Nordheim, *A Program of Research and Calculation of Resonance Absorption*, GA-2527, 1961.
12. Internal Technical Report, *ENDF/B Version 6 Nuclear Data Processing at INEL*, W. Y. Yoon, R. A. Grimesey, and C. A. Wemple, NRRT-N-91-034, 1991. Internal Letter Report, W. Y. Yoon to D. W. Nigg, *COMBINE-6 Cycle*, WYY-01-94, E&G Idaho, 1994.
13. Amouyal, P. Benoist and J. Horowitz, "New Method for Determining the Thermal Utilization Factor in a Unit Cell," *Journal of Nuclear Energy*, 6, 1957.
14. G. D. Joanou and J. D. Dudek, *GAM-I: A Consistent P-1 Multigroup code for the Calculation of Fast Neutron Spectra and Multigroup Constants*, GA-1850, June 1961.
15. ANISN/PC Manual, D. Kent Parsons, EGG-2500, Idaho National Engineering Laboratory, December, 1988.
16. *NJOY99.0 Code System for Producing Pointwise and Multigroup Neutron and Photon Cross Sections from ENDF/B data*, RSICC PSR-480, March 2000. *Processing ENDF/VII.0 with NJOY99.161* (the latest being *NJOY99.259*), National Nuclear Data Center, December 15, 2006.
17. D. Selengut, *Critical Mass Calculations for Bare Hydrogen Moderated Reactors by Means of Transport Theory*, APEX-121, September 1952.
18. R. E. MacFarlane, R. B. Kidman, and R. J. LaBauve, "The Background Cross Section Method as A General Tool for Reactor Analysis," CONF-78040, Proc. ANS Topical Meeting, Gatlinburg, Tennessee, April 1978, E. G. Silver, Ed. 1978.

19. M. G. Stamtelatos, R. J. LaBauve (LASL), "Space Shielding Cross Sections for Pebble-Bed High-Temperature Reactors," *American Nuclear Society Transactions*, 1972, pp. 600–601.
20. M. Weinberg and E. P. Wigner, *The Physical Theory of Neutron chain Reactors*, Chicago: The University of Chicago Press, 1958.
21. K. M. Case, F. de Hoffman, and G. Placzek, Introduction to the theory of Neutron Diffusion, Los Alamos, NM: Los Alamos Scientific Laboratory, 1953.
22. Sauer, "Thermal Utilization in the Square Cell," *Journal of Nuclear Energy*, 18, 1964, p. 425.
23. G. D. Joanou and J. S. Dudek, *GAM-II A B3 Code for the Calculation of Fast Neutron Spectra and Associated Multigroup Constants*, GA-4265, September 1963L. Dresner, *Resonance Absorption in Nuclear Reactors*, New York: Pergamon Press, 1960.
24. L. Dresner, *Resonance Absorption in Nuclear Reactors*, New York; Pergamon Press, 1960.
25. D. E. Cullen, "Program SIGMA1 (version 77-1): Doppler Broaden Evaluated Cross Sections in the Evaluated Nuclear Data File/Version B (ENDF/B) Format," Lawrence Livermore National Laboratory report UCRL-50400, Vol. 17, Part B, 1977
26. N. M. Greene, L. M. Petrie, and R. M. Westfall, "NITAWL-III: SCALE System Module for Performing Resonance Shielding and Working Library Production," NUREG/CR-0200, Rev 7, Volume II, Section F2, 2004, pp. F2.3.2.
27. K. R. Knight, *SUPERDAN: Computer Programs for Calculating the Dancoff Factor of Spheres, Cylinders, and Slabs*, ORNL/NUREG/CSO/Tm-2, March 1978.
28. G. I. Bell, "A simple Treatment for Effective Resonance Absorption Cross Sections in Dense Lattices," *Nuclear Science and Engineering*, Vol. 5, Issue 2, 1959, pp.138, 139.
29. H. Gelling and A.Sauer, *Programmbechreibung zu Dancoff Jr.*, IBM-7040, KEA-114, April 1964.
30. W. Maynard, *Blackness Theory and Coefficients for Slab Geometry*, WAPD-TN-168, May 1959.
31. F. Henry, *A theoretical Method for Determining the Worth of Control Rods*, WAPD-218, August 1959.
32. D. Voorhis et al., *Experimental and theoretical Study of Critical Slabs: Effect of Absorbing Membranes of Cadmium, Gold, and Boron*, WAPD-170, April 1957.
33. Radkowsky (ed.), *Naval Reactors Handbook*, Volume I, "Selected Basic Techniques," TID-7050, 1964.
34. J. B. Fussell ltr to H. L. McMurry, "SCAMP S<sub>n</sub> Code Consolidation and Modification," EG&G Idaho, JBF-8-70, August 7, 1970,
35. J. Lieberoth and A. Stojadinovic, "Neutron Streaming in Pebble Beds," *Nuclear Science and Engineering*, Vol. 76, 1980, pp. 336–344.
36. J. K. Kloosterman and A. M. Ougouag *Computation of Dancoff Factors for Fuel Elements Incorporating Randomly Packed TRISO Particles*, INEEL/EXT-05-02592, January 2005.

**APPENDIX A**

**INL CROSS-SECTION FORMAT DESCRIPTION**

# Appendix A—INL Cross-Section Format Description

The internal INL format is based on a word-addressable card image file structure. The following tables describe this structure. A nonzero value in Column 1 of a data record for a material signifies the end of data for that material. The scatter matrices do not have the  $2L + 1$  term multiplied into them.

**Table A-1. The library material title record summary.**

<b>Information or Mnemonic Name of Data</b>	<b>Record Columns</b>	<b>Description or Function</b>
IAD	2–3	A nonzero value means update rather than replace or add this material to the library file.
IDIFF	4–5	A nonzero value means the SIGMU(J,IM) values are computed from the input D(J,IM) values instead of read directly.
MTLNO (or LM)	6–10	Library material identifying number.
MAC	11–13	0 for microscopic cross section 1 for macroscopic cross section
EPFISS	14–25	Energy per fission (MeV), 0 for macro.
AKINF	26–37	Eigenvalues, $k_{\text{inf}}$ for the region.
AKEFF	38–49	Eigen value, $k_{\text{eff}}$ for the region.
ADEN	50–60	Atomic density, 0 for macro.
TIT	62–80	Library material title information.

Table A-2. The library material floating point data summary.

Index 1 Card Cols. 2-3	Index 2 Card Cols. 4-5	Index 3 Card Cols. 6-8	Index 4 Card Cols. 9-10	Mnemonic Name of Data	Description or Function of Data (index which increases as more data words are added across a card is enclosed in parenthesis)
1		J	1	TD(J)	Diffusion coefficient for group J. From Equation (148) of Fick's law. Maybe negative or unreliable. 1-D only.
1		J	2	SIGA(J)	Absorption cross section for group J.
1		J	3	SIGNU(J)	Neutron per fission times fission cross section for group J.
1		J	4	SIGFIS(J)	Fission cross section for group J.
1		J	5	CHI(J)	Fission source for group J.
1		J	6	TAVFLUX(J)	Flux for group J.
1		J	7	BUCKPAR(J)	Parallel Buckling (cm <sup>-2</sup> ) for group J. From Equation (156). 1-D only.
1		J	8	BUCKTRANS(J)	Transverse Buckling (cm <sup>-2</sup> ) for group J. From input.
2		J	1	DCR(J)	Radial diffusion coefficient for group J. From Equation (149) of Fick's law pseudo extension. 1-D only.
2		J	2	DCZ(J)	Axial diffusion coefficient for group J. From Equation (149). 1-D only.
3		J	K	TRMAT(J,K)	General scattering transfer cross section, $\Sigma_{s_0}$ , from group J to group K. (K may be less than, equal to, or greater than J).
4		J	0	SIGMU(J)	Transport cross section for group J. For 0-D macro, from Equation (125) of Fick' law. For 0-D micro, from Equation (133) of $B_1$ approximation to transport. When 1-D calculation is performed, Equation (150) is used for both macro and micro. If negative, the positive value among from Equations (151), (152), and (153) is selected. If the value is less than 0.5 or greater than that from Equation (151), use that from Equation (151), which is always positive. <b>Recommended for diffusion theory code (D=1/(3SIGMU)).</b>
4		J	1	S2AVERI(J)	Inner radial surface to average flux ratio for group J. From Equation (161). 1-D only.
4		J	2	S2AVERO(J)	Outer radial surface to average flux ratio for group J. From Equation (162). 1-D only.

4		J	3	S2AVEZI(J)	Inner axial surface to average flux ratio for group J. From Equation (161). 1-D only.
4		J	4	S2AVEZO(J:LM)	Outer axial surface to average flux ratio for group J. From Equation (162). 1-D only.
1		J	11	SNG(J,LM)	Capture cross section. Index 4=11 through 52 for micro only.
1		J	12	SGP(J,LM)	Proton production cross section.
1		J	13	SGD(J,LM)	Deuteron production cross section.
1		J	14	SGT(J,LM)	Triton production cross section.
1		J	15	SGH(J,LM)	He-3 (h) production cross section.
1		J	16	SGA(J,LM)	He-4 ( $\alpha$ ) production cross section.
1		J	17	SN2N(J,LM)	(n,2n) cross section.
1		J	18	SN3N(J,LM)	(n,3n) cross section.
1		J	19	SN4N(J,LM)	(n,4n) cross section.
1		J	20	HEATN(J,LM)	Heating cross sections (eV-barns).
1		J	21	KERMA(J,LM)	Kerma cross sections (eV-barns).
1		J	22	DAMEN(J,LM)	Damage energy production cross sections (eV-barns).
1		J	23	SNP(J,LM)	(n,p) cross section.
1		J	24	SND(J,LM)	(n,d) cross section.
1		J	25	SNT(J,LM)	(n,t) cross section.
1		J	26	SNH(J,LM)	(n,h) cross section.
1		J	27	SNA(J,LM)	(n, $\alpha$ ) cross section.
1		J	28	SN2A(J,LM)	(n,2 $\alpha$ ) cross section.
1		J	29	SN3A(J,LM)	(n,3 $\alpha$ ) cross section.
1		J	30	SN2P(J,LM)	(n,2p) cross section.
1		J	31	SNPA(J,LM)	(n,p $\alpha$ ) cross section.
1		J	32	SNT2A(J,LM)	(n,t2 $\alpha$ ) cross section.
1		J	33	SND2A(J,LM)	(n,d2 $\alpha$ ) cross section.
1		J	34	SNPD(J,LM)	(n,pd) cross section.
1		J	35	SNPT(J,LM)	(n,pt) cross section.
1		J	36	SNNA(J,LM)	(n,n $\alpha$ ) cross section.
1		J	37	SNN3A(J,LM)	(n,n3 $\alpha$ ) cross section.

1		J	38	SN2NA(J,LM)	(n,2n $\alpha$ ) cross section.
1		J	39	SN3NA(J,LM)	(n,3n $\alpha$ ) cross section.
1		J	40	SNNP(J,LM)	(n,np) cross section.
1		J	41	SNN2A(J,LM)	(n,n2 $\alpha$ ) cross section.
1		J	42	SN2N2A(J,LM)	(n,2n2 $\alpha$ ) cross section.
1		J	43	SNND(J,LM)	(n,nd) cross section.
1		J	44	SNNT(J,LM)	(n,nt) cross section.
1		J	45	SNNH(J,LM)	(n,nh) cross section.
1		J	46	SNND2A(J,LM)	(n,nd2 $\alpha$ ) cross section.
1		J	47	SNNT2A(J,LM)	(n,nt2 $\alpha$ ) cross section.
1		J	48	SN2NP(J,LM)	(n,2np) cross section.
1		J	49	SN3NP(J,LM)	(n,3np) cross section.
1		J	50	SNDA(J,LM)	(n,da) cross section.
1		J	51	SNN2P(J,LM)	(n,n2p) cross section.
1		J	52	SNNPA(J,LM)	(n,np $\alpha$ ) cross section.
6		J	K	TRMAT1(J,K)	Same as INDEX1 = 3 for values of $\sum_{s_1}$ .
7		J	K	TRMAT2(J,K)	Same as INDEX1 = 3 for values of $\sum_{s_2}$ .
8		J	K	TRMAT3(J,K)	Same as INDEX1 = 3 for values of $\sum_{s_3}$ .
11		J	1	THEAT(J)	Photon heating cross sections (eV-barns). Index1= 1 through 11 when NPROB=-2.
11		J	2	TGABS(J)	Photon absorption cross sections (eV-barns).
11		J	3	TGTOT(J)	Photon total cross sections (eV-barns).
11	1	J	K	TGG(J,K,1)	Photon transfer cross section from group J to group K for Legendre Order (L) 1.
11	2	J	K	TGG(J,K,2)	Photon transfer cross section from group J to group K for L=2.
11	3	J	K	TGG(J,K,3)	Photon transfer cross section from group J to group K for L=3.
11	4	J	K	TGG(J,K,4)	Photon transfer cross section from group J to group K for L=4.
11	5	J	K	TGG(J,K,5)	Photon transfer cross section from group J to group K for L=5.
11	9	J	K	TTGNP(J,K)	Photon production cross section from neutron group J to photon group K

**APPENDIX B**

**ANISN CROSS-SECTION FORMAT DESCRIPTION**

## Appendix B—ANISN Cross-Section Format Description

If the ANISN output format is selected, all cross sections are output in the standard ANISN card image 14\*\* format (see Reference B-1 for details). The absorption, nu-sigma-fission, and total cross sections are always present regardless of the scattering order of the material or the current group number. For scattering orders beyond  $e = 0$ , the absorption, nu-sigma-fission, and total cross sections are 0.0.

The upscatter cross sections are present only when (HIS-IHT) is greater than 1. If they are present, there are  $NUS = (HIS - IHT - 1)$  locations present for every group and for every scattering order (material). This includes the physically nonexistent quantities such as  $\sigma$  upscattering from group (IGM + NUS) to the lowest energy group IGM. In this way, the number of upscatter cross sections for each group in the cross-section table remains constant. The cross-section arrangement is summarized in Table B-1.

**Table B-1. Cross-section arrangement.**

Cross Section	Group	Position Description
$\sigma$ absorption	g	
$\nu\sigma$ fission	g	
$\sigma$ total or $\sigma$ transport	g	IHT
$\sigma$ upscatter	$(g + NUS) \rightarrow g$	
•	•	
•	•	
•	•	
$\sigma$ upscatter	$(g + 1) \rightarrow g$	IHS
$\sigma$ self-scatter	$g \rightarrow g$	
$\sigma$ downscatter	$(g - 1) \rightarrow g$	
•	•	
•	•	
•	•	
$\sigma$ downscatter	$(g - NDS) \rightarrow g$	IHM
$\sigma$ upscatter (code calculated)	From g	IHP = IHM + 1

Finally, it should be noted that the higher-order scattering materials are output by COMBINE/PC without the  $(2\ell + 1)$  term pre-multiplied into them.

### B. REFERENCE

1. D. K. Parsons, *ANISN/PC Manual*, EGG-2500, December 1988.

**APPENDIX C**

**CCCC INTERFACE FILE FORMATS AND  
CONVENTIONS**

# Appendix C—CCCC Interface File Formats and Conventions<sup>a</sup>

## ISOTXS—Nuclide (Isotope) Ordered, Multigroup Neutron Cross Sections

The changes in ISOTXS-IV relative to ISOTXS-III are in the main part, clarifications of ambiguities present in the latter. The changes reflected in Version IV are:

- If scattering bandwidth, JBAND(J,N), is zero, no scatter data are present in block N. (see 4D record.)
- The position of self-(or within-group-) scatter must lie within the scattering bandwidth unless the bandwidth is zero, i.e.,  $I < IJJ(J,N) < JBAND(J,N)$  if  $JBAND(J,N) \neq 0$ . (See 4D record.)
- The Legendre expansion coefficient factor  $(2l + 1)$  is not included in the  $P_l$  weighted transport and total cross sections. (See 5D record.)
- The  $n,2n$  principal cross section (see 5D record) is clarified as the  $n,2n$  reaction cross section while the  $n,2n$  scatter matrix terms are clarified (see 4D record NOTE) as emission (production) based, i.e.,

$$\sigma_{n,2n(g)} = 0.5 \sum_{g'} \sigma_{n,2n}(g \rightarrow g') \quad (C-1)$$

The following is included to clarify the meaning of the vectors IDSCT(N) and LORD(N) contained in the ISOTOPE CONTROL AND GROUP-INDEPENDENT DATA (4D) record and to remove an ambiguity in the sub-blocking of scattering data.

IDSCT(N) specifies the identity and ordering of scattering data blocks, and LORD(N) specifies the number of Legendre orders contained in each block. Each block of scattering may be sub-blocked into NSBLOCK records (sub-blocks) where NSBLOCK is found on the FILE CONTROL (ID) record. With the single exception below, sub-blocking shall not be used ( $NSBLOCK > 1$ ) if the individual blocks defined by IDSCT and LORD contain more than one Legendre order of scattering. The single exception is that sub-blocking may be used with more than one Legendre order per record (sub-block) only if each record (sub-block) contains data for a single “scattered-into” group.

Finally, the following information is reproduced from the Version III specifications for the sake of completeness.

The  $P_l$  weighted transport and total cross sections can be defined<sup>b</sup> as

$$\sigma_{trl}^g = \sigma_{tl}^g - \sum_{g'} \sigma_{sl}(g \rightarrow g') \quad l = 1, \dots, LTRN, \quad (C-2)$$

and

$$\sigma_{tl}^g \equiv \frac{\int_g \sigma_l(E) dE}{\int_g \sigma_l(E) dE} \quad l = 0, 1, \dots, LTOT-1. \quad (C-3)$$

a. Extracted from LA-6941-MS, Standard Interface Files and Procedures for Reactor Physics Codes Version IV by R. Douglas O'Dell.

b. Other definitions of the weighted transport cross section are also possible.

The  $P_l$  weighted scattering cross sections given in the scattering blocks are defined as

$$\sigma_{sl}(g \rightarrow g') \equiv \frac{\int_g \int_{g'} \sigma_{sl}(E \rightarrow E') \Phi(E) dE' dE}{\int_g \Phi(E) dE}. \quad (C-4)$$

For the transport cross section, STRPL, Equation (125) for macro and Equation (133) for micro are used when 0-D calculation is performed. When 1-D calculation is performed, Equation (150) is used for SIGMU for both macro and micro. If negative, the positive value among Equations (151), (152), and (153) is selected. If the value is less than 0.5 or greater than that from Equation (151), use that from Equation (151), which is always positive.

```

C*****
C*****
C
C             REVISED 11/30/76
C
CF             ISOTXS-IV
CE             MICROSCOPIC GROUP NEUTRON CROSS SECTIONS
C
CN             THIS FILE PROVIDES A BASIC BROAD GROUP
CN             LIBRARY, ORDERED BY ISOTOPE.
C
CN             FORMATS GIVEN ARE FOR FILE EXCHANGE ONLY
C
C*****
C
C
C-----
CS             FILE STRUCTURE
CS
CS             RECORD TYPE                PRESENT IF
CS             =====
CS             FILE IDENTIFICATION        ALWAYS
CS             FILE CONTROL                ALWAYS
CS             FILE DATA                  ALWAYS
CS             FILE-WIDE CHI DATA        ICHIST.GT.1
CS
CS             ***** (REPEAT FOR ALL ISOTOPES)
CS             *             ISOTOPE CONTROL AND GROUP
CS             *             INDEPENDENT DATA        ALWAYS
CS             *             PRINCIPAL CROSS SECTIONS  ALWAYS
CS             *             ISOTOPE CHI DATA        ICHI.GT.1
CS             *
CS             *             ***** (REPEAT TO NSCMAX SCATTERING BLOCKS)
CS             * *             ***** (REPEAT FROM 1 TO NSBLOK)
CS             * * *             SCATTERING SUB-BLOCK        LORDN (N) .GT.0
CS             *****
C
C-----
CR             FILE IDENTIFICATION
C
CL             HNAME, (HUSE (I) , I=1, 2) , IVERS, MULT

```

```

C
CW 1+3*MULT
C
CB FORMAT(4H OV ,A8,1H*,2A6,1H*,2I6)
C
CD HNAME HOLLERITH FILE NAME - MATXS - (A8)
CD HUSE HOLLERITH USER IDENTIFIATION (A8)
CD IVERS FILE VERSION NUMBER
CD MULT DOUBLE PRECISION PARAMETER
CD 1- A6 WORD IS SINGLE WORD
CD 2- A6 WORD IS DOUBLE PRECISION WORD
C
C-----
C
C-----
CR FILE CONTROL (1D RECORD)
C
CL NGROUP,NISO,MAXUP,MAXDN,MAXORD,ICHIST,NSCMAX,NSBLOK
C
CW 8=NUMBER OF WORDS
C
CB FORMAT(4H 1D ,4I6)
C
CD NGROUP NUMBER OF ENERGY GROUPS IN FILE
CD NISO NUMBER OF ISOTOPES IN FILE
CD MAXUP MAXIMUM NUMBER OF UPSCATTER GROUPS
CD MAXDN MAXIMUM NUMBER OF DOWNSCATTER GROUPS
CD MAXORD MAXIMUM SCATTERING ORDER (MAXIMUM VALUE OF
CD LEGENDRE EXPANSION INDEX USED IN FILE) .
CD ICHIST FILE-WIDE FISSION SPECTRUM FLAG
CD ICHIST.EQ.0 NO FILE-WIDE SPECTRUM
CD ICHIST.EQ.1 FILE-WIDE CHI VECTOR
CD ICHIST.GT.1 FILE-WIDE CHI MATRIX
CD NSCMAX MAIMUM NUMBER OF BLOCKS OF SCATTERING DATA
CD NSBLOK SUB-BLOCKING CONTROL FOR SCATTER MATRICES. THE
CD SCATTERING DATA ARE SUB-BLOCKED INTO NSBLOK
CD RECORDS (SUB-BLOCKS) PER SCATTERING BLOCK.
C
C-----
C
C-----
CR FILE DATA
C
CL (HSETID(I),I=1,12),(HISONM(I),I=1,NISO),
CL 1(CHI(J),J=1,NGROUP),(VEL(J),J=1,NGROUP,
CL 2(EMAX(J),J=1,NGROUP),EMIN,(LOCA(I),I=1,NISO)
C
CW (NISO+12)*MULT+1+NISO
CW +NGROUP*(2+ICHIST*(2/(ICHIST+1)))=NUMBER OF WORDS
C
CB FORMAT(4H 2D ,1H*,11A6,1H* HSETID,HISONM
CB 11H*,A6,1H*,9(1X,A6)/(10(1X,A6)))
CB FORMAT(6E12.5) CHI (PRESENT IF ICHIST.EQ.1)
CB FORMAT(6E12.5) VEL,EMAX,EMIN
CB FORMAT(12I6) LOCA

```

```

C
CD HSETID(I) HOLLERITH IDENTIFICATION OF FILE (A6)
CD HISONM(I) HOLLERITH ISOTOPE LABEL FOR ISOTOPE I (A6)
CD CHI(J) FILE-WIDE FISSION SPECTRUM(PRESENT IF ICHIST.EQ.1)
CD VEL(J) MEAN NEUTRON VELOCITY IN GROUP J (CM/SEC)
CD EMAX(J) MAXIMUM ENERGY BOUND OF GROUP J (EV)
CD EMIN MINIMUM ENERGY BOUND OF SET (EV)
CD LOCA(I) NUMBER OF RECORDS TO BE SKIPPED TO READ DATA FOR
CD ISOTOPE I.
C
-----
C
C
C
CR FILE-WIDE CHI DATA (3D RECORD)
C
CC PRESENT IF ICHIST.GT.1
C
CL ((CHI(K,J),K=1,ICHIST),J=1,NGROUP),(ISSPEC(I),I=1,NGROUP)
C
CW NGROUP*(ICHIST+1)=NUMBER OF WORDS
C
CB FORMAT(4H 3D ,1P5E12.5/(6E12.5)) CHI
CB FORMAT(12I6) ISSPEC
C
CD CHI(K,J) FRACTION OF NEUTRONS EMITTED INTO GROUP J AS A
CD RESULT OF FISSION IN ANY GROUP, USING SPECTRUM K
CD ISSPEC(I) ISSPEC(I)=K IMPLIES THAT SPECTRUM K IS USED
CD TO CALCULATE EMISSION SPECTRUM FROM FISSION
CD IN GROUP I
C
-----
C
C
C
CR ISOTOPE CONTROL AND GROUP INDEPENDENT DATA (4D RECORD)
C
CL HABSID,HIDENT,HMAT,AMSS,EFISS,ECAPT,TEMP,SIGPOT,ADENS,KBR,ICHI,
CL 1IFIS,IALF,INP,IN2N,IND,INT,LTOT,LTRN,ISTRPD,
CL 2(IDSCT(N),N=1,NSCMAX),(LORD(N),N=1,NSCMAX),
CL 3((JBAND(J,N),J=1,NGROUP),N=1,NSCMAX),
CL 4((IJJ(J,N),J=1,NGROUP),N=1,NSCMAX)
C
CW 3*MULT+17+NSCMAX*(2*NGROUP+2)=NUMBER OF GROUPS
C
CB FORMAT(4H 4D ,3(1X,A6)/6E15.5/(12I6))
C
CD HABSID HOLLERITH ABSOLUTE ISOTOPE LABEL - SAME FOR ALL
CD VERSIONS OF THE SAME ISOTOPE IN FILE (A6)
CD HIDENT IDENTIFIER OF LIBRARY FROM WHICH BASIC DATA
CD CAME (E.G. ENDF/B) (A6)
CD AMASS GRAM ATOMIC WEIGHT
CD EFISS TOTAL THERMAL ENERGY YIELD/FISSION (W.SEC/FISS)
CD ECAPT TOTAL THERMAL ENERGY YIELD/CAPTURE (W.SEC/FISS)
CD TEMP ISOTOPE TEMPERATURE (DEGREES KELVIN)
CD SIGPOT AVERAGE EFFETIVE POTENTIAL SCATTERING IN
CD RESONANCE RANGE (BARNS/ATOM)

```

CD	ADENS	DENSITY OF ISOTOPE IN MIXTURE IN WHICH ISOTOPE	-
CD		CROSS SECTIONS WERE GENERATED (/BARN-CM)	-
CD	KBR	ISOTOPE CLASSIFICATION	-
CD		0=UNDEFINED	-
CD		1=FISSILE	-
CD		2=FERTILE	-
CD		3=OTHER ACTINIDE	-
CD		4=FISSION PRODUCT	-
CD		5=STRUCTURE	-
CD		6=COOLANT	-
CD		7=CONTROL	-
CD	ICHI	ISOTOPE FISSION SPECTRUM FLAG	-
CD		ICHI.EQ.0 USE FILE-WIDE CHI	-
CD		ICHI.EQ.1 ISOTOPE CHI VECTOR	-
CD		ICHI.GT.1 ISOTOPE CHI MATRIX	-
CD	IFIS	(N,F) CROSS SECTION FLAG	-
CD		IFIS.EQ.0 NO FISSION DATA IN PRINCIPAL	-
CD		CROSS SECTION RECORD	-
CD		IFIS.EQ.1 FISSION DATA PRESENT IN PRINCIPAL	-
CD		CROSS SECTION RECORD	-
CD	IALF	(N,ALPHA) CROSS SECTION	-
CD		SAME OPTIONS AS IFIS	-
CD	INP	(N,P) CROSS SECTION	-
CD		SAME OPTIONS AS IFIS	-
CD	IN2N	(N,2N) CROSS SECTION	-
CD		SAME OPTIONS AS IFIS	-
CD	IND	(N,D) CROSS SECTION	-
CD		SAME OPTIONS AS IFIS	-
CD	INT	(N,T) CROSS SECTION	-
CD		SAME OPTIONS AS IFIS	-
CD	LTOT	NUMBER OF MOMENTS OF TOTAL CROSS SECTION PROVIDED	-
CD		IN PRINCIPAL CROSS SECTIONS RECORD	-
CD	ITRN	NUMBER OF MOMENTS OF TRANSPORT CROSS SECTION	-
CD		PROVIDED IN PRINCIPAL CROSS SECTIONS RECORD	-
CD	ISTRPD	NUMBER OF COORDINATE DIRECTIONS FOR WHICH	-
CD		COORDINATE DEPENDENT TRANSPORT CROSS SECTIONS	-
CD		ARE GIVEN. IF ISTRPD=0, NO COORDINATE DEPENDENT	-
CD		TRANSPORT CROSS SECTIONS ARE GIVEN.	-
CD	IDSCT(N)	SCATTERING MATRIX TYPE IDENTIFICATION FOR	-
CD		SCATTERING BLOCK N. SIGNIFICANT ONLY IF	-
CD		LORD(N) .GT.0	-
CD		IDSCT(N)=000 + NN, TOTAL SCATTERING, (SUM OF	-
CD		ELASTIC, INELASTIC, AND N2N SCATTERING	-
CD		MATRIX TERMS) .	-
CD		100 + NN, ELASTIC SCATTERING	-
CD		200 + NN, INELASTIC SCATTERING	-
CD		300 + NN, (N,2N) SCATTERING, ----SEE	-
CD		NOTE BELOW----	-
CD		WHERE NN IS THE LEGENDRE EXPANSION INDEX OF THE	-
CD		FIRST MATRIX IN BLOCK N	-
CD	LORD(N)	NUMBER OF SCATTERING ORDERS IN BLOCK N. IF	-
CD		LORD(N)=0, THIS BLOCK IS NOT PRESENT FOR THIS	-
CD		ISOTOPE. IF NN IS THE VALUE TAKEN FROM	-
CD		IDSCT(N), THEN THE MATICES IN THIS BLOCK	-
CD		HAVE LEGENDRE EXPANSION INDICES OF NN, NN+1,	-
CD		NN+2, . . . , NN+LORD(N) -1	-
CD	JBAND(J,N)	NUMBER OF GROUPS THAT SCATTER INTO GROUP J,	-

```

CD          INCLUDING SELF-SCATTER, IN SCATTERING BLOCK N.      -
CD          IF JBAND(J,N)=0, NO SCATTERING DATA IS PRESENT     -
CD          IN BLOCK N.                                          -
CD  IJJ(J,N)  POSITION OF IN-GROUP SCATTERING CROSS SECTION IN   -
CD          SCATTERING DATA FOR GROUP J, SCATTERING BLOCK     -
CD          N, COUNTED FROM THE FRIST WORD OF GROUP J DATA.   -
CD          IF JBAND(J,N).NE.0 THEN IJJ(J,N) MUST SATISFY     -
CD          THE RELATION 1.LE.IJJ(J,N).LE.JAND(J,N)            -
C
CD          NOTE- FOR N,2N SCATTER, THE MATRIX CONTAINS TERMS, -
CD          SCAT(J TO G), WHICH ARE EMISSION (PRODUCTION)-    -
CD          BASED, I.E., ARE DEFINED SUCH THAT MACROSCOPIC    -
CD          SCAT(J TO G) TIMES THE FLUX IN GROUP J GIVES     -
CD          THE RATE OF EMISSION (PRODUCTION) OF NEUTRONS    -
CD          INTO GROUP G.                                       -
C
C-----
C
C-----
CR          PRINCIPAL CROSS SECTIONS      (5D RECORD)          -
C
CL          ((STRPL(J,L),J=1,NGROUP),L=1,LTRN),                -
CL          1((STOPL(J,L),J=1,NGROUP)L=1,LTOT),(SNGAM(J),J=1,NGROUP), -
CL          2(SFIS(J),J=1,NGROUP),(SNUTOT(J),J=1,NGROUP),    -
CL          3(CHISO(J),J=1,NGROUP),(SNALF(J),J=1,NGROUP),    -
CL          4(SNP(J),J=1,NGROUP),(SN2N(J),J=1,NGROUP),      -
CL          5(SND(J),J=1,NGROUP),(SNT(J),J=1,NGROUP),        -
CL          6(STRPD(J,I),J=1,NGROUP),I=1,ISTRPD)             -
C
CW          (1+LTRN+LTOT+IALF+INP+IN2N+IND+INT+ISTRPD+2*IFIS+  -
CW          ICHI*(2/(ICHI+1)))*NGROUP=NUMBER OF WORDS        -
C
CB          FORMAT(4H 5D ,5E12.5/(6E12.5))                    -
C
CD  STRPL(J,L)  PL WEIGHTED TRANSPORT CROSS SECTION          -
CD          THE FIRST ELEMENT OF ARRAY STRPL IS THE          -
CD          CURRENT (P1) WEIGHTED TRANSPORT CROSS SECTION    -
CD          THE LEGENDRE EXPANSION COEFFICIENT FACTOR (2L+1) -
CD          IS NOT INCLUDED IN STRPL(J,L).                    -
CD  STOTPL(J,L) PL WEIGHTED TOTAL CROSS SECTION              -
CD          THE FIRST ELEMENT OF ARRAY STOTPL IS THE        -
CD          FLUX (P0) WEIGHTED TOTAL CROSS SECTION           -
CD          THE LEGENDRE EXPANSION COEFFICIENT FACTOR (2L+1) -
CD          IS NOT INCLUDED IN STRPL(J,L).                    -
CD  SNGAM(J)    (N,GAMMA)                                     -
CD  SFIS(J)     (N,F)          (PRESENT IF IFIS.GT.0)         -
CD  SNUTOT(J)   TOTAL NEUTRON YIELD/FISSION (PRESENT IF IFIS.GT.0) -
CD  SCHISO(J)   ISOTOPE CHI   (PRESENT IF ICHI.EQ.1)         -
CD  SNALF(J)    (N,ALPHA)    (PRESENT IF IALF.GT.0)          -
CD  SNP(J)      (N,P)        (PRESENT IF INP.GT.0)           -
CD  SN2N(J)     (N,2N)       (PRESENT IF IN2N.GT.0)  -----SEE -
CD          NOTE BELOW-----                                -
CD  SND(J)      (N,D)        (PRESENT IF IND.GT.0)           -
CD  SNT(J)      (N,T)        (PRESENT IF INT.GT.0)           -
CD  STRPD(J,I)  COORDINATE DIRECTION I TRANSPORT CROSS SECTION -
CD          (PRESENT IF ISTRPD.GT.0)                          -

```

```

C
CN          NOTE - THE PRINCIPAL N,2N CROSS SECTION SN2N(J)
CN          IS DEFINED AS THE N,2N REACTION CROSS SECTION,
CN          I.E., SUCH THAT MACROSCOPIC 2N2N(J) TIMES THE
CN          FLUX IN GROUP J GIVES THE RATE AT WHICH N,2N
CN          REACTIONS OCCUR IN GROUP J.  THUS, FOR N,2N
CN          SCATTERING, SN2N(J) = 0.5*(SUM OF SCAT(J TO G)
CN          SUMMED OVER ALL G) .
C
C-----
C
C
C-----
CR          ISOTOPE CHI DATA      (6D RECORD)
C
CC          PRESENT IF ICHI.GT.1
C
CL          ((CHIISO(K,J),K=1,ICHI),J=1,NGROUP), (ISOPEC(I),I=1,NGROUP)
C
CW          NGROUP*(ICHI+1)=NUMBER OF WORDS
C
CB          FORMAT(4H 6D ,5E12.5/(6E12.5))  CHIISO
CB          FORMAT(12I6)                      ISOPEC
C
CD          CHIISO(K,J) FRACTION OF NEUTRONS EMITTED INTO GROUP J AS A
CD          RESULT OF FISSION IN ANY GROUP, USING SPECTRUM K
CD          ISOPEC(I)   ISOPEC(I)=K IMPLIES THAT SPCTRUM K IS USED
CD          TO CALCULATE EMISSION SPECTRUM FROM FISSION
CD          IN GROUP I
C
C-----
C
C
C-----
CR          SCATTERING SUB-BLOCK    (7D RECORD)
C
CL          ((SCAT(K,L),K=1,KMAX),L+1,LORDN)
C
CC          KMAX=SUM OVER J OF JBAND(J,N) WITHIN THE J-GROUP RANGE OF THIS
CC          SUB-BLOCK.  IF M IS THE INDEX OF THE SUB-BLOCK, THE J-GROUP
CC          RANGE CONTAINED WITHIN THIS SUB-BLOCK IS
CC          JL=(M-1)*((NGROUP-1)/NSBLOK+1)+1 TO JU=MIN0(NGROUP,JUP),
CC          WHERE JUP=M*((NGROUP-1)/NSBLOK+1) .
C
CC          LORDN=LORD(N)
CC          N IS THE INDEX FOR THE LOOP OVER NSCMAX (SEE FILE STRUCTURE)
C
CW          KMAX*LORDN=NUMBER OF GROUPS
C
CB          FORMAT(4H 7D ,5E12.5/(6E12.5))
C
CD          SCAT(K,L)   SCATTERING MATRIX OF SCATTERING ORDER L, FOR
CD          REACTION TYPE IDENTIFIED BY IDSCT(N) FOR THIS
CD          BLOCK.  JBAND(J,N) VALUES FOR SCATTERING INTO
CD          GROUP K ARE STORED AT ;PCATOPMS L=SUM FROM 1
CD          TO (J-1) ( OF JBAND(J,N) PLUS 1 TO K-1+JBAND(J,N) .
CD          THE SUM IS ZERO WHEN J=1.  J-TO-J SCATTER IS

```

```
CD          THE IJJ(J,N)-TH ENTRY IN THE RANGE JBAND(J,N) .      -
CD          VALUES ARE STORED IN THE ORDER (J+JUP) ,            -
CD          (J+JUP-1) , . . . , (J+1) , J , (J-1) , . . . , (J-JDN) , -
CD          WHERE JUP=IJJ(J,N)-1 AND JDN=JBAND(J,N)-IJJ(J,N) . -
C-----
C-----
CEOF
```

**APPENDIX D**

**VALIDATION OF COMBINE7.1 CRITICALITY  
SEQUENCES**

# Appendix D—Validation of COMBINE7.1 Criticality Sequences

Criticality validation calculations were performed as part of verification and validation of the code. The COMBINE7.1 criticality validation suite is a collection of 19 benchmarks taken from the *International Handbook of Evaluated Criticality Benchmark Experiments* (IHECB) [1]. The designations by the Cross Section Evaluation Working Group Benchmark Specifications (CSEWG [2]) are interchangeably used with those from IHECB when applicable. The cases in the suite were selected to compass a variety of fissile materials in configurations that produce fast, intermediate, and thermal spectra, but were limited to those configurations which COMBINE7.1 calculation sequence, i.e., COMBINE7.1/ANISN, can afford. Some independent Monte Carlo Neutral Particle (MCNP) [3] calculations were also performed, all based on ENDF/B-VII.0 nuclear data. The distribution of cases by fuel material and spectrum is shown in Table D.1, followed by a brief summary of each case. The results are listed in Table D.2. The experiment  $k_{\text{eff}}$  values have some uncertainties involved and estimated to be mostly within  $1.0000 \pm 0.0050$  [1]. The  $k_{\text{eff}}$  values from MCNP calculations are also included. The results show the sensitivity to the deterministic nature of the method. The results are very robust despite these limitations and are very comparable to the experiments or the MCNP results. Some sensitivity can be digested from these calculations. All the relevant input files are included in the code package.

**Table D.1. Criticality Validation Suite**

Spectrum		Fast		Intermediate		
Geometry	Bare	Heavy Reflector	Light Reflector	Any	Solution	
					Bare	Reflector
HEU	GODIVA	FLATTOP-25		hci004	ORNL-1, ORNL-2, ORNL-10,	L-7, L-11
<sup>233</sup> U	JEZEBEL-23	umf002-1, umf002-2	umf005-1, umf005-2			
Pu	JEZEBEL, JEZEBEL-Pu	FLATTOP- PU		pci001	PNL-3, PNL- 4	

### GODIVA (hmf001)

This is a bare sphere of enriched uranium metal modeled as a homogeneous sphere of radius 8.7407 cm with the composition shown in the following table (number densities are given in nuclides per barn-cm).

Isotope	Density
<sup>235</sup> U	$4.4994 \times 10^{-2}$
<sup>238</sup> U	$2.4984 \times 10^{-3}$
<sup>234</sup> U	$4.9184 \times 10^{-4}$

### FLATTOP-25 (hmf028)

This is a spherical system consisting of a highly enriched uranium core in a thick natural uranium reflector. The core radius is 6.1156 cm and the outer radius of the reflector is 24.1242 cm. The compositions for the two regions (nuclides per bar-cm) are given in the following table.

Isotope	Core	Reflector
<sup>235</sup> U	4.4482x10 <sup>-2</sup>	3.4610 <sup>-4</sup>
<sup>238</sup> U	2.7038x10 <sup>-3</sup>	4.7721 <sup>-2</sup>
<sup>234</sup> U	4.8869x10 <sup>-4</sup>	2.6438 <sup>-6</sup>

#### FLATTOP-PU (pmf006)

This is a spherical system consisting of a plutonium core in a thick natural uranium reflector. The radius of the core is 4.5332 cm and the outer radius of the reflector is 24.142 cm. The compositions of the two regions are given in the following table.

Isotope	Core	Reflector
<sup>239</sup> Pu	3.6697x10 <sup>-2</sup>	
<sup>240</sup> Pu	1.8700x10 <sup>-3</sup>	
<sup>241</sup> Pu	1.1639x10 <sup>-4</sup>	
Ga	1.4755x10 <sup>-3</sup>	
<sup>234</sup> U		2.6438x10 <sup>-6</sup>
<sup>235</sup> U		3.4610x10 <sup>-4</sup>
<sup>238</sup> U		4.7721x10 <sup>-2</sup>

#### JEZEBEL (pmf001)

This is a bare sphere of plutonium modeled as a homogeneous sphere of radius 6.3849 cm with the composition shown in the following table (all number of densities are given as nuclides per barn-cm).

Isotope	Density
<sup>239</sup> Pu	3.7047x10 <sup>-2</sup>
<sup>240</sup> Pu	1.7512x10 <sup>-2</sup>
<sup>241</sup> Pu	1.1674x10 <sup>-4</sup>
Ga	1.3752x10 <sup>-3</sup>

#### JEZEBEL-23 (umf001)

This is a bare sphere of enriched <sup>233</sup>U metal (98.13%) with radius 5.9838 cm and the composition shown in the following table (all number of densities are given as nuclides per barn-cm).

Isotope	Density
<sup>233</sup> U	4.6712x10 <sup>-2</sup>
<sup>234</sup> U	5.9026x10 <sup>-4</sup>
<sup>235</sup> U	1.4281x10 <sup>-5</sup>
<sup>238</sup> U	2.8561x10 <sup>-4</sup>

#### JEZEBEL-Pu (pmf002)

This is a bare sphere of enriched plutonium meta, containing 20.1% <sup>240</sup>Pu. It is modeled as a homogeneous sphere of radius 6.6595 cm with the composition shown in the following table (all number of densities are given as nuclides per barn-cm).

Isotope	Density
<sup>239</sup> Pu	2.9934x10 <sup>-2</sup>
<sup>240</sup> Pu	7.8754x10 <sup>-3</sup>
<sup>241</sup> Pu	1.2146x10 <sup>-3</sup>
<sup>242</sup> Pu	1.5672x10 <sup>-4</sup>
Ga	1.3723x10 <sup>-3</sup>

### U233-met-fast-002 (umf002)

This is a spherical system consisting of a highly enriched <sup>233</sup>U surrounded by highly enriched <sup>235</sup>U.

Case (1) The core radius is 5.0444 cm and the outer radius of the surrounding highly enriched <sup>235</sup>U is 6.2661 cm.

Case (2) The core radius is 4.5999 cm and the outer radius of the surrounding highly enriched <sup>235</sup>U is 6.5887 cm.

Both critical experiments were performed at Los Alamos Scientific Laboratory.

The compositions for the two regions (nuclides per bar-cm) of these cases are given in the following table. Temperature is at 293 °K.

Isotope	Case 1	Case 2
<sup>233</sup> U core		
<sup>233</sup> U	4.7253x10 <sup>-2</sup>	4.7312x10 <sup>-2</sup>
<sup>234</sup> U	5.2705x10 <sup>-4</sup>	5.2770x10 <sup>-4</sup>
<sup>238</sup> U	3.2975x10 <sup>-4</sup>	3.3015x10 <sup>-4</sup>
<sup>235</sup> U Surroundings		
<sup>235</sup> U	4.4892x10 <sup>-1</sup>	4.4892x10 <sup>-1</sup>
<sup>238</sup> U	3.2340x10 <sup>-3</sup>	3.2340x10 <sup>-3</sup>

### U233-met-fast-005 (umf005)

This is a spherical system consisting of a highly enriched <sup>233</sup>U, reflected by beryllium.

Case (1) The core radius is 5.0444 cm and the outer radius of the reflector is 7.0891 cm.

Case (2) The core radius is 4.5999 cm and the outer radius of the reflector is 8.7960 cm.

Both critical experiments were performed at Los Alamos Scientific Laboratory.

The compositions for the two regions (nuclides per bar-cm) of these cases are given in the following table. Temperature is at 293 °K.

Isotope	Case 1	Case 2
<sup>233</sup> U core		
<sup>233</sup> U	4.7253x10 <sup>-2</sup>	4.7312x10 <sup>-2</sup>
<sup>234</sup> U	5.2705x10 <sup>-4</sup>	5.2770x10 <sup>-4</sup>
<sup>238</sup> U	3.2975x10 <sup>-4</sup>	3.3015x10 <sup>-4</sup>
Beryllium Reflector		
Be	1.1984x10 <sup>-1</sup>	1.1984x10 <sup>-1</sup>
O	1.3776x10 <sup>-3</sup>	1.3776x10 <sup>-3</sup>

### Pu-Comp-Inter-001 (pci001)

This is a  $k_{\infty}$  experiment at the HECTOR reactor (Winfrith, UK, 1960s): a graphite moderated plutonium oxide core (5%  $^{240}\text{Pu}$ ). The benchmark model is an infinite medium with a material composition appropriate to the interpolated boron/ $^{239}\text{Pu}$  ratio. It is modeled as a homogeneous infinite medium with the composition shown in the following table (all number of densities are given as nuclides per barn-cm).

Isotope	Density
$^{239}\text{Pu}$	$2.7350 \times 10^{-4}$
$^{240}\text{Pu}$	$1.5490 \times 10^{-5}$
$^{241}\text{Pu}$	$1.0720 \times 10^{-6}$
$^{242}\text{Pu}$	$5.8000 \times 10^{-8}$
$^1\text{H}$	$1.0770 \times 10^{-4}$
$^{10}\text{B}$	$1.0151 \times 10^{-4}$
$^{11}\text{B}$	$4.0859 \times 10^{-4}$
C	$7.0900 \times 10^{-2}$
$^{16}\text{O}$	$2.7070 \times 10^{-3}$
$^{40}\text{Ca}$	$8.0267 \times 10^{-4}$
$^{42}\text{Ca}$	$5.3572 \times 10^{-6}$
$^{43}\text{Ca}$	$1.1178 \times 10^{-6}$
$^{44}\text{Ca}$	$1.7272 \times 10^{-5}$
$^{46}\text{Ca}$	$3.3120 \times 10^{-8}$
$^{48}\text{Ca}$	$1.5484 \times 10^{-6}$

### HEU-Comp-Inter-004 (hci004)

This is a  $k_{\infty}$  experiment at the HECTOR reactor (Winfrith, UK, 1960s): a graphite moderated uranium oxide core. The benchmark model is an infinite medium with a material composition appropriate to the interpolated boron/ $^{235}\text{U}$  ratio. It is modeled as a homogeneous infinite medium with the composition shown in the following table (all number of densities are given as nuclides per barn-cm).

Isotope	Density
$^{234}\text{U}$	$3.1200 \times 10^{-6}$
$^{235}\text{U}$	$2.5020 \times 10^{-4}$
$^{236}\text{U}$	$4.2670 \times 10^{-7}$
$^{238}\text{U}$	$1.7190 \times 10^{-5}$
$^1\text{H}$	$1.1260 \times 10^{-4}$
$^{10}\text{B}$	$5.7849 \times 10^{-5}$
$^{11}\text{B}$	$2.3285 \times 10^{-4}$
C	$7.5650 \times 10^{-2}$
$^{16}\text{O}$	$1.6500 \times 10^{-2}$
$^{40}\text{Ca}$	$5.5227 \times 10^{-4}$
$^{42}\text{Ca}$	$3.6860 \times 10^{-6}$
$^{43}\text{Ca}$	$7.6909 \times 10^{-7}$
$^{44}\text{Ca}$	$1.1884 \times 10^{-5}$
$^{46}\text{Ca}$	$2.2788 \times 10^{-8}$
$^{48}\text{Ca}$	$1.0653 \times 10^{-6}$

## AQUEOUS THERML CRITICALS

Three unreflected spheres from the ORNL series were computed. These benchmarks contain  $^{235}\text{U}$  in the form of uranyl nitrate dissolved in water. One of the devices was poisoned with boron. Benchmarks ORNL-1 (hst013 Case 1) and ORNL-2 (hst013 Case 2) are of inner sphere radius 34.5948 cm. ORNL-10 (hst032) has inner sphere radius of 61.011 cm. The sphere wall, which is made of 1100 Al, is 0.32-cm thick for ORNL1 and ORNL2, 0.775-cm thick for ORNL10. The solution compositions specified for the models are as follows.

Material	ORNL-1	ORNL-2	ORNL-10
$^{10}\text{B}$	0.0	$1.0366 \times 10^{-6}$	0.0
$^{11}\text{B}$	0.0	$4.1724 \times 10^{-6}$	0.0
H	$6.6041 \times 10^{-2}$	$6.5892 \times 10^{-2}$	$6.6409 \times 10^{-2}$
O	$3.3642 \times 10^{-2}$	$3.3667 \times 10^{-2}$	$3.3601 \times 10^{-2}$
N	$1.8685 \times 10^{-4}$	$2.1276 \times 10^{-4}$	$1.1212 \times 10^{-4}$
$^{233}\text{U}$			$3.9124 \times 10^{-9}$
$^{234}\text{U}$	$5.3850 \times 10^{-7}$	$6.2962 \times 10^{-7}$	$4.0905 \times 10^{-7}$
$^{235}\text{U}$	$4.8042 \times 10^{-5}$	$5.6171 \times 10^{-5}$	$3.6157 \times 10^{-5}$
$^{236}\text{U}$	$1.3862 \times 10^{-7}$	$1.6207 \times 10^{-7}$	$2.0858 \times 10^{-7}$
$^{238}\text{U}$	$2.8050 \times 10^{-6}$	$3.2796 \times 10^{-6}$	$1.9878 \times 10^{-6}$

In order to get a case with higher leakage, two additional spheres from the L series of uranyl fluoride assemblies were calculated. The L-7 (hst009-3) assembly is modeled as an aluminum-clad sphere with an inner radius of 11.5177 cm. The aluminum container has a thickness of 0.1587 cm, and the aluminum number density is taken to be 0.06024 per barn-cm. The L-11 (hst012) assembly is modeled as an aluminum-clad sphere with inner radius of 27.9244 cm. The aluminum container has a thickness of 0.2 cm, and the aluminum number density is taken to be 0.06024 per barn-cm. The number densities for the solutions are given in the following table.

Material	L-7	L-11
H	$6.33620 \times 10^{-2}$	$6.6722 \times 10^{-2}$
O	$3.3467 \times 10^{-2}$	$3.3473 \times 10^{-2}$
F	$1.7864 \times 10^{-3}$	$1.1249 \times 10^{-4}$
$^{234}\text{U}$	$8.7965 \times 10^{-6}$	$5.5393 \times 10^{-7}$
$^{235}\text{U}$	$8.3281 \times 10^{-4}$	$5.2444 \times 10^{-5}$
$^{236}\text{U}$	$4.4499 \times 10^{-6}$	$2.8022 \times 10^{-7}$
$^{238}\text{U}$	$4.7124 \times 10^{-5}$	$2.9675 \times 10^{-6}$

The L-7 assembly has an additional 23.3236 cm of water outside the aluminum shell (the number densities for the hydrogen and oxygen are .066659 and .033329 per bar-cm, respectively). The L-11 assembly has an additional 15.0 cm of water outside the aluminum shell (the number densities for the hydrogen and oxygen are .0666883 and .0333442 per bar-cm, respectively).

Two unreflected spheres of plutonium nitrate solution were also computed. The PNL-3 (pst001 Case 18-1) and PNL-4 (pst011 Case 18-6) benchmarks have an inner sphere radius of 22.6974 cm of solution surrounded by 0.127-cm thick stainless steel shell, which is then covered with 0.0508 cm of cadmium. The isotopic compositions of the solutions are given in the following table.

Material	PNL-3	PNL-4
H	$6.5147 \times 10^{-2}$	$6.0264 \times 10^{-2}$
O	$3.4534 \times 10^{-2}$	$3.7209 \times 10^{-2}$
N	$7.3930 \times 10^{-4}$	$2.7753 \times 10^{-3}$
Fe	$1.2940 \times 10^{-6}$	$1.5204 \times 10^{-6}$
<sup>239</sup> Pu	$5.3938 \times 10^{-5}$	$6.6343 \times 10^{-5}$
<sup>240</sup> Pu	$2.3549 \times 10^{-6}$	$2.8964 \times 10^{-6}$

**Table D.2. Calculated ( $B_1$ )  $k_{\text{eff}}$  eigenvalues against the measured  $k_{\text{eff}} = 1.000$ .**

IHECB/CSEWGBenchmarks	$k_{\text{eff}}$		
	MCNP5*	COMBINE7.1**	
		Bondarenko Self Shielding	Bondarenko + Nordheim Self Shielding
hmf001 (GODIVA), 300K	0.99993	1.00011	1.00010
hmf028 (FLATTOP-25), 296K	1.00309	0.99950	0.99949
pmf006 (FLATTOP-Pu), 293K	1.00036	0.99404	0.99402
pmf001 bare (JEZEBEL), 293K	1.00020	0.99920	0.99920
umf001 (JEZEBEL-23), 296K	1.00032	0.99937	0.99937
pmf002 (JEZEBEL-Pu), 293.15K	1.00041	0.99978	0.99978
umf002-1, 293K	0.99867	0.99862	0.99862
umf002-2, 293K	1.00072	0.99990	0.99990
umf005-1, 293K	0.99393	0.99078	0.99078
umf005-2, 293K	0.99216	0.98449	0.98449
pci001, 293K	1.01217	1.01184	1.00781
hci004, 293K	0.98804	0.99195	0.99102
hst013 Case 1(ORNL-1), 293.6K	0.99751	0.99744	0.99735
hst013 Case 2 (ORNL-2), 293.6K	0.99578	0.99652	0.99645
hst032 (ORNL-10), 293.6K	0.99897	0.99820	0.99815
hst009-3 (L-7), 298K	0.99937	0.99908	0.99846
hst012 (L-11), 298K	0.99954	0.99097	0.99098
hst012 (L-11), 293.6K	0.99954	0.99929	0.99921
pst011 Case 18-1 (PNL-3), 298K	0.99379	0.99690	0.99588
pst011 Case 18-6 (PNL-4), 300K	0.99973	1.00233	1.00111

\* within  $\pm 0.0025$ , all at 293.6K

\*\* Temperatures correspond to those in Column 1. 28 groups for fast spectrum and 18 groups for intermediate and thermal spectra are used.

## D. REFERENCE

1. *International Handbook of Evaluated Criticality Safety Benchmark Experiments*, OECD Nuclear Energy Agency report NEA/NSC/DOC(95)03, September 2005 Edition.
2. *Cross Section Evaluation Working Group Benchmark Specifications*, ENDF-202, BNL-19302, November, 1974 and September 1991 Update.
3. MCNP 5.1.40, LA-UR-08-2216, November, 2005.

**APPENDIX E**

**FILES CONTENT of the SAMPLE INPUTS**

## Appendix E—Files Content of Sample Inputs

COMBINE input	ANISN input	Description
godiva.28b <sup>*</sup> , godiva.28r <sup>**</sup>	godiva.sn1	See Appendix D.
flattop25.28b, flattop25.28r	flattop25.sn1	See Appendix D.
flattoppu.28b, flattop.28r	flattoppu.sn1	See Appendix D.
jezebel.28b, jezebel.28r	jezebel.sn1	See Appendix D.
jezebel23.28b, jezebel23.28r	jezebel23.sn1	See Appendix D.
jezebelpu.28b, jezebelpu.28r	jezebelpu.sn1	See Appendix D.
umf002-1.18b,umf002-1.18r	umf002-1.sn1	See Appendix D.
umf002-2.18b,umf002-2.18r	umf002-2.sn1	See Appendix D.
umf005-1.18b,umf005-1.18r	umf005-1.sn1	See Appendix D.
umf005-2.18b,umf005-2.18r	umf005-2.sn1	See Appendix D.
pci001.b, pci001.r		See Appendix D.
hci004.b, hci004.r		See Appendix D.
orn1.18b, orn1.18r	orn1.sn1	See Appendix D.
orn2.18b, orn2.18r	orn2.sn1	See Appendix D.
orn10.18b, orn10.18r	orn10.sn1	See Appendix D.
17.18b, 17.18r	17.sn1	See Appendix D.
111.18b, 111.18r	111.sn1	See Appendix D.
111A.18b, 111A.18r	111.sn1	See Appendix D.
com.ani		COMBINE input for 1-D transport only. Requires anisn.inp.
bench.bat		Run batch file for the benchmarks (see Table D-2)
uriso.1_6		Homogenized UO <sub>2</sub> TRISO fuel.
uriso.1_6		One stage TRSIO fuel.
uebble.1_4	uebble.s1_4	Two stage pebble.
doppu.b0	oned.snu	UO <sub>2</sub> Doppler case.
cmb_pbmr268Az12g16.inp_test1	pb268.sn1	Three stage core, isotxs format.
cmb_pbmr268Az12g16.inp_test2		Three stage core, inl format
cmb_pbmr268Az12g16.inp_test3		Three stage core, inl format, extra micros.
cmb_pbmr268Az12g16.inp_test4		Three stage core, inl format, extra micros, group and regionwise buckling.
cmb_pbmr268Az12g16.inp_test5	pb268.sn1	Three stage core, isotxs format, extra micros, group and regionwise buckling.

COMBINE input	ANISN input	Description
cmb_pbmr268Az12g16.inp_test6		Three stage core, isotxs format, extra micros, group and regionwise buckling, generates photon cross section file (photon.sig).
com.pho	pb268.sn1	Photon transport.
pg268Ag6.inp1	pb268Ag6.sn1	One stage multiregion, isotxs format, forward (regular) transport.
	pb268Ag6.sn2	Adjoint transport.
pb268Ag6.inp3, com.adjnt	p268Ag6.sn1	Generates adjoint cross sections and run regular transport for adjoint flux
cmb_pbmr268Az12g6.inp1	pb268.sna	Three stage, isotxs format, forward transport .
	pb268.sna2	Adjoint transport.
cmb_pbmr268Az12g6.inp3, com.adjnt	pb268.sna	Generates adjoint cross sections and run regular transport for adjoint flux.
sample.bat		Run batch file for those other than benchmarks.

\* Bondarenko selfshielding only.

\*\* Bondarenko+ Nordheim self shielding.